11176-H532-R0-00

PROJECT TECHNICAL REPORT

TASK E-9G

LUNAR FAR SIDE COMMUNICATIONS ANALYSIS FOR SATELLITE RELAY SYSTEMS

NAS 9-8166 20 April 1970

Prepared for

NATIONAL AERONAUTICS AND SPACE ADMINISTRATION
MANNED SPACECRAFT CENTER
HOUSTON, TEXAS

Prepared by

Communications and Sensor Systems Department
Electronics Systems Laboratory

TRW
SYSTEMS GROUP

11176-H532-RO-00

PROJECT TECHNICAL REPORT

TASK E-9G

LUNAR FAR SIDE COMMUNICATIONS ANALYSIS FOR SATELLITE RELAY SYSTEMS

NAS 9-8166

20 April 1970

Prepared for

NATIONAL AERONAUTICS AND SPACE ADMINISTRATION
MANNED SPACECRAFT CENTER
HOUSTON, TEXAS

Prepared by

G. W. Breland
L. A. Lorio
J. C. Miller
P. A. Penzo
D. R. Perron

Approved by: J. G. Prothro

J. G. Prothro, Manager
Task E-9E

Approved by: John DeVillier

John DeVillier, Manager
Communications and Sensor
Systems Department

TRW
SYSTEMS GROUP

PRECEDING PAGE BLANK NOT FILMED.

CONTENTS

ILLUSTRATIONS

ILLUSTRATIONS (Continued)

ILLUSTRATIONS (Continued)

PRECEDING PAGE BLANK NOT FILMED.

TABLES

I. INTRODUCTION

A comprehensive lunar exploration program should naturally proceed from the present efforts concentrated on the earth side to landings on the far side of the moon. Because the far side is never visible from the earth, communications with a lunar far side terminal from earth (or a point on the near side of the moon) will involve some form of intermediate relay. The requirements for such a relay are already apparent in the current Apollo missions since the orbiting CSM and LM experience a loss of communications when passing behind the moon. This restriction of communications is serious because of critical operations (such as SPS ignition for insertion on the return to earth trajectory) which occur behind the moon. Real time communications to the lunar far side become a prerequisite for far side landings and exploration. It should be noted, however, that at present, there are no firm plans for such a far side mission.

1. STUDY PLAN

The overall study plan is illustrated schematically in Figure 1.

Following a brief requirements survey, the study program encompassed four tasks:

(1) Satellite coverage and visibility analysis
(2) Communication system parametric analysis
(3) Trajectory and vehicle considerations
(4) Survey of applicable technology

The communications system parametric analysis is based upon a mathematical model of a satellite communications system. Requirements for relay satellite system parameters such as effective radiated power, noise, temperature, etc., are investigated for two systems:

(1) Current Apollo systems
(2) Improved Apollo systems

The types of lunar relay systems which have been investigated are the current Apollo system, and a modified system in which the lunar terminal is

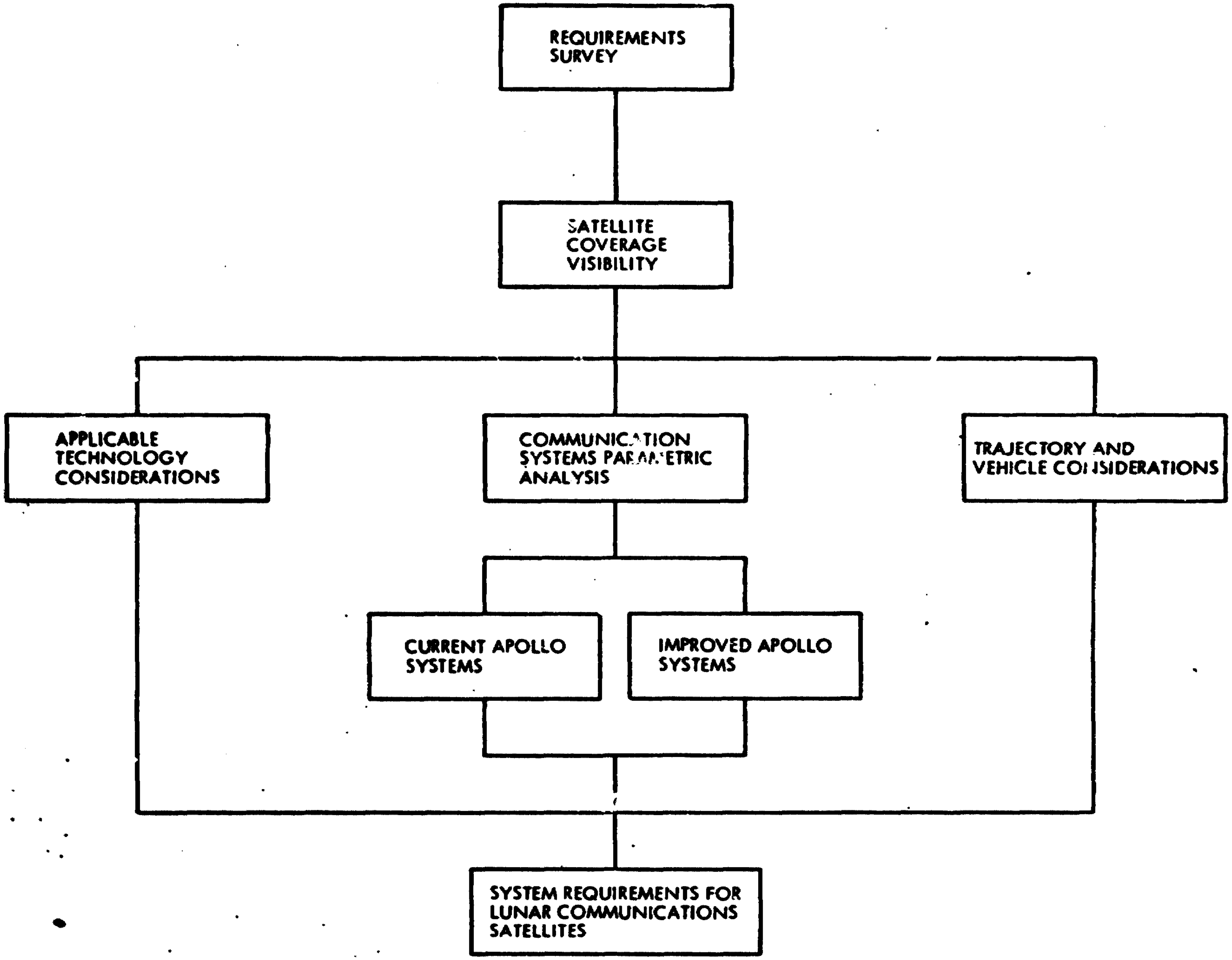

FIGURE 1. PROGRAM PLAN

similar to the Apollo system, and the earth to lunar relay satellite link is an X-band system.

Trajectory and vehicle considerations include performance, trajectory, and guidance analysis which includes the following items:

(1) ΔV requirements for entering selected lunar orbits
(2) Payload capabilities of candidate launch vehicles
(3) Perturbative effects on selected lunar orbits
(4) Orbit stabilization and phase control

The survey of applicable communications satellite technology is directed toward an assessment of the current state-of-the-art in major system items such as antenna design and RF power capabilities. The survey to date has been on antenna design, RF power generation, and low noise receivers.

As part of a continuing study, the results of these analyses should be integrated into a definitive statement of system requirements for a lunar communications satellite system. These requirements, based upon firm supporting analyses, would be the point of departure for a preliminary design of a lunar communications satellite.

2. COMMUNICATIONS REQUIREMENTS

It is instructive to briefly examine the communications requirements for the current Apollo missions and to estimate projected communications requirements for possible future lunar exploration. A summary of these requirements is shown in Table 1. Note that only the first two entries on Apollo G-H missions and Apollo J missions are firm requirements at the present. The remaining entries are the authors' projections. As shown in the table, it is expected that initial far side Apollo missions would closely

parallel the near side activities currently planned. Initial far side exploration would then require communications relay to earth from single lunar surface terminals (LM, rovers) whose location and surface activity time would be known well in advance of the mission. As will be discussed later, knowledge of mission time and landing site have substantial impact on relay communication system design.

Beyond Apollo type missions, one might expect future lunar surface explorations to involve the establishment of a near side lunar base, followed by a system of near side bases. This in turn might be followed by an initial far side base and possibly a system of far side bases. Wide ranging surface exploration from this base or system of bases might include long range EVA using large mobile surface laboratory vehicles. Finally, a lunar orbiting space station/base might be established.

This brief discussion has thus indicated that the goal of any lunar communications system should be coverage of the entire lunar sphere all the time. Transmission requirements start with those of the current Apollo system and proceed to those associated with comprehensive systems of bases and orbiting stations. One might expect these latter requirements to be similar to those projected for earth orbiting space bases, i.e., multiple two-way TV channels, high data rate telemetry channels, multiple channel EVA communications, etc.

While the long term goals are complete and continuous coverage, the time phasing of the operational requirements is such that the establishment of a lunar far side relay communications system may be phased in concert with developing requirements. It is important to note that the communications relay systems required to support initial Apollo missions would be substantially less complicated than the full coverage system.

Table 1. Communications Summary for Lunar Exploration

Phase of Lunar Exploration	Surface Stay Time	Activities	Communications Requirements Possible Modes	 Possible Links	Remarks
Current Apollo Missions* (G-H type missions)	up to 35 hrs	Limited EVA within 1500 ft. of LM - duration 2 hrs. 40 minutes	USB-voice	LM-CSM	See mission time line.
Apollo Earth-side Lunar Exploration Missions* (J-type missions)	up to 78 hrs	Expanded walking EVA within 1-2 KM of LM for 3 hrs. 40 minutes Mobile EVA within 5 KM of LM using rover	USB-voice USB-data USB-TV USB-ranging VHF-voice VHF-data VHF-ranging	LM-CSM LM-EVA LM-earth CSM-earth Rover-CSM Rover-LM Rover-earth Rover-EVA	See mission time line
Initial Far Side Apollo Missions	Short similar to G-H missions	Limited EVA similar to G-H missions	USB-voice USB-data USB-TV USB-ranging VHF-voice VHF-data VHF-ranging	LM-CSM LM-EVA LM-earth CSM-earth	No far side missions planned before 1975 at present
Apollo Far Side Lunar Exploration Missions	Similar to J-type missions	Expanded EVA similar to J-type missions	USB-voice USB-data USB-TV USB-ranging VHF-voice VHF-data VHF-ranging	LM-CSM LM-EVA LM-earth CSM-earth Rover-CSM Rover-LM Rover-earth Rover-EVA	

*Reference: "Program and Mission Definition Apollo Lunar Exploration" NASA/MSC Report No. SPD-9P-052 August 15, 1969.

Table 1. Communications Summary for Lunar Exploration - Continued

Phase of Lunar Exploration	Surface Stay Time	Activities	Communications Requirements		Remarks
			Possible Modes	Possible Links	
Initial Lunar Base	Indef-inite	Comprehensive surface science and exploration. Long duration EVA using large surface rovers.	Voice Data TV Ranging	Base-orbiters Base-EVA Base-rovers Orbiters-earth	Post 1975
System of Lunar Bases	Indef-inite	Multiple sites for comprehensive surface science and exploration.	Voice Data TV Ranging	Base-orbiters Base-EVA Base-rovers Base-earth Inter-base links	Post 1975
Lunar Orbiting Space Station		Similar activity to earth orbiting space station	Voice Data TV Ranging	Station-earth Station-orbiters Station-lunar Station-surface Station-terminals Station-EVA	Post 1980

3. METHODS FOR LUNAR FAR SIDE COMMUNICATIONS RELAY

There are a variety of possible methods for relay communications from the far side of the moon. These possibilities are briefly summarized in the discussions below.

One approach is that of providing a lunar surface link from a far side terminal to a near side terminal with subsequent relay to an earth station. The surface mode of transmission could be one or a combination of the following techniques:

(1) Lunar surface point-to-point relay

a. Microwave

b. VHF or UHF radio relay

(2) Surface wave transmission (generally limited to frequencies below the high frequency region of the spectrum)

While attractive for special applications, the relay mode is primarily limited by the difficulty and expense of establishing a sufficiently extensive network to provide area coverage for the lunar far side. The surface wave transmission mode can provide area coverage, but because of the frequency limitation can provide limited information bandwidth. This mode is, however, very attractive for backup communications, and is also attractive for specific applications where wide bandwidth is not a primary consideration. For example, far side experiment packages with low data rates might use this mode for relaying scientific information to a near side terminal with subsequent relay to an earth station.

Lunar communications satellites provide the most direct method of complete area coverage for the lunar sphere. There are basically three configurations for such satellites

a. Lunar orbiting satellites

b. Libration point satellite at position L_2

c. A "Hummingbird" lunar synchronous satellite

There is no stable synchronous orbit for the moon due to the effect of the earth's potential. A lunar synchronous orbit would be possible in principle using continuous propulsion on-board the satellite. This concept has been investigated by GSFC (Reference 3-1).

It should be noted, also, that passive or active relay satellites are possible in this application. Terminal effective radiated power limitations are such that only active relay satellites represent practical possibilities. Coverage and visibility observations developed in this report, however, apply to both active and passive satellites.

This report specifically considers the coverage and visibility factors for a lunar orbiting system of communications satellites. Since the characteristics on the L_2 libration point are well documented, (Reference 3-2) no specific attention has been devoted to the coverage and visibility analysis for this type of satellite.

It should also be noted that only circular orbits are considered. Other orbits such as a highly elliptical earth orbit which has an apogee behind the moon could be considered in further studies.

II. SUMMARY AND CONCLUSIONS

This report addresses itself to an analysis of orbiting lunar relay satellites. Since full coverage of the lunar far-side surface is not possible from an equatorial orbit, a system of polar orbiting relay satellites is proposed. For continuous coverage of the entire lunar sphere, the minimum network of relay satellites is composed of three sets of three orbiting satellites, equally spaced in circular orbits. For orbit plane separations of sixty degrees; orbit altitudes of approximately 6000 statute miles will provide lunar grazing angles of 5 degrees.

Since the most attractive possibility for partial coverage is a network of three equally spaced satellites in circular polar orbit, it is proposed that such a system be established as an interim step in providing full coverage with the nine satellite system. It can be shown that such an orbit may be positioned to provide continuous coverage for a specific mission whose landing site and mission time are known during substantial fractions of a lunar cycle.

A review of Part IV indicates that off-the-shelf boosters possess the capability of delivering up to 6400 pounds to lunar orbit. It would thus appear to be within reason to postulate that three lunar relay satellites could be orbited using a single booster. It also appears reasonable that the approximately 2000 pounds available for each satellite should be enough to provide for the on-board propulsion required for initial phasing control and for station keeping to cancel the perturbation effects for a lifetime of several years. It is obvious that further study will be necessary to determine the actual feasibility of any satellite system, depending upon the weight and complexity of the system chosen.

Assuming a lunar relay satellite system with separate antennas for the MSFN-satellite link and for the satellite-lunar vehicle link, analysis of the required effective radiated power (ERP) and receive antenna gains for a 3 satellite system is presented in Part V.

Figures 30 and 31 of Part V are consolidated plots showing a wide range of combinations of lunar relay satellite effective receive gain and effective radiated power (ERP) which will produce the required signal to noise ratio at the terminal receiver (lunar vicinity vehicle or MSFN). Table 2 in Part V lists the minimum satellite ERP and receive gain shown in Figures 30 and 31 as well as those required for a back-up baseband voice system and system using a VHF link from the lunar terminal to the satellite. The satellite minimum required receiver gain varies from approximately -33 dB for the uplink (MSFN to satellite, modified system) to +40 dB for the downlink (lunar vehicle to satellite, Apollo system); while the minimum required ERP varies from +20 dbm for the downlink (satellite to MSFN, Apollo system with the VHF back-up link from lunar terminal to satellite) to +84 dbm for the uplink (satellite to lunar terminal with omni antenna, Apollo system).

Selecting two of the allowable receive gain - ERP combinations, two examples of antenna gains and transmitted powers are provided - one for the Apollo system and one for a modified Apollo system (where the MSFN-satellite link is X-Band). Using parabolic antennas, the example for the modified system provides the antenna specifications shown in Table 3 . Table 3 shows that a relay satellite with the reasonable parameters of an S-Band transmitter of 10 watts and S-Band antenna approximately 13 feet in diameter; together with an X-Band transmitter of one watt and an antenna of approximately 4 feet in diameter will provide the required margins for omni-narrowband system which is the worst case requirement.

Appendix A lists the ground rules and parameters used to establish the required antenna gains and ERP for lunar relay satellites.

Appendix B is a brief summary of applicable RF technology available for lunar relay satellites. Antenna gains up to 44 dB at S-Band and 55 dB at X-Band appear to be the present state-of-the-art. RF power generators of approximately 20 watts are available at S-Band and X-Band, while receiver noise figures are in the 2 to 2.5 dB range.

III. COVERAGE AND VISIBILITY ANALYSIS FOR SATELLITE RELAY SYSTEMS

The use of lunar orbiting communications satellite offers an attractive solution to the problem of lunar far side communications. The technology of communications relay by satellite is well advanced through the current efforts in terrestrial applications. Relay of communications from spacecraft to ground terminals is being actively explored through the planned ATS-F and ATS-G experiments and the initial work on geosynchronous tracking and data relay satellites (TDRS).

1. COVERAGE OF THE LUNAR SURFACE

The basic problem in the design of a satellite communications network is that of providing adequate coverage. The most optimistic goal would be a system where any lunar surface terminal or any vehicle in lunar orbit could communicate with earth at any time. Due to the evolutionary nature of the lunar exploration program as it is currently defined or projected, it may neither be practical or desirable to attempt to achieve this goal with the initial efforts in providing lunar far side communications relay. For initial Apollo-type far side missions, it will only be necessary to provide coverage during short periods of a few days at infrequent intervals.

A second factor of interest is the desirability of eliminating requirements for satellite-to-satellite relay. This factor has a substantial impact upon the design of a communications satellite system. For example, if the line of sight path from earth to the communications satellite visible from the lunar far side terminal is occulted by the moon, then there is no possibility of direct relay to earth, and a second relay link through a satellite would be required. This satellite-to-satellite relay mode imposes severe requirements upon the communications system. The studies described in this report will assume that no satellite-to-satellite relay is to be provided.

1.1 Choice of Orbit for the Communications Satellite Network

It is impossible to cover all points on the lunar sphere simultaneously from satellites in a single orbital plane. The degree of coverage varies with the altitude of the satellite orbit, the number of satellites and the minimum elevation of the satellite above the horizon viewed from the lunar surface at acquisition. For example, if a lunar equatorial orbit is utilized

then the polar regions will never be covered. An inclined orbit will allow coverage of all points on the lunar surface, but not simultaneously. A system of polar orbits is probably the most promising candidate for realizing the long term goal of 100% coverage of the lunar surface 100% of the time. An equatorial orbit may be most effective, however, if all Apollo missions operate over a region confined to latitudes of, say, $\pm 40°$ of the lunar equator. In summary, the choice of orbit rests upon projected operational requirements. Subsequent discussion on the orbital configuration of candidate communication satellite systems will be directed toward three objectives:

(1) A single system of equatorial satellites oriented toward support of current Apollo missions.

(2) A system of polar orbiting satellites oriented toward the long term goal of 100% coverage for any time.

(3) A system for partial coverage to support Apollo or other specific missions.

2. BASIC COVERAGE CONSIDERATIONS

Consider the geometry illustrated in Figure 2. A system of N satellites is to be positioned in circular orbit about the moon to provide communications between points on earth and terminals on the lunar surface as well as vehicles in orbit around the moon. In order to provide continuous communications with lunar terminals, some overlap in coverage must be provided in the orbital plane of the communications satellites. It is convenient to measure this overlap in terms of the selenocentric angle α as shown in Figure 2. The third parameter of interest is the elevation angle at acquisition, ϵ. This is the angle above the horizon viewed from the lunar terminal at which the acquisition of a signal from the communications satellite could first be accomplished. There are therefore, three independent quantities which determine the altitude of the circular orbits of the communications satellite network

(1) Number of satellites, N.

(2) Selenocentric angle of overlap α, for coverage in the orbital plane

(3) Elevation angle at acquisition ϵ.

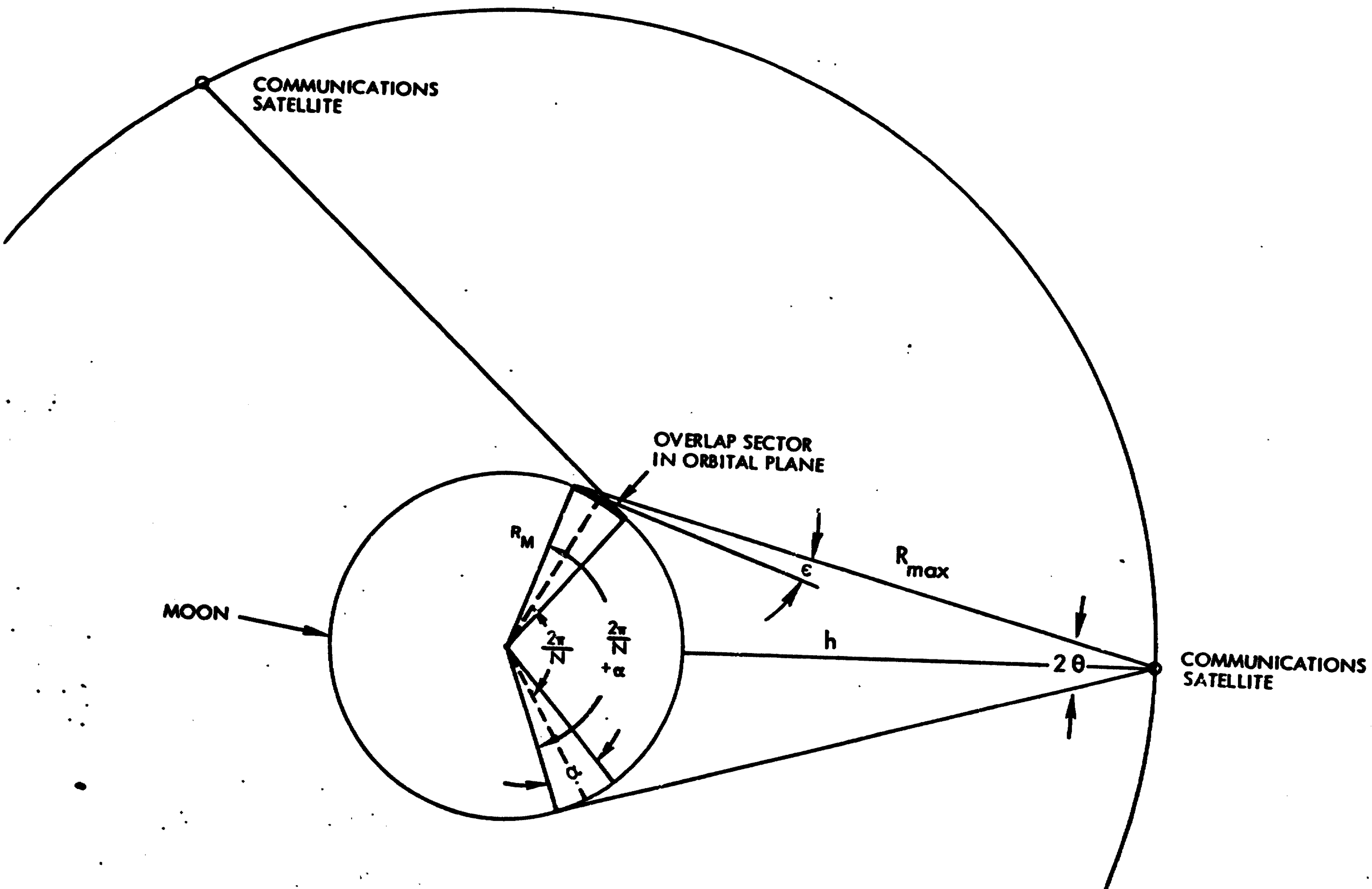

FIGURE 2. BASIC COVERAGE GEOMETRY

Referring to the simplified diagram of Figure 2 , the law of sines may be applied to obtain

$$\frac{\sin\left(\frac{\pi}{N}+\frac{\alpha}{2}\right)}{R_{max}} = \frac{\sin\left(\frac{\pi}{2}+\epsilon\right)}{R_M + h} = \frac{\sin\theta}{R_M} \qquad (1)$$

where:

R_M = radius of moon

h = altitude of communications satellite above the lunar surface

R_{max} = communications distance at acquisition

The angle θ may be expressed in terms of the other angles as follows

$$\theta = \pi\left(\frac{1}{2}-\frac{1}{N}\right) - \left(\epsilon+\frac{\alpha}{2}\right), \; N \geq 3 \qquad (2)$$

It is easily shown from (1) that the satellite altitude is given by

$$h = R_M \frac{(\cos\epsilon - \sin\theta)}{\sin\theta} \qquad (3)$$

The maximum communications distances will be

$$R_{max} = R_M \frac{\sin\left(\frac{\pi}{N}+\frac{\alpha}{2}\right)}{\sin\theta} \qquad (4)$$

3. DERIVATION OF EXTENT OF MUTUAL VISIBILITY ZONES

The requirement of continuous communications dictates that a period of mutual visibility must be provided for two communications satellites and the lunar terminal. Specification of a selenocentric angle of overlap for coverage in the orbital plane of communications satellites meets this requirement. It is of interest to determine the extent of this mutual visibility region. The mutual visibility regions for adjacent satellites is illustrated in Figure 3 . Figure 4 illustrates the orientation of the intersection of the cone representing the satellite coverage sector and the

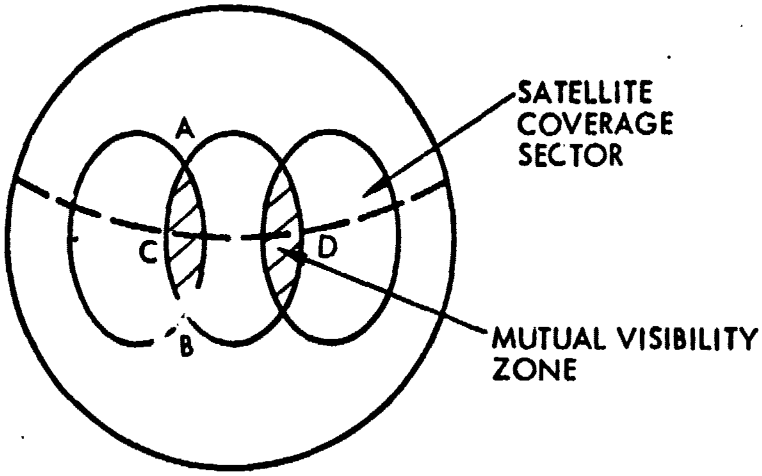

B.1 (a) MUTUAL VISIBILITY ZONES

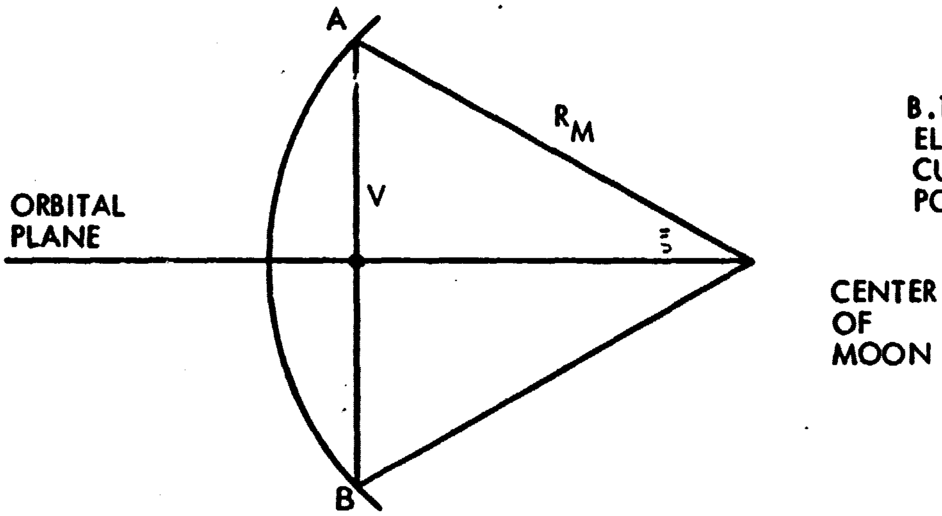

B.1 (b)
ELEVATION
CUT THROUGH
POINTS A AND B

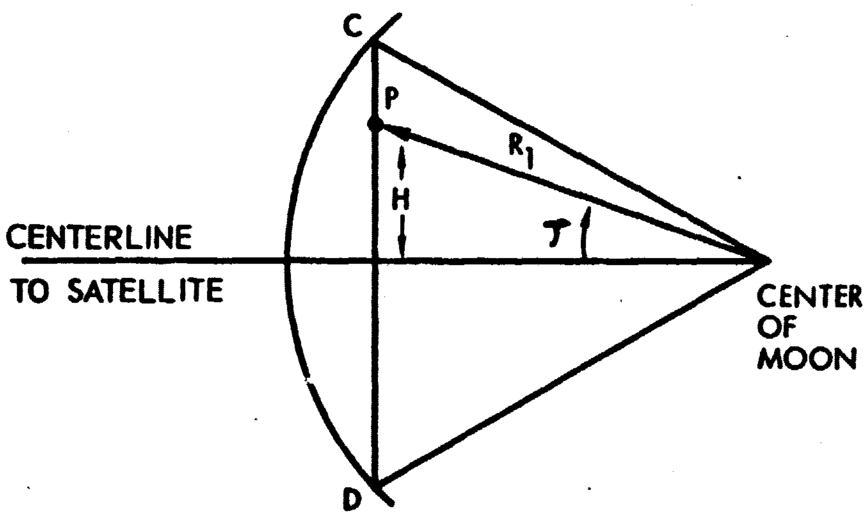

B.1 (c)
AZIMUTHAL CUT
THROUGH C AND D

FIGURE 3. MUTUAL VISIBILITY ZONES

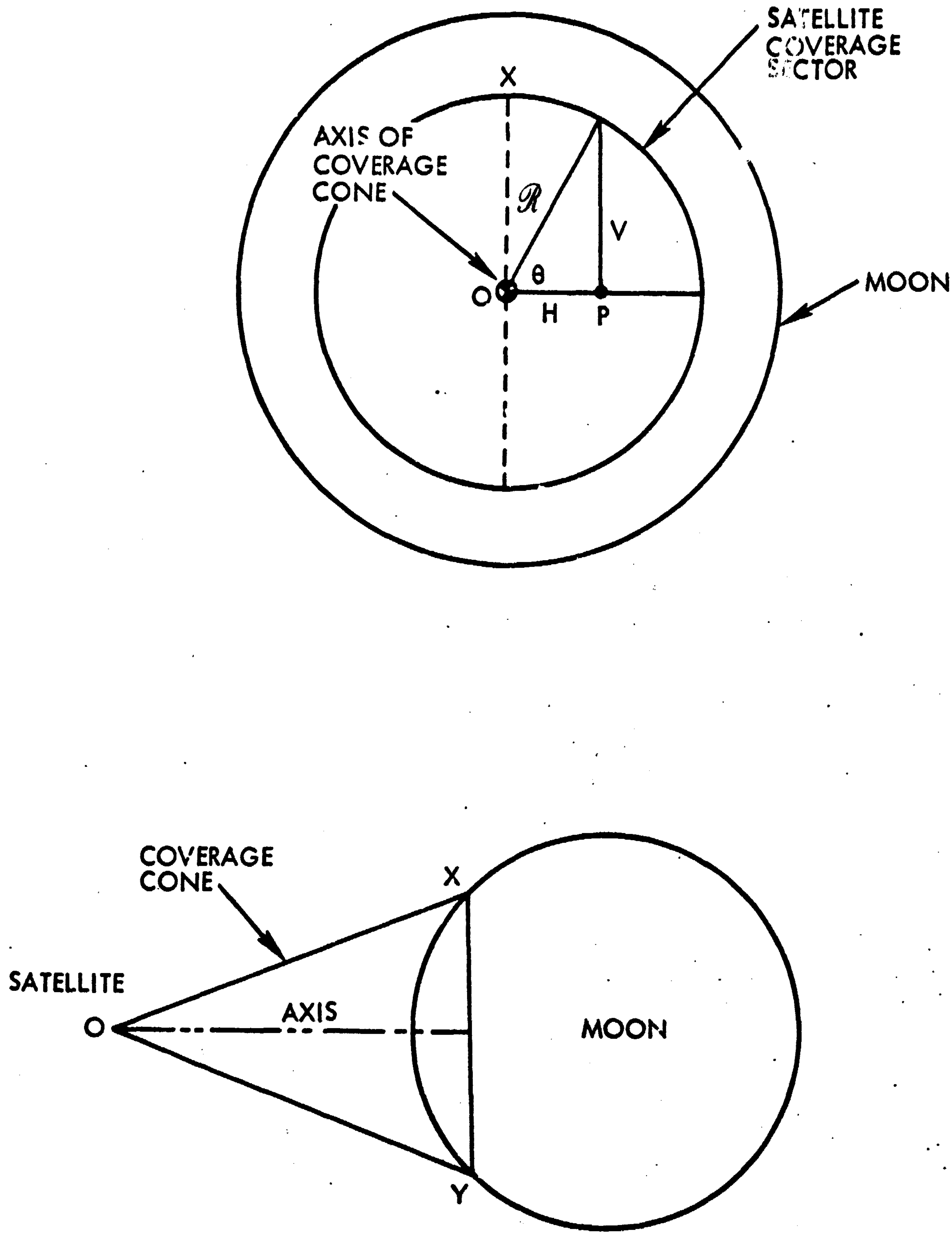

FIGURE 4. ORIENTATION OF SATELLITE COVERAGE SECTOR

lunar sphere. Referring to these diagrams it may be seen that the radius R is related to the lunar radius by

$$R = R_M \sin\left(\frac{\pi}{N} + \frac{\alpha}{2}\right) \tag{5}$$

where:

R_M = lunar radius

N = number of satellites ($N \geq 3$)

α = selenocentric angle of overlap for coverage sectors in orbital plane of satellites.

If the center line of the right circular coverage cone is taken as reference, then the angular coordinates (τ, ξ) define the intersection of the coverage cone with the lunar sphere. For example, if an equatorial system of communications satellites is being considered, then τ will be the longitudinal coordinate from the centerline of the coverage cone, while ξ will be the latitudinal coordinate for the intersection. These coordinates for every point on the intersection are conveniently expressed in terms of the angle θ shown in Figure 4. It may be seen that

$$\begin{aligned} V &= R \sin \theta \\ H &= R \cos \theta \end{aligned} \tag{6}$$

and,

$$R_1 = R_M \cos \xi$$

$$\begin{aligned} \sin \tau &= \frac{H}{R_1} \\ \sin \xi &= \frac{V}{R_M} \end{aligned} \tag{7}$$

Using (6) - (7) the angles τ and ξ may be determined to be

$$\begin{aligned} \xi &= \sin^{-1} \left\{ \sin\left(\frac{\pi}{N} + \frac{\alpha}{2}\right) \sin \theta \right\} \\ \tau &= \sin^{-1} \left\{ \frac{\sin\left(\frac{\pi}{N} + \frac{\alpha}{2}\right) \cos \theta}{\cos \xi} \right\} \end{aligned} \tag{8}$$

Of particular interest is the angle ξ at which the coverage zones intersect since this is the maximum extent of the mutual visibility zone. Figure 5 illustrates the geometry to be considered in determining this angle. The orbital plane of the satellites in Figure 5 is the plane of the paper. Figure 6 is a vertical cut in the plane of OV shown in Figure 5. From triangle OXR it is seen that

$$OR = R_M \cos\left(\frac{\pi}{N} + \frac{\alpha}{2}\right) \tag{9}$$

while from triangle OVR, it may be determined that

$$OV = OR \sec\frac{\pi}{N} \tag{10}$$

and

$$OV = R_M \cos\left(\frac{\pi}{N} + \frac{\alpha}{2}\right) \sec\frac{\pi}{N} \tag{11}$$

The central angle for the point of intersection is then

$$\xi_{\text{intersection}} = \cos^{-1}\left\{\cos\left(\frac{\pi}{N} + \frac{\alpha}{2}\right) \sec\frac{\pi}{N}\right\} \tag{12}$$

The extent of the mutual visibility region in fact determines the effective coverage limits for a system of equally spaced coplanar satellites. Figure 7 illustrates these coverage limits. Note that there are two regions where there is no continuous communications coverage. The extent of these regions is determined by interdependent quantities such as the altitude of the relay satellite network, number of satellites, and required elevation angle at acquisition. Figures 8 and 9 illustrates the dependence of the selenocentric angle subtended by the coverage region for systems of three, five, and six satellites upon the selenocentric angle of coverage overlap in the orbital plane of the satellites.

The impact of this coverage limitation is obvious for an equatorial system of lunar communications relay satellites. As will be discussed

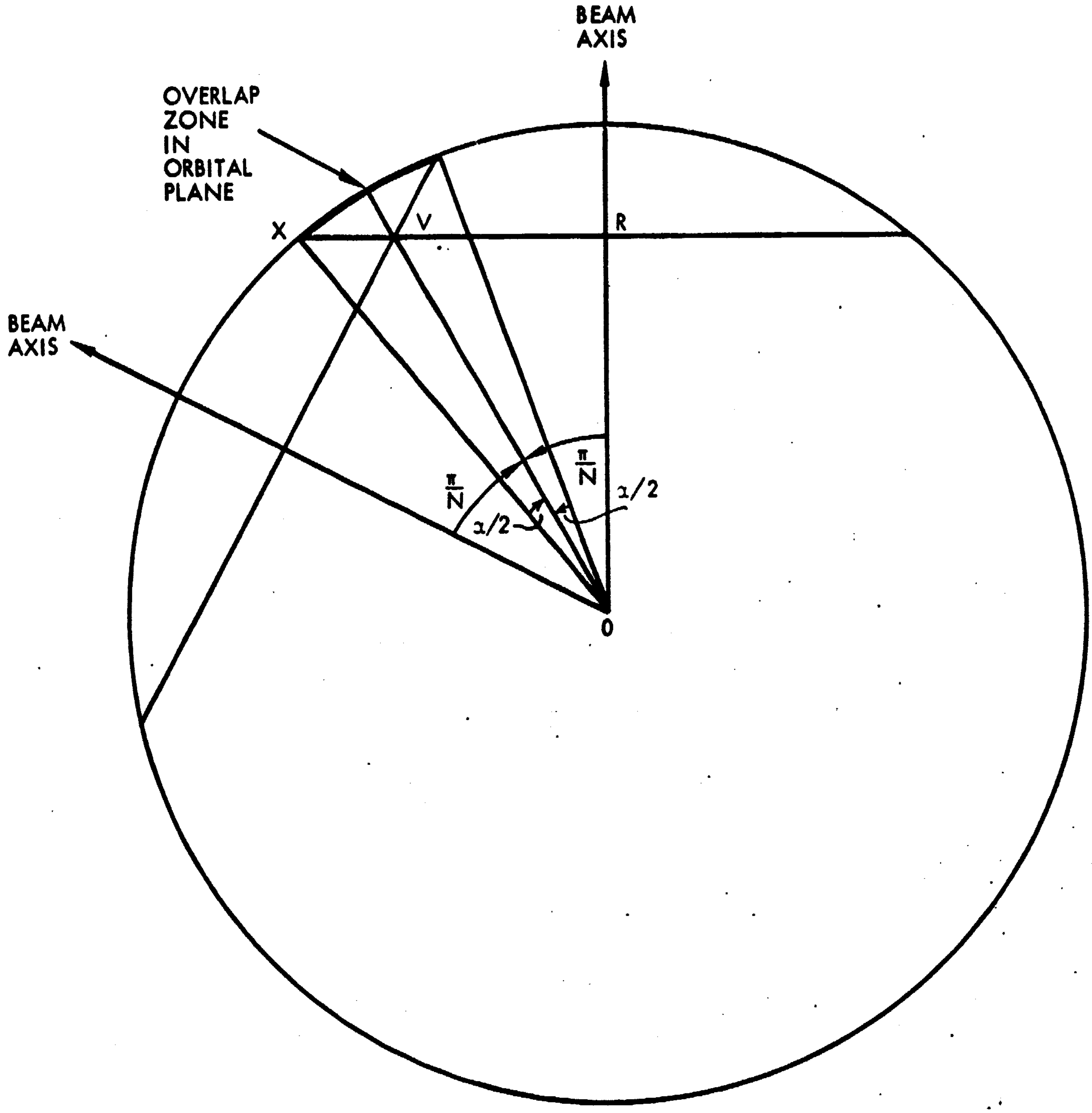

FIGURE 5. GEOMETRY PERTINENT TO OUT-OF-PLANE COVERAGE ANALYSIS

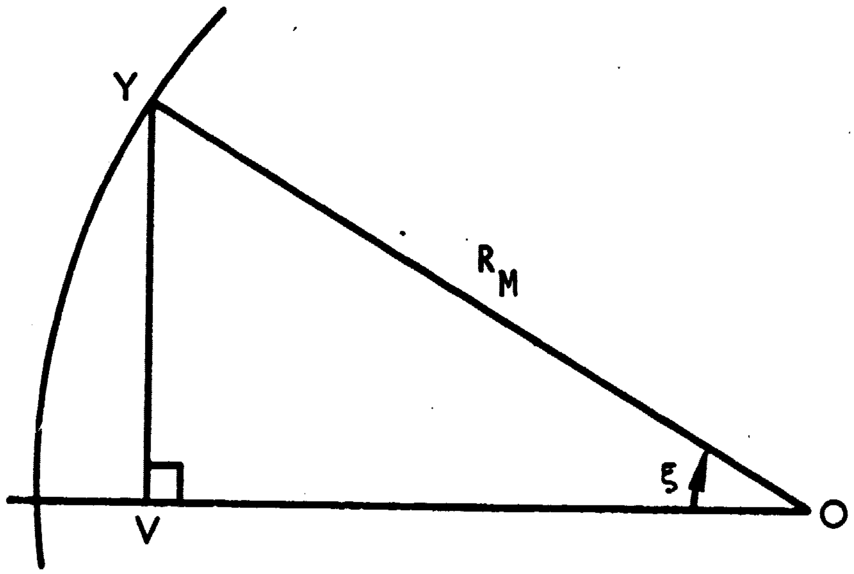

FIGURE 6. VERTICAL CUT THROUGH POINTS O AND V OF FIGURE 5.

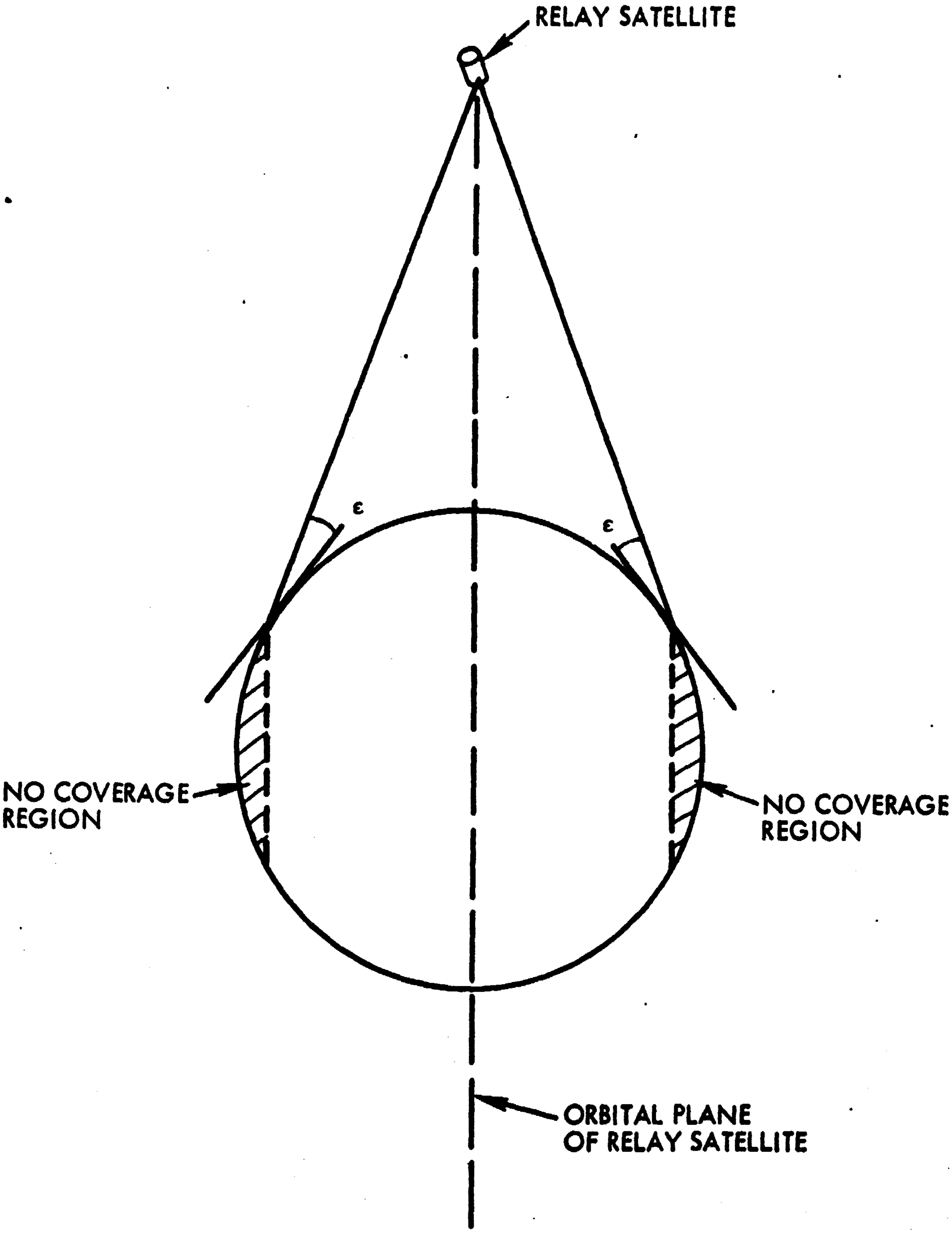

FIGURE 7. COVERAGE RESTRICTION DUE TO PROVISION OF NON-ZERO ELEVATION ANGLE AT ACQUISITION

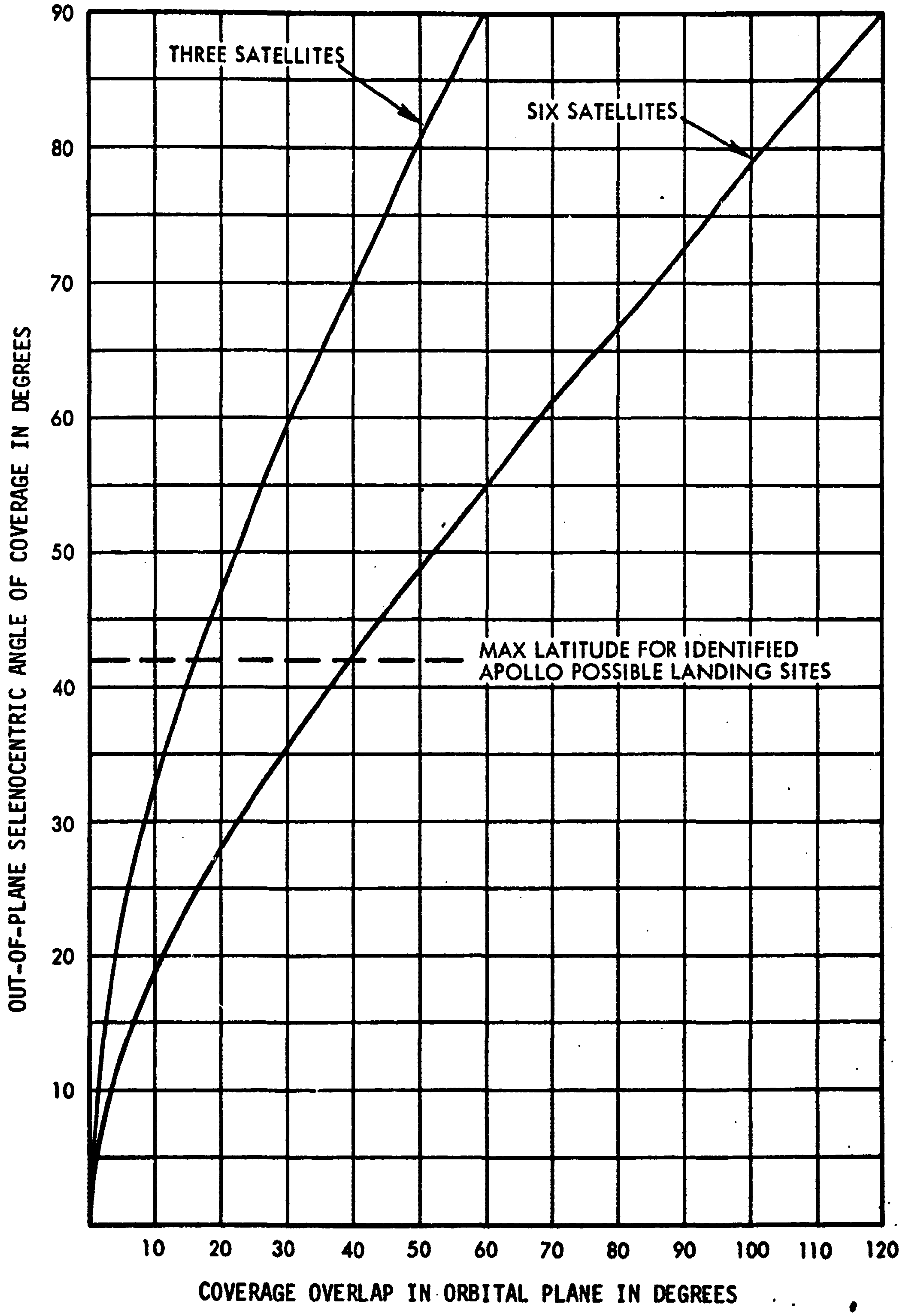

FIGURE 8. OUT-OF-PLANE COVERAGE FOR SELECTED SATELLITE SYSTEMS

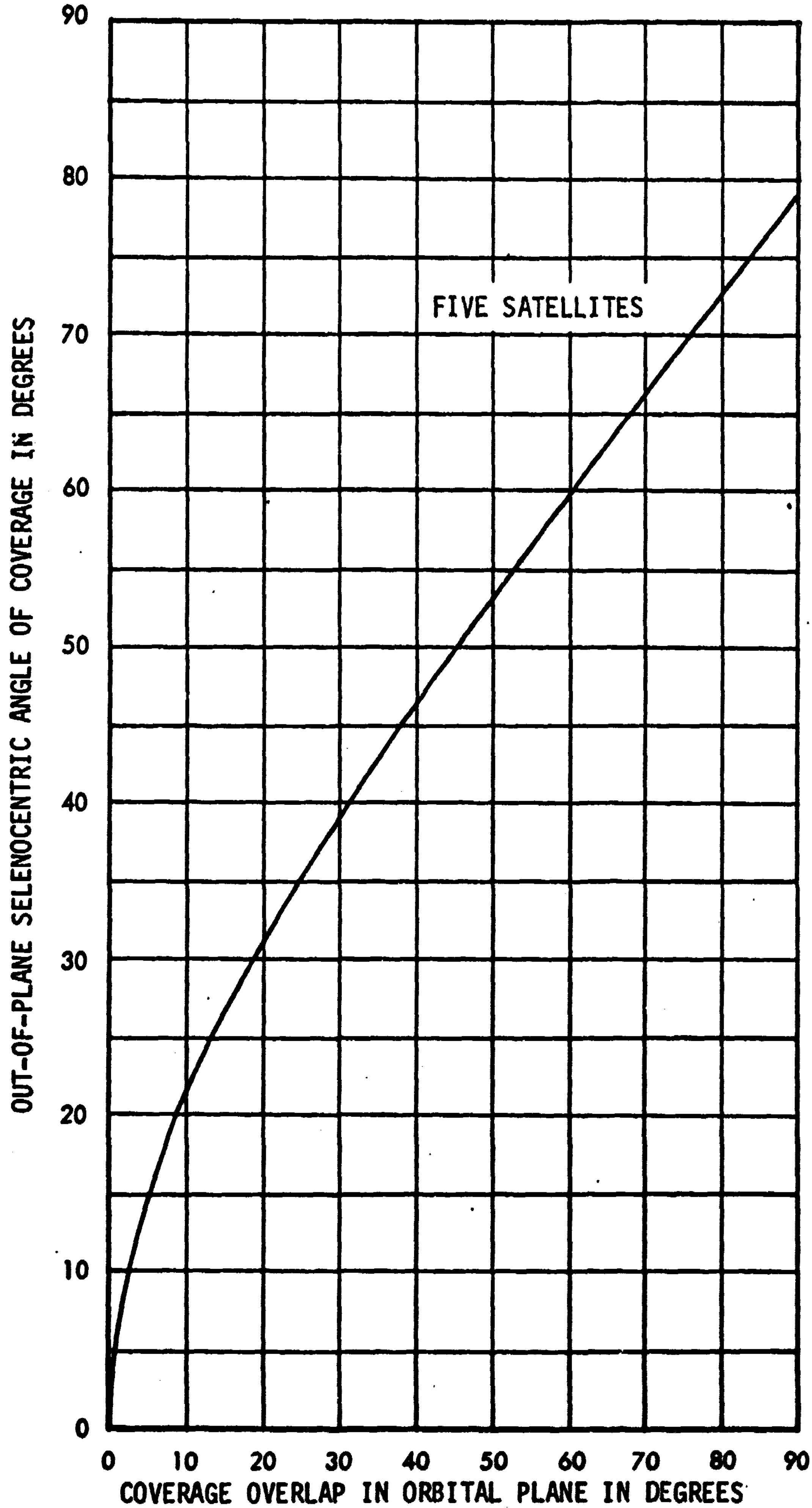

FIGURE 9. OUT-OF-PLANE COVERAGE FOR SELECTED SATELLITE SYSTEMS

in a subsequent section of this report, this factor also imposes a requirement for three non-coplanar sets of polar orbiting satellites if continuous coverage of the entire lunar surface is to be achieved.

Figures 10 - 14 illustrate the dependence of satellite altitude and surface coverage for selected systems.

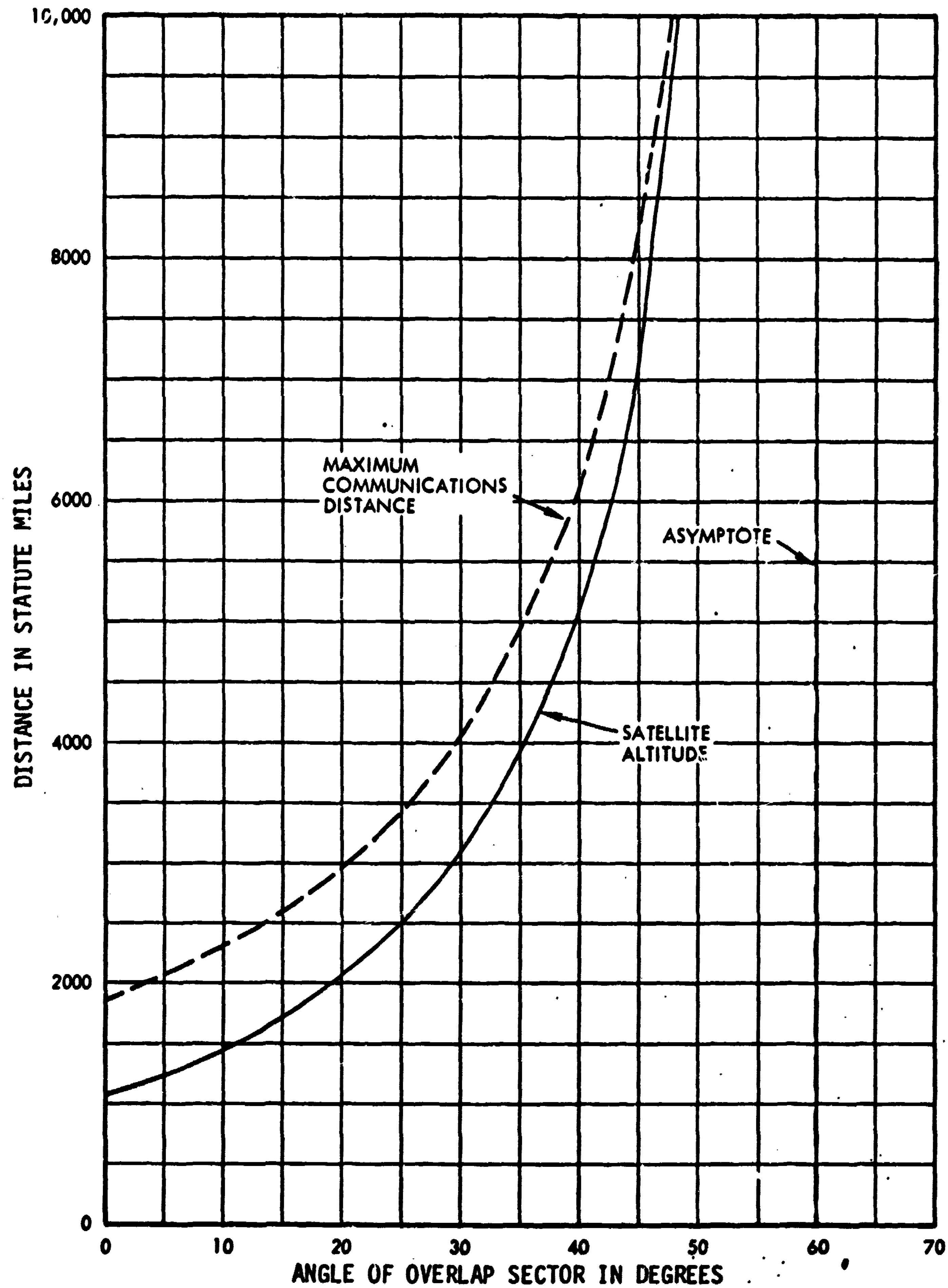

FIGURE 10. SATELLITE ALTITUDE AND MAXIMUM COMMUNICATIONS DISTANCE vs. ANGULAR OVERLAP SECTOR FOR THREE (3) EQUI-SPACED SATELLITES IN CIRCULAR ORBIT

ELEVATION ANGLE AT ACQUISITION IS 0°

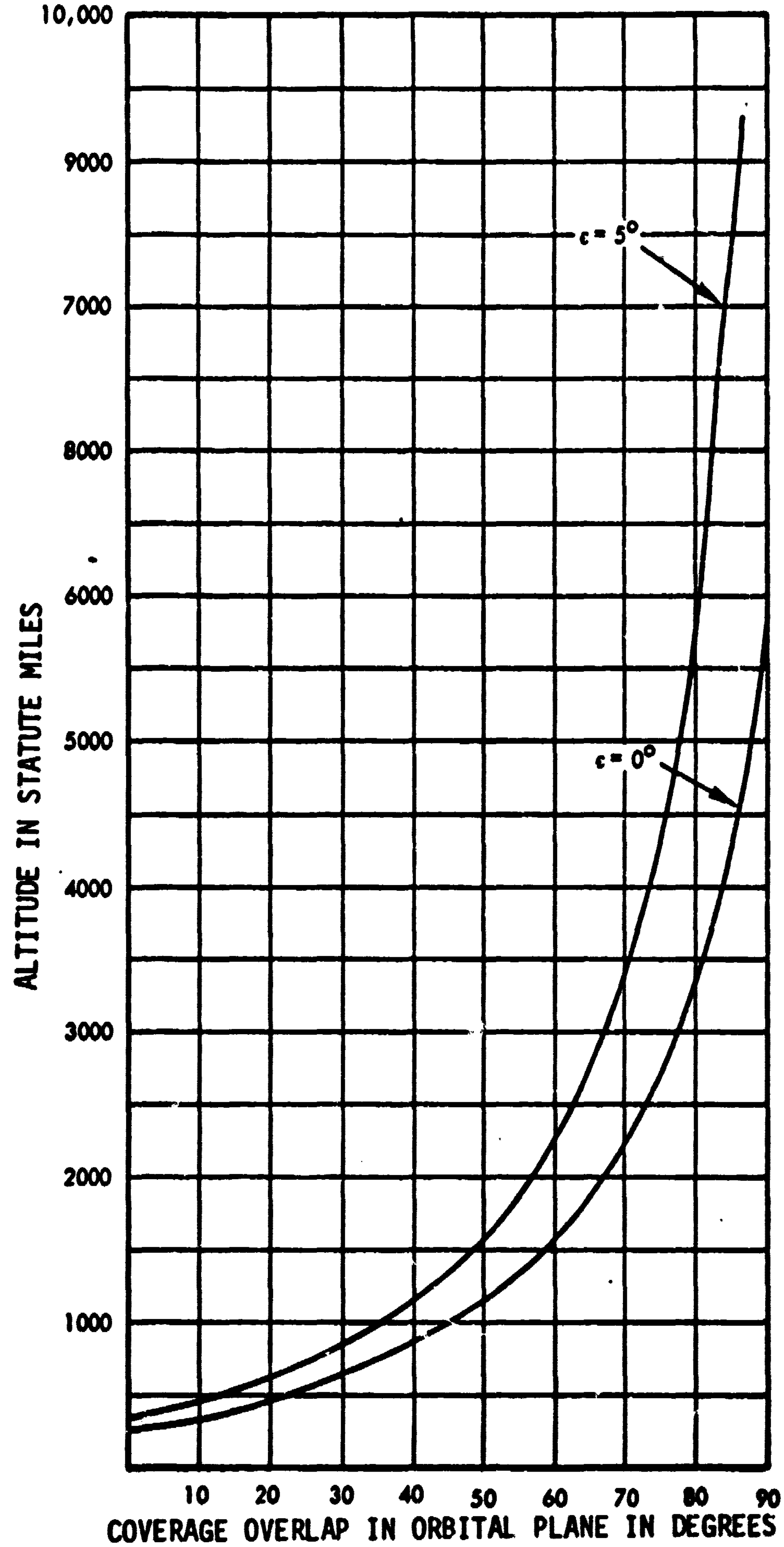

FIGURE 11. ORBITAL ALTITUDE VS. SELENOCENTRIC ANGLE OF COVERAGE OVERLAP FOR FIVE EQUI-SPACED COPLANAR SATELLITES IN CIRCULAR ORBIT

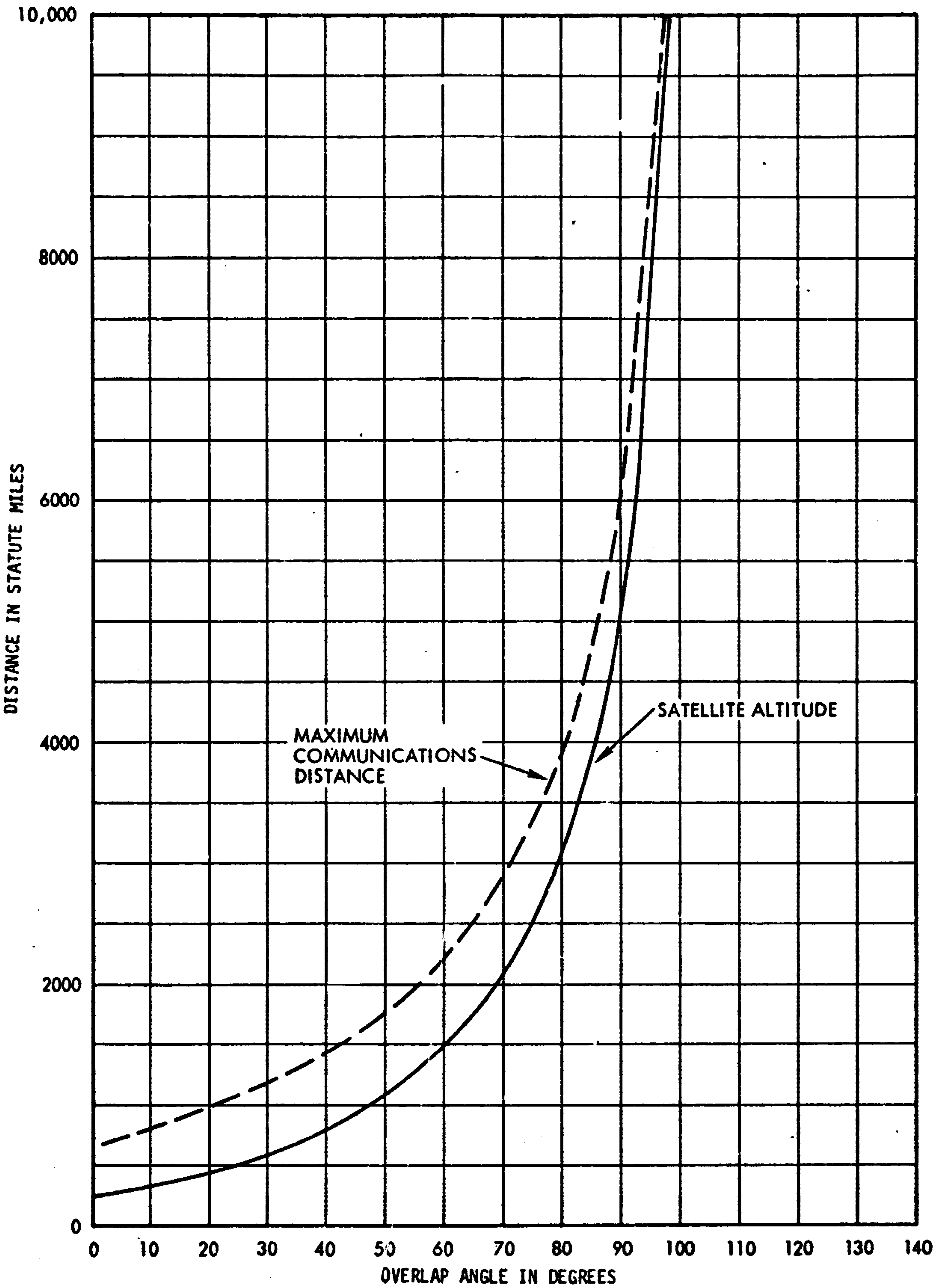

FIGURE 12. SATELLITE ALTITUDE VS. OVERLAP SECTOR FOR SIX (6) EQUI-SPACED SATELLITES

$\epsilon = 5°$

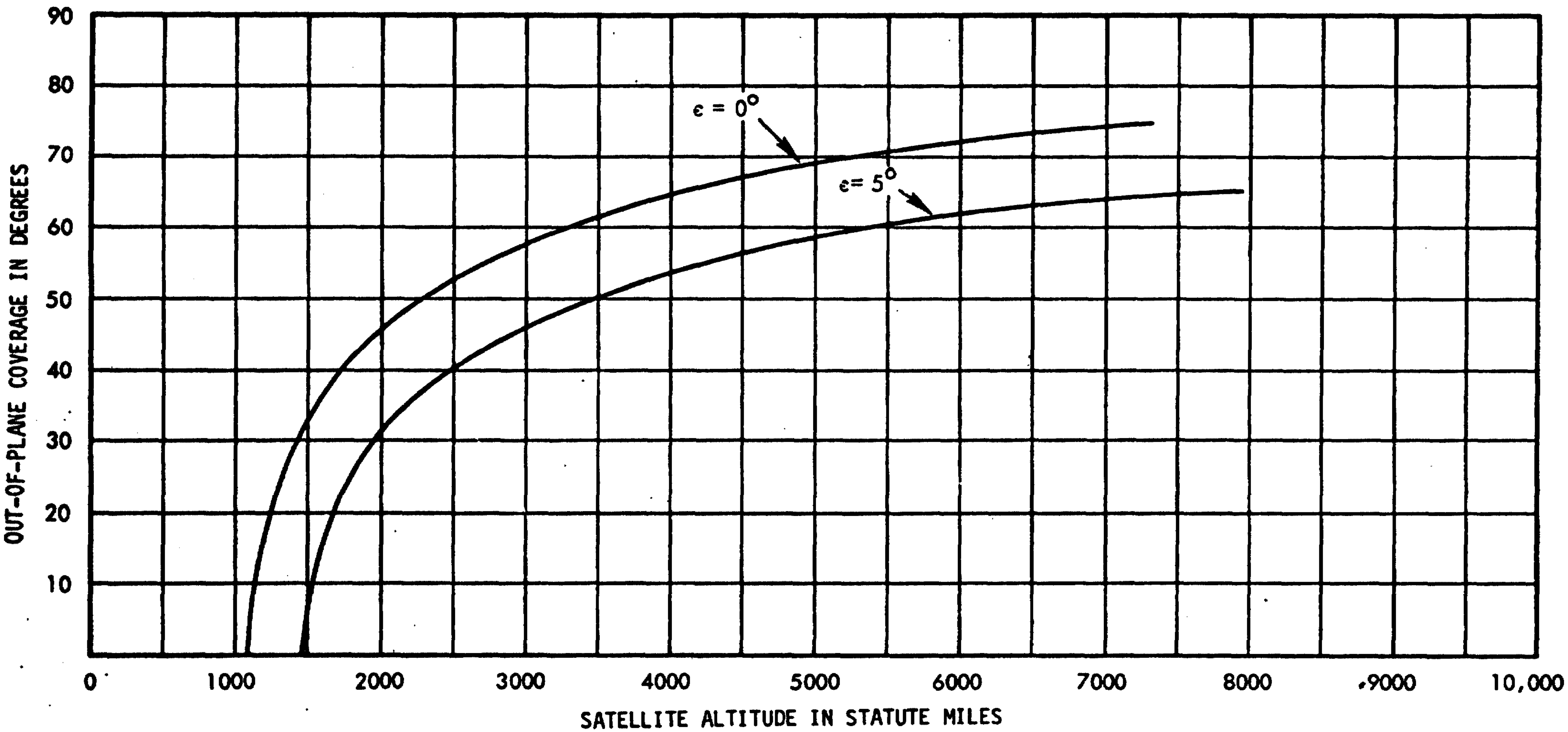

FIGURE 13. OUT-OF-PLANE COVERAGE FOR THREE SATELLITES EQUI-SPACED IN CIRCULAR LUNAR ORBIT

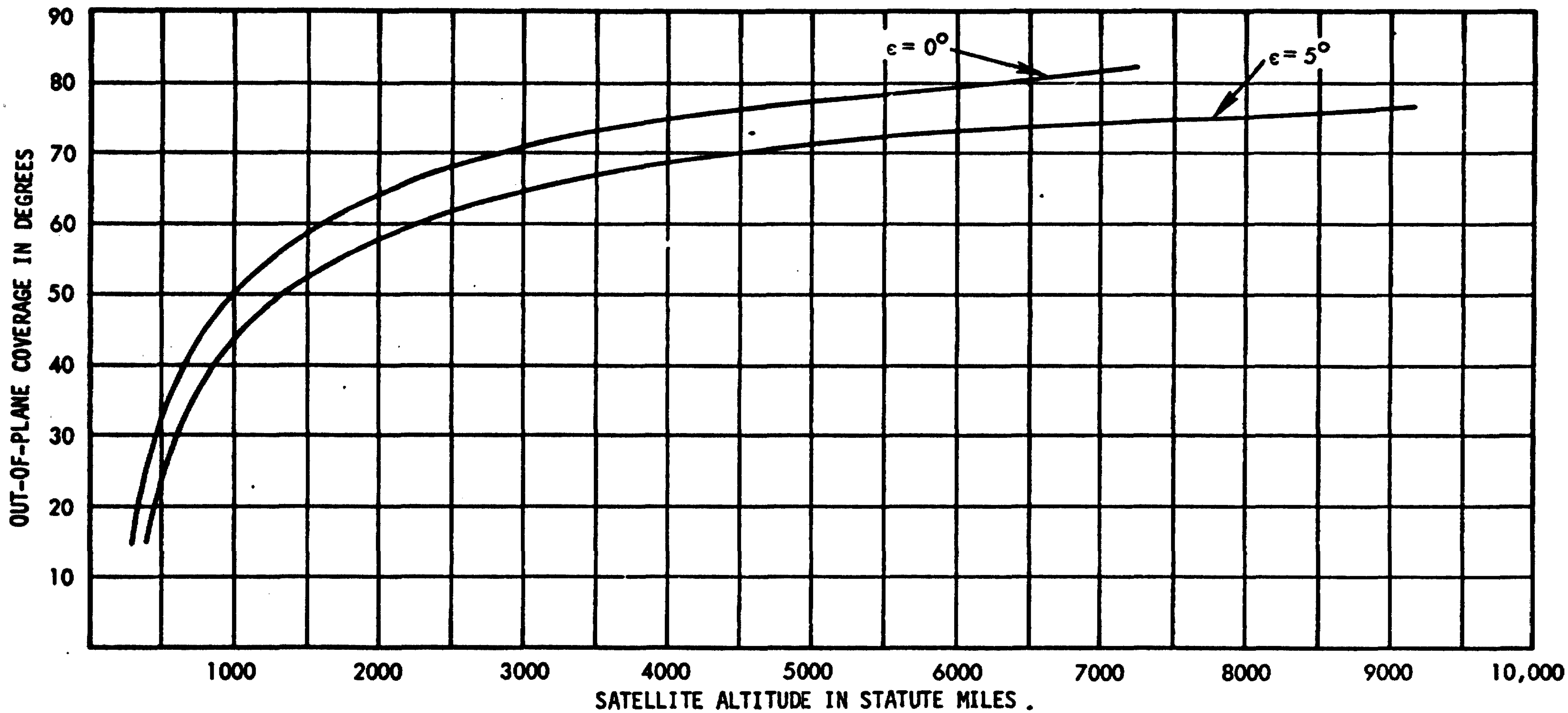

FIGURE 14. OUT-OF-PLANE COVERAGE FOR FIVE SATELLITES EQUI-SPACED IN CIRCULAR LUNAR ORBIT

4. AN EQUATORIAL SYSTEM OF COMMUNICATIONS SATELLITES

An equatorial system of satellites for lunar far side relay applications is limited by two factors:

(1) Each of the communications satellites is occulted by the moon during each orbital period.

(2) Coverage of extreme polar regions of the moon is impossible.

The first of these limitations may be overcome by providing a sufficient number of satellites properly phased in equatorial orbit. The second limitation is impossible to counter using only satellites in lunar equatorial orbit.

To further illustrate this first observation, consider the diagram of Figure 15. An equatorial system of five satellites is shown, and this system is arranged to provide uninterrupted service for a point on the lunar far side located in the plane of the orbit of the satellite network. This uninterrupted service is possible because of the complete overlap in coverage between adjacent satellites in the system.

For example, if the lunar far side surface terminal is located at point T, and the earth-moon orientation is as shown on the diagram of Figure 15, then satellite 1 will not be visible from earth. Satellite 5 will be passing out of view of the surface terminal while satellite 2 is just coming into view. Relay may thus be accomplished using 2 until 1 emerges from the occultation zone.

Note that uninterrupted service is possible only for points in the orbital plane. In order to provide this service to points out of plane, more than the indicated amount of overlap would be required. Note also that five satellites is the minimum number for uninterrupted service in the orbital plane since four or less cannot be arranged so as to provide complete overlap in plane.

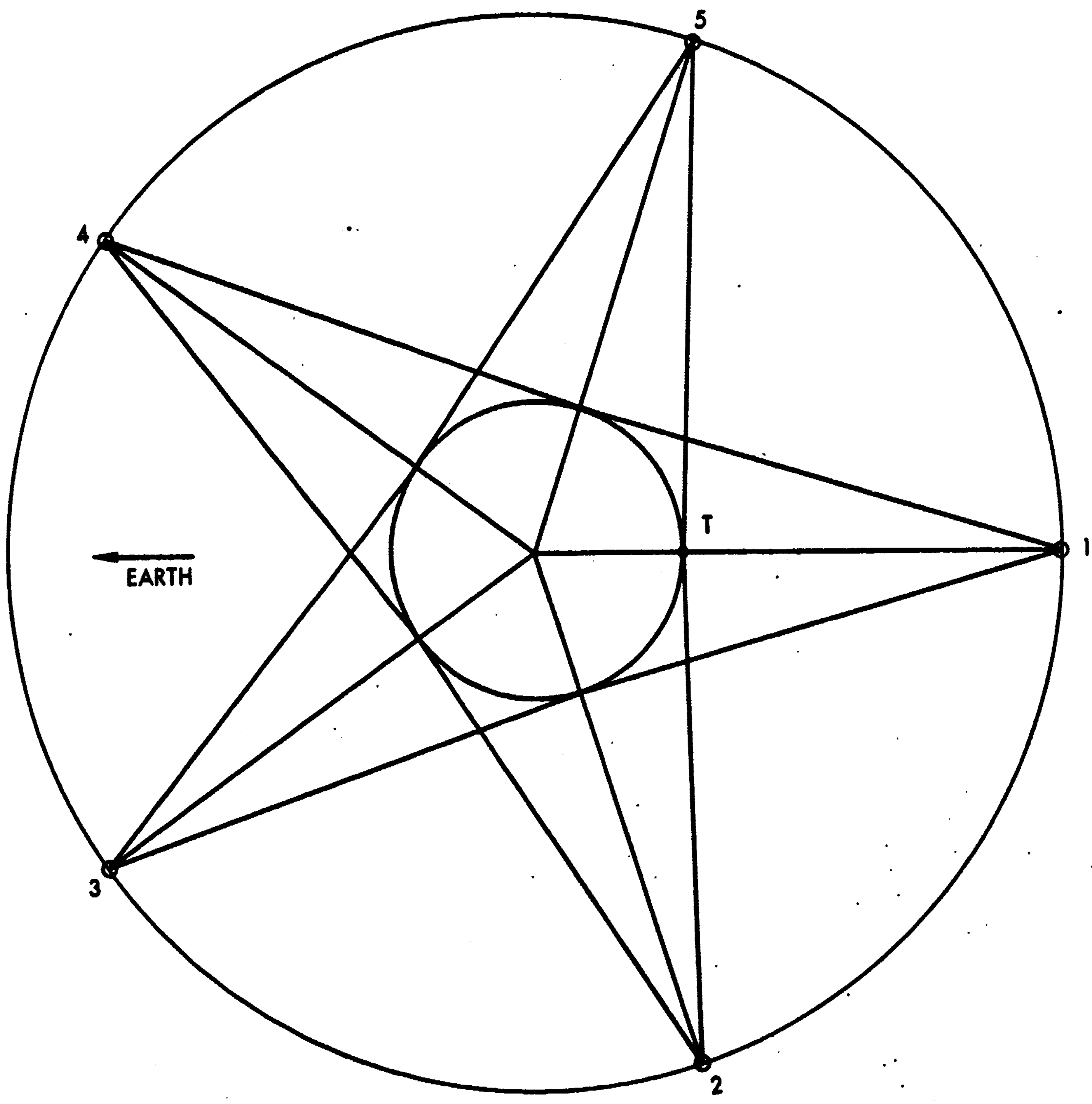

FIGURE 15. FIVE SATELLITE SYSTEM-EQUATORIAL ORBIT

5. A POLAR SYSTEM OF LUNAR COMMUNICATIONS SATELLITES

An equatorial system of lunar communications satellites cannot provide coverage for the lunar polar regions. This limitation may be directly overcome by utilizing systems of polar orbiting satellites. There are some special coverage requirements caused by the fact that the moon may occult the line-of-sight path between the active satellite and an earth station for certain fractions of lunar cycle. This occultation is illustrated graphically in Figure 16 , where for simplicity, two orthogonal polar orbits are shown for the communications satellites. In the neighborhood of positions A and C, satellites in polar planes 1-1' will be occulted by the moon, while in the neighborhood of positions B and D, satellites in orbital plane 2-2' will be occulted.

As in the case for an equatorial system of satellites, it is possible to overcome this occultation problem by using five or more equispaced satellites in each orbital plane. For orthogonal orbits, a minimum of ten satellites would be required for continuous coverage of the entire lunar sphere.

If three orbital planes are established, it would be possible to continuously cover the lunar surface with a total of nine satellites with three equispaced satellites in each plane. The angular separation between orbital planes is clearly a function of the width of the coverage sector for each set of coplanar communications satellites. If the selenocentric angle from the orbital plane to the limit of mutual visibility (i.e., the crossover point for adjacent coverage zones) is ξ_{max} (see Equation 12), then the required plane separation between the orbits is given by

$$\theta_{\substack{\text{plane} \\ \text{separation}}} = 2\left(\frac{\pi}{2} - \xi_{max}\right) . \qquad (13)$$

If the coverage sector is $\pm$ 75 degrees on either side of the orbital plane, then a plane separation of 30 degrees is necessary. Three satellites equally spaced in an orbit of approximately 7200 statute miles altitude (zero degrees grazing angle) will provide this coverage. If a grazing angle at

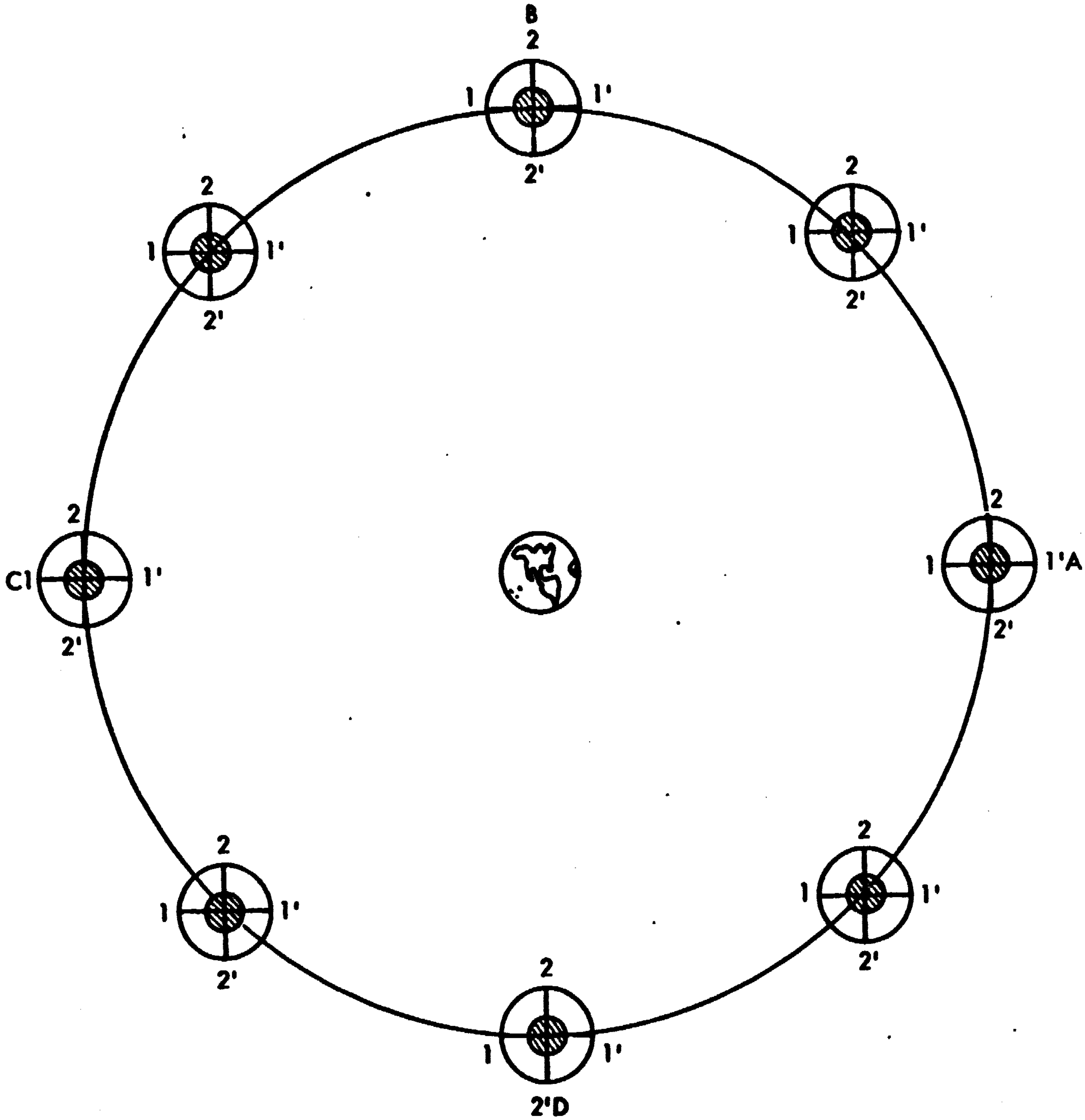

FIGURE 16. POLAR ORBIT ORIENTATIONS

acquisition of five degrees is required, the altitude for a three satellite configuration increases to approximately 23,600 statute miles. As previously noted, these very high orbits should be avoided if long orbital lifetimes are to be achieved. Equally spaced orbital planes would be separated by sixty degrees which corresponds to a coverage sector width of $\pm$ 60 degrees from the orbital plane of one set of three coplanar satellites. For an acquisition grazing angle of zero degrees, the required satellite altitude is approximately 3300 statute miles, increasing to approximately 6000 statute miles for a grazing angle of five degrees. Note that sixty degrees is the maximum orbital plane separation for a three orbit system.

As shown in Figure 16, it is possible to establish lunar polar orbits such that every point in the orbit is visible from any point on earth for large fractions of a lunar cycle. Consider the diagram of Figure 17 which further illustrates the geometry of the lunar communications relay problems. The line 1-1' is the edge of a lunar polar orbit. Note that in lunar position A, satellites in oribt 1-1' would be occulted when passing behind the moon. In lunar position B, all points in oribt 1-1 would just be visible from any point on earth. It is of interest to determine for what fraction of a lunar cycle a polar orbit would be completely visible. If α, β, θ are as labeled in Figure 17, and R_M is the radius of the moon, R_E is the radius of the earth, d_M is the distance from the earth to the moon, and h is the altitude of the satellite, then it is clear that

$$\alpha = \sin^{-1}\left\{\frac{R_M}{R_M + h}\right\} \tag{14}$$

$$\beta = \sin^{-1}\left\{\frac{R_E + R_M}{d_M}\right\}$$

The angle θ is then the sum $(\beta + \alpha)$ and is written as

$$\theta = \sin^{-1}\left\{\frac{R_M}{R_M + h}\right\} + \sin^{-1}\left\{\frac{R_E + R_M}{d_M}\right\} \tag{15}$$

The fraction of a lunar cycle during which all points in orbit 1-1' will not be visible from any point on the earth is

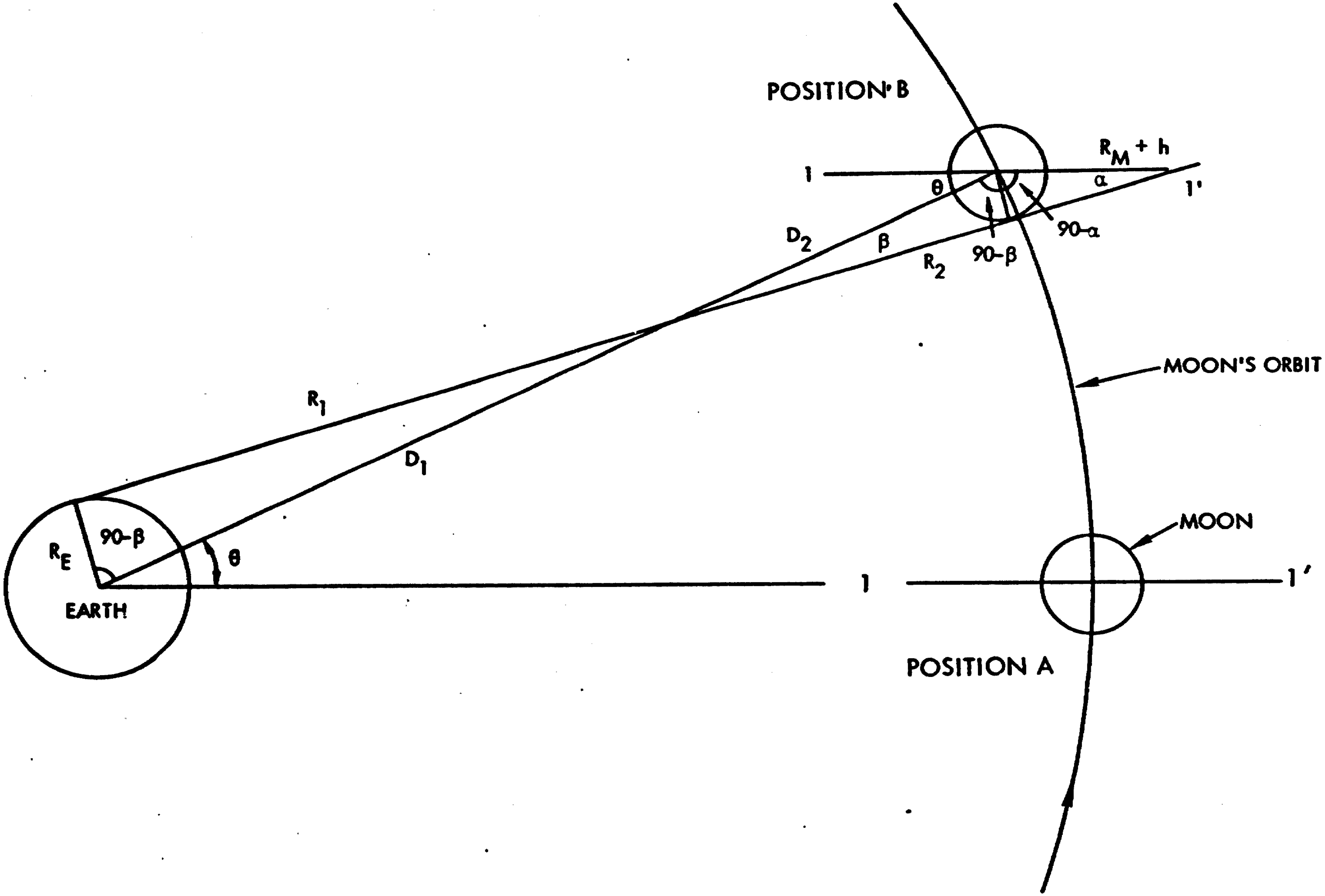

FIGURE 17. ORBIT ORIENTATION DURING OCCULTATION

$$VT = \frac{4\theta}{2\pi} \qquad (16)$$

Noting that the geometry of Figure 17 would be repeated when the moon passes to a point diametrically opposite the position illustrated.

Note also that this visibility factor is strongly dependent upon the altitude of the orbit. Figure 18 illustrates the visibility time as a function of satellite altitude.

6. POSSIBILITIES FOR PARTIAL COVERAGE

The preceding discussions on equatorial and polar orbiting systems of lunar communications satellites has emphasized continuous coverage of the complete lunar sphere. While this complete coverage would be a firm long term requirement for comprehensive lunar exploration, the current pace of Apollo missions would allow the establishment of systems for partial coverage.

From an economic point of view, it would be desirable to initially establish the minimum number of relay satellites which could support the projected Apollo G, H, and J type missions. The basic characteristics of these missions are summarized in Table 1 (pp 1-5 and 1-6).

The fundamental problem is thus to provide communications during the lunar orbit and surface stay phases of an Apollo mission. Other longer term relay requirements resulting from Apollo missions might include relay of scientific data from surface experiment packages left on the lunar surface.

The simplest situation one might consider is that of a single satellite which would be positioned to be mutually visible from earth and lunar stations during the mission. The absolute minimum coverage acceptable would be from the initiation of the lunar descent phase until insertion of the LM on the ascent trajectory. As indicated in Table 1 , this phase would be substantially in excess of 35 hours, the surface stay time for G - H type missions. For Apollo 11, the period between the undocking maneuver prior to LM descent and the docking after LM ascent was approximately 28 hours, of which lunar surface stay accounted for approximately 22 hours. This surface stay increases to about 78 hours for J type missions. Thus, if a lunar far side exploration mission were based on G - H type missions, the single communications

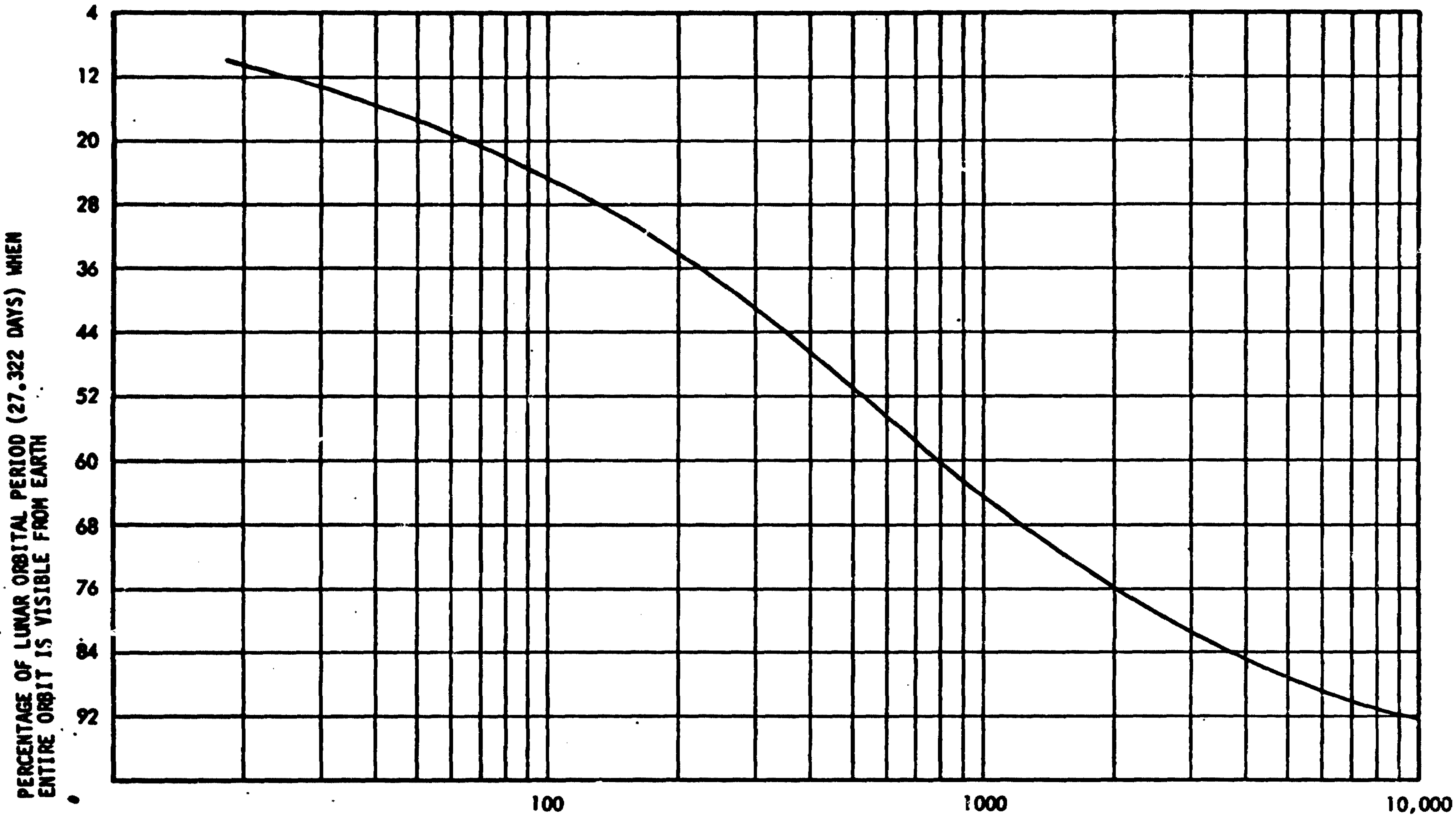

FIGURE 18. VISIBILITY FACTOR FOR LUNAR POLAR ORBIT

relay satellite must be mutually visible by earth LM and CSM for approximately 40 hours, this figure increasing to about 82 hours if J type mission were undertaken.

Consider the situation illustrated schematically in Figure 19 Simplifying assumptions are

(1) Lunar rotation is negligible during satellite passage from acquisition to loss of communications (i.e. from horizon to horizon).

(2) Surface terminal is in plane of orbit.

(3) Orbit is polar and positioned so as to be visible from earth during mission time.

It is clear from the diagram that the total time when relay communications will be possible will be given by

$$T = \frac{\theta_{ca}}{2\pi} T \tag{17}$$

where θ_{ca} is the control angle traversed by the relay satellite as it moves from horizon to horizon, and T is the orbital period of the satellite. Using the laws of sines, θ_{ca} may be found to be

$$\theta_{ca} = \pi - 2\epsilon - 2 \sin^{-1} \left\{ \frac{R_M}{R_M + h} \cos \epsilon \right\} \tag{18}$$

where h is the satellite altitude, R_M is the lunar radius, and ϵ is the elevation of the satellite above the lunar horizon at acquisition.

Figure 20 illustrates the graph of orbital period in hours versus satellite altitude and shows on the same plot the visibility time for a single satellite. Note that for satellite altitude less than 10,000 miles above the lunar surface, the satellite will be visible for less than 28 hours. This visibility time is insufficient to support on Apollo type far side lunar exploration missions.

It should also be noted that the influence of earth and sun were neglected in the determination of orbital period for the relay satellite. At the higher altitudes, these effects become important. It is probable

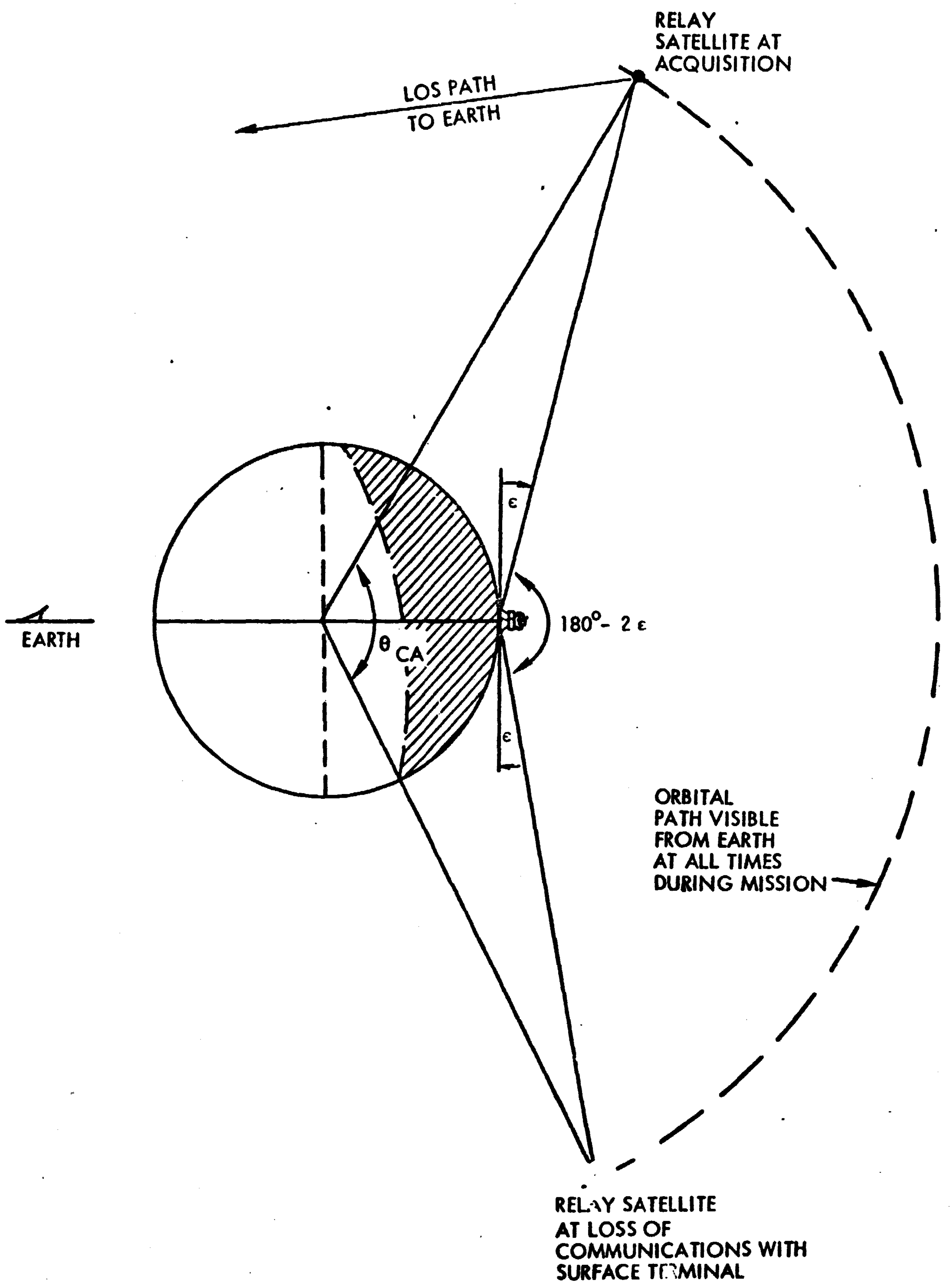

FIGURE 19. VISIBILITY GEOMETRY FOR SINGLE SATELLITE

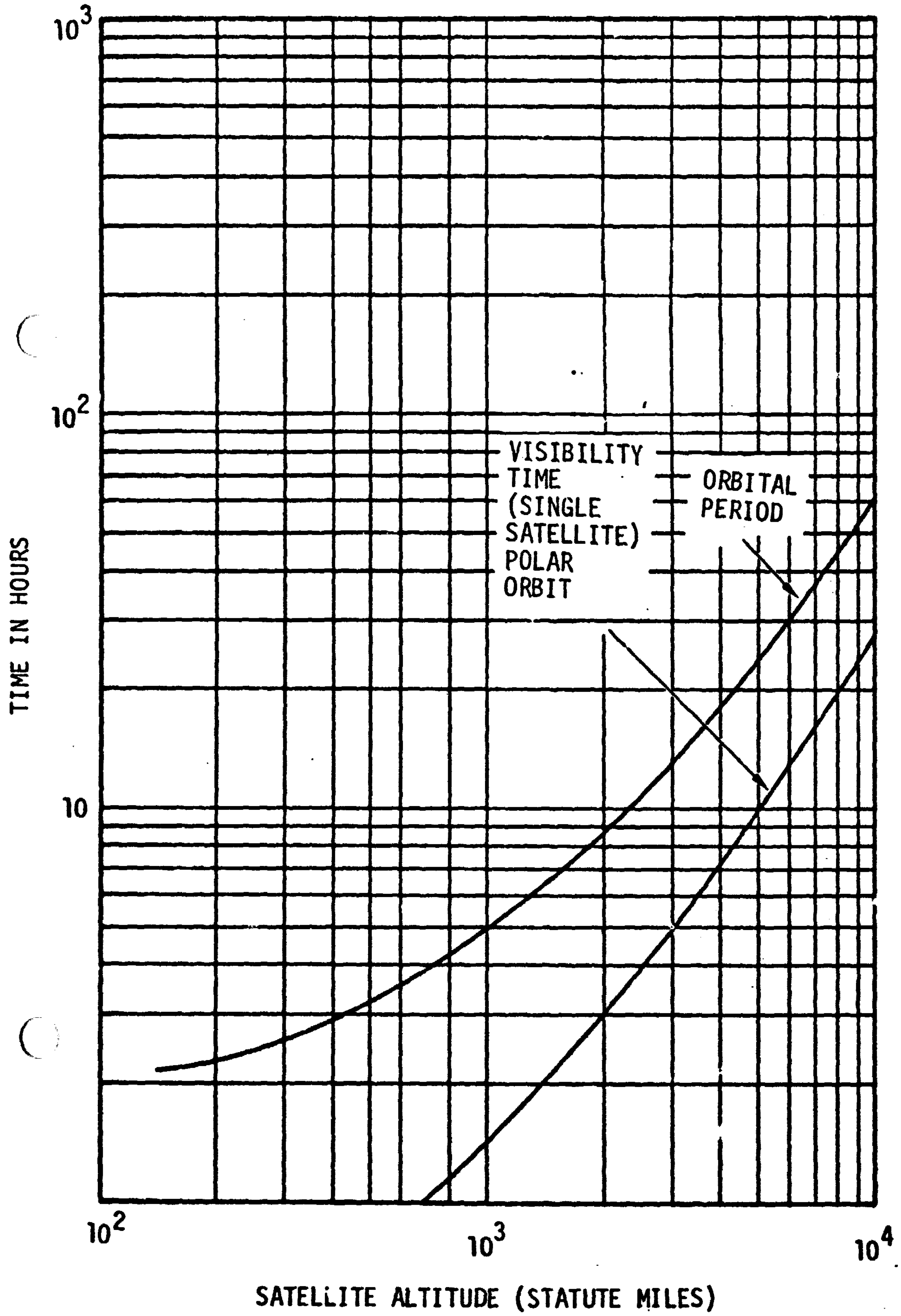

Figure 20. Visibility Time and Orbital Period for Single Satellite

that altitudes greater than 10,000 miles may not be usable.

7. A MINIMUM FULL COVERAGE COMMUNICATIONS SATELLITE NETWORK FOR A SPECIFIC APOLLO TYPE MISSION

The minimum communications network which could provide continuous coverage during an Apollo type mission is a system of three equispaced satellites in polar orbit. It is clear that the orbital plane of these satellites must be properly positioned relative to the earth-moon line. This positioning constraint is illustrated graphically in Figure 21. In this diagram the moon's orbital plane is in the plane of the paper. Three communications satellites are equally spaced in circular polar orbit, the edge of which is illustrated. Note that the invisible region is only on the lunar far side since the near side always will be completely visible from earth. If the landing site is located so that it falls within the visibility region, the orbital plane of the communications satellites would be adjusted with respect to the earth-moon line so that all points of the communications satellite orbit would be visible from earth for the maximum length of time from initiation of the landing phase of a lunar mission.

Note that if the selected landing site for the mission falls within the invisible region, the orbital plane would be positioned such that the landing zone at the time of landing would be just passing into view of the satellite as the moon rotates in the direction shown. If the landing site is within the visible region, there is no constraint imposed upon the orientation of the orbit other than the previously discussed visibility from earth.

This continuous coverage is, of course, specific mission oriented. Later missions would either have to be properly timed with respect to be original mission for which the satellite network was established, or the network could be repositioned. The advantages of establishing such a single three satellite system are:

(1) Basic coverage for Apollo missions is possible.
(2) It allows for a time phased establishment of a full coverage system.

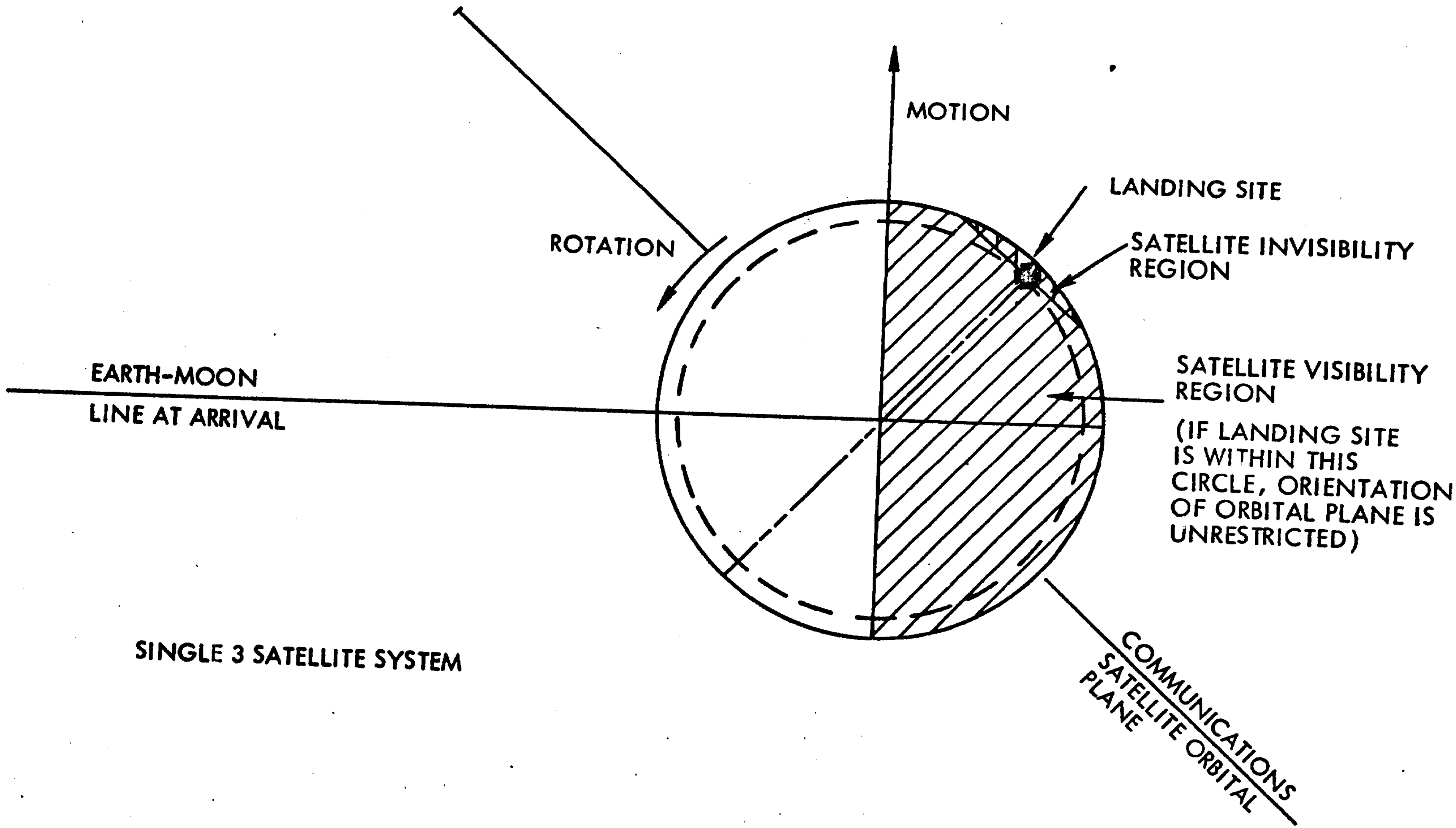

FIGURE 21. EFFECT OF LANDING SITE ON ORIENTATION OF SATELLITE ORBIT.

8. SUMMARY AND CONCLUSIONS

The coverage and visibility analysis summarized in this report is based on two basic ground rules:

(1) Continuous coverage of the full lunar sphere should be the long term goal for a lunar satellite communications system.

(2) The communications relay mode is assumed to be a two way earth-relay satellite-lunar terminal mode. No satellite-satellite relay capability is assumed.

For continuous coverage of the entire lunar sphere, the minimum network of relay satellites is composed of three sets of three polar orbiting satellites. The satellites are equally spaced in circular orbit, and the orbital plane separation between adjacent orbits ranges from thirty to sixty degrees. The sixty degree separation is most desirable in that satellite altitudes are considerably less than those required for the thirty degree separation. For a plane separation of sixty degrees (the maximum for a three orbit system), an orbit altitude of approximately 6000 statue miles will provide a lunar grazing angle of 5 degrees).

If only two orbital planes are established, ten satellites are required for full continuous coverage. Five satellites would be equally spaced in each of two orthogonal circular orbits. These orbits may both be polar, or one polar and one equatorial.

Full coverage is not possible from equatorial orbit. For continuous coverage of an equatorial sector, five satellites equally spaced in equatorial orbit are required.

The most attractive possibility for partial coverage is a network of three equally spaced satellites in circular polar orbit. It is shown that such an orbit may be positioned to provide continuous coverage for a specific mission whose landing site and mission time are known during substantial fractions of a lunar cycle. Such a network is a member of the minimum network of nine polar orbiting satellites required for continuous coverage of

the entire lunar sphere. Therefore, the full network may be established over a period of time, this time depending upon the evolution of operational requirements. It might develop that a single three satellite network would serve to support a wide variety of Apollo type missions if the missions were properly timed.

Single satellites (other than the libration point satellite) cannot provide continuous coverage for an Apollo mission. Two satellite networks increase coverage time for an Apollo type mission, but cannot provide complete coverage.

REFERENCES

3-1. Schmid, P. A. "Lunar Far Side Communications Satellites", NASA Technical Note D-4509, June 1968.

3-2. Godfrey, R. D., Coffman, J. W., Burr, P. T., "Lunar Backside Communications Study", Goddard Space Flight Center, Greenbelt, Maryland, X-830-69-509, November 1969.

IV. TRAJECTORY AND VEHICLE CONSIDERATIONS

1. INTRODUCTION

Additional considerations, other than communications, coverage and visibility analyses, are required to establish the feasibility of a lunar communications satellite system. These fall naturally into two major categories. The first includes all of the requirements necessary to establish the satellites of the system into their desired lunar orbits. Such considerations include the following:

(1) Launch vehicle and payload available with this vehicle,

(2) Velocity requirements for translunar injection and lunar orbit insertion,

(3) Launch opportunities satisfying all mission constraints and resulting in the desirable payload in lunar orbit,

(4) Tracking and midcourse guidance requirements for orbit determination and establishment of each satellite in the desired lunar orbit.

The first, or launch vehicle, consideration is probably the most important in establishing the satellite system that is finally implemented. This vehicle will most likely be "off the shelf" and two candidate vehicles will be discussed in the following subsection. The payload capability will determine whether it is feasible to launch several satellites into lunar orbit with a single launch vehicle. Also, the number of launch opportunities may be affected by the second stage restart capabilities. These considerations, and others concerned with launch and possible mission modes, are discussed briefly in Subsection 4.

In the second consideration, the velocity requirements are essentially vehicle independent. This information provides inputs for launch opportunities, translunar flight times, lunar orbit altitude, and vehicle sizing. This information is essential to a preliminary analysis and is provided in Subsection 2.

Considerations in (3) and (4) are important in implementing the chosen communications satellite system; however, they do not greatly impact on the preliminary design. The daily and monthly launch windows

will be very similar to the lunar orbiter missions. They will be greater, in fact, because no lighting constraint at the moon is imposed. Also, the considerable experience in lunar midcourse guidance and orbit determination should apply directly to this mission and not impact greatly on mission design.

The second major category is concerned with maintaining the lunar communications satellites within their proper orbits (within limits) over a long period of time. Since the earth and sun can cause sizable perturbations on the lunar orbits, the satellites can deviate from their nominal orbit to the point where the communications coverage requirements are no longer being met. Also affected will be the phase angle between consecutive satellites in the same orbit. Thus, orbit and phase control maneuvers will be required. An analysis of the perturbations and a technique for control are presented in Subsection 3.

2. VELOCITY AND PAYLOAD DATA

The purpose of this section is to provide performance and trajectory information which will be useful in the design of a lunar satellite communications system. Specifically, the problems considered are the following:

1. What are the payload capabilities of two vehicles, Atlas/Centaur and Titan IIIC, for launch into lunar orbit?
2. What are the velocity and flight time requirements to enter a high circular orbit about the moon?
3. What will the orientations of these orbits be at lunar orbit insertion (LOI)?

Considering the first question, the velocity requirements to inject out of a 100 nautical mile circular earth parking orbit will be primarily dependent on the translunar flight time and the distance of the moon from the earth at the time of LOI. This circular velocity excess (CVE) is plotted in Figure 22 for the range of translunar flight times expected to be considered. Specifically, for lower flight times than 60 hours, the CVE requirements increase considerably. The upper limit on flight time is set by the minimum energy requirements to get to the moon. For

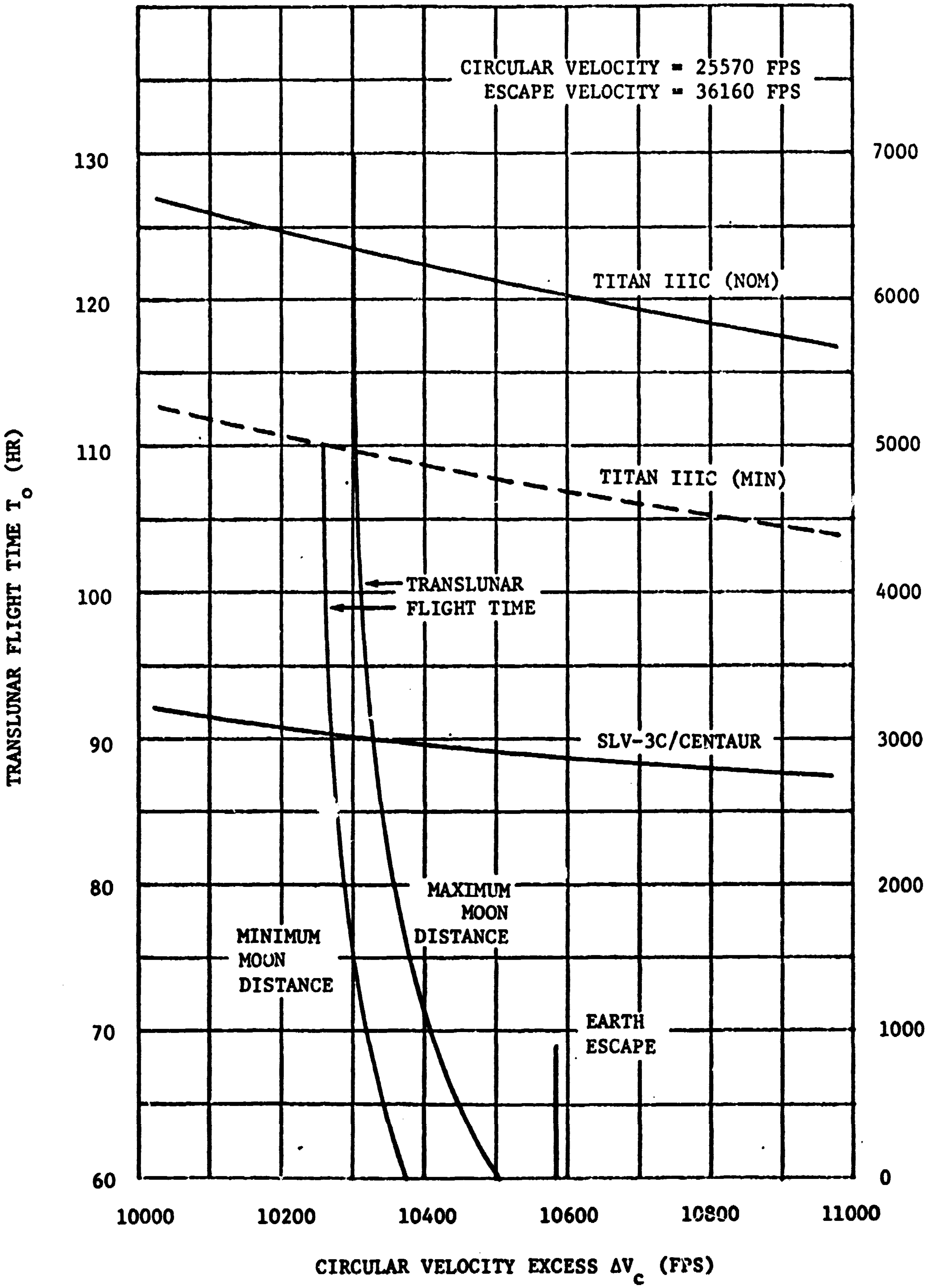

FIGURE 22. EARTH PARKING ORBIT (100 N.MI.) CIRCULAR VELOCITY EXCESS VERSUS TRANSLUNAR FLIGHT TIME AND PAYLOAD CAPABILITY

the moon at minimum distance (about 56.0 earth radii), this time is about 110 hours. For the moon at maximum distance (about 63.7 earth radii), this time is about 130 hours. For longer flight times, where the approach to the moon will be from the back side, the required velocities will increase. As stated above, the circular velocity excess requirements, assuming an inplane translunar injection (TLI), will be fairly independent of other parameters.

Also on Figure 22 are the payload capability curves for the Atlas/ Centaur SLV-3C, and for the Titan IIIC, as a function of the CVE requirements. Reference 4-1 gives two capability curves for the Titan IIIC, differing by about 1400 pounds, which represent the nominal and minimum expected payload. An updated curve is not expected to vary significantly from the nominal curve shown in Figure 22. For the CVE requirements of the mission being considered, which ranges from 10260 to 10500 feet per second, the Titan IIIC nominal payload capability ranges from 6400 to 6100 pounds. For the same CVE range, the Atlas/Centaur payload (Reference 4-2) ranges from 3000 to 2900 pounds, or about half of that of the Titan IIIC. In either case, the variation in payload will only be 200 or 300 pounds for any lunar mission that may be considered.

The velocity requirements to enter high altitude lunar orbits are shown in Figure 23. Three representative altitudes are shown: 2000, 6000, and 10,000 nautical miles. These curves are sufficiently close so that interpolation for other altitudes is easily accomplished. These requirements are primarily a function of the flight time from TLI to LOI, the inclination of the outbound (earth centered) trajectory to the moon's plane, and the moon's distance at the time of LOI.

The velocity requirements shown here may be associated with the TLI CVE requirements through the flight time values, which are shown as tick marks on the four scales at the bottom of Figure 23. The four scales correspond to the combinations of maximum and minimum moon distance with 0 and 60 degrees outbound inclinations to the moon's plane. Actually, when 0 and 60 degrees are written, it is implied that the outbound

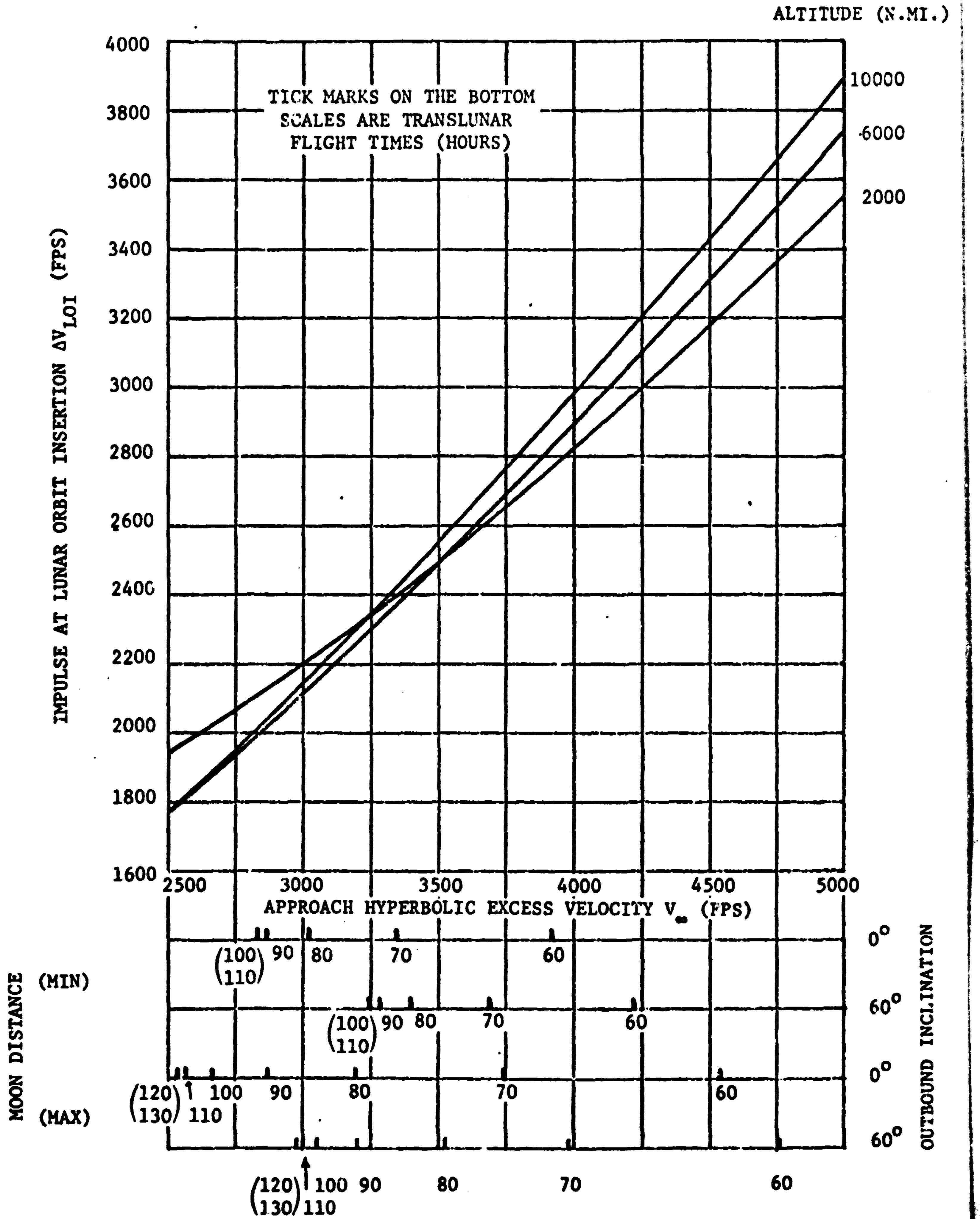

FIGURE 23. VELOCITY REQUIRED TO ENTER A CIRCULAR LUNAR ORBIT FOR VARIOUS TRANSLUNAR FLIGHT TIMES, OUTBOUND INCLINATIONS AND DISTANCES OF THE MOON

inclination is within a few degrees of these values. For example, if the translunar flight time is 70 hours for maximum moon distance, and the outbound inclination is zero, then the velocity required to enter a 6000 nautical mile orbit will be about 2700 feet per second. From Figure 22, the CVE is seen to be 10410 feet per second and the Titan IIIC payload 6200 pounds.

The LOI velocity requirement in Figure 23 is plotted against the moon centered approach hyperbolic excess velocity, since the latter is a measure of the total spacecraft energy. Thus, at a given orbit altitude (fixed potential energy), the kinetic energy (or velocity) will depend only on the total energy. Empirical data from computer runs were used to relate the hyperbolic excess velocity to the flight time, moon's distance, and outbound inclination.

It is interesting to note that these curves lie fairly close together and even cross each other. The greatest separation of about 300 feet per second exists for the extreme 60 hour flight time. For the longer flight times, the separation can decrease to 50 feet per second, indicating that payload in orbit will be relatively insensitive to orbit altitude. The velocity requirements for variations in other parameters, however, can vary considerably. For example, for a 6000 nautical mile orbit, the insertion velocity will vary from 1800 to 3340 feet per second for maximum moon distance and zero outbound inclination. Then, for this moon distance, the variation with outbound inclination can be 300 feet per second. It is clear from this that, if possible, the longer translunar flight times and zero outbound inclination should be used if maximum payload in orbit is to be achieved.

The conditions of flight time, outbound inclination, and moon's distance at LOI affect the orientation of the approach to the moon as well as energy. Effectively, these parameters cause the approach hyperbola to the moon to contain a vector which is close to the moon's orbit plane, and displaced 35 to 90 degrees west of the moon-to-earth line at the time of LOI. If the outbound inclination is zero, then this

vector will lie in the moon's orbit plane. If the outbound inclination is close to 60 degrees, then this vector may make an angle of as much as 10 degrees with the earth-moon plane. The moon's equator is inclined about 6.5 degrees to the the moon's orbit plane, indicating that the angle of this vector can be as great as 16.5 degrees to the moon's equator. Thus, if equatorial orbits are desired, either favorable launch days and conditions must be found to minimize this angle, or a plane-change penalty will be incurred at LOI.

For highly inclined or polar orbits, no plane change maneuver will be required at LOI. That is, it is always possible to insert into a polar orbit with an in-plane deboost. The nodal location of this orbit, however, will be constrained by the above mentioned vector which the oribt must contain. Neglecting the librations of the moon (which amount to about 7 degrees in longitude), the selenographic location of the nodal line for polar orbits is approximated in Figure 24. As with the approach energy (represented by V_∞), this longitude will vary with translunar flight time, outbound inclination, and the moon's distance at the time of LOI. For longer translunar flight times, which represent lower LOI velocities as shown in Figure 23, the nodal location will be between 70 and 90 degrees west longitude. Because of the longitudinal librations of the moon, the actual value may vary by ± 7 degrees from the value indicated in Figure 23. Finally, Figure 25 represents the period and velocity of a circular lunar orbit as a function of its altitude above the lunar surface.

3. SATELLITE STABILITY AND PHASE CONTROL

At this point of the analysis, it is assumed that the satellites have been placed in the desired lunar orbit and that they are properly phased with respect to each other. If the moon represented a central force field and no other gravitational bodies were nearby, the satellites would remain in their respective Keplerian orbits. The nonspherical effects of the moon and the third body effects of the earth and sun, however, cause the orbits and the phase angle between satellites to deviate from nominal. Thus, if it is desired to utilize the system for some length of time, say several years, it may be necessary to apply occasional trim maneuvers to adjust the orbit and cancel the perturbation effects.

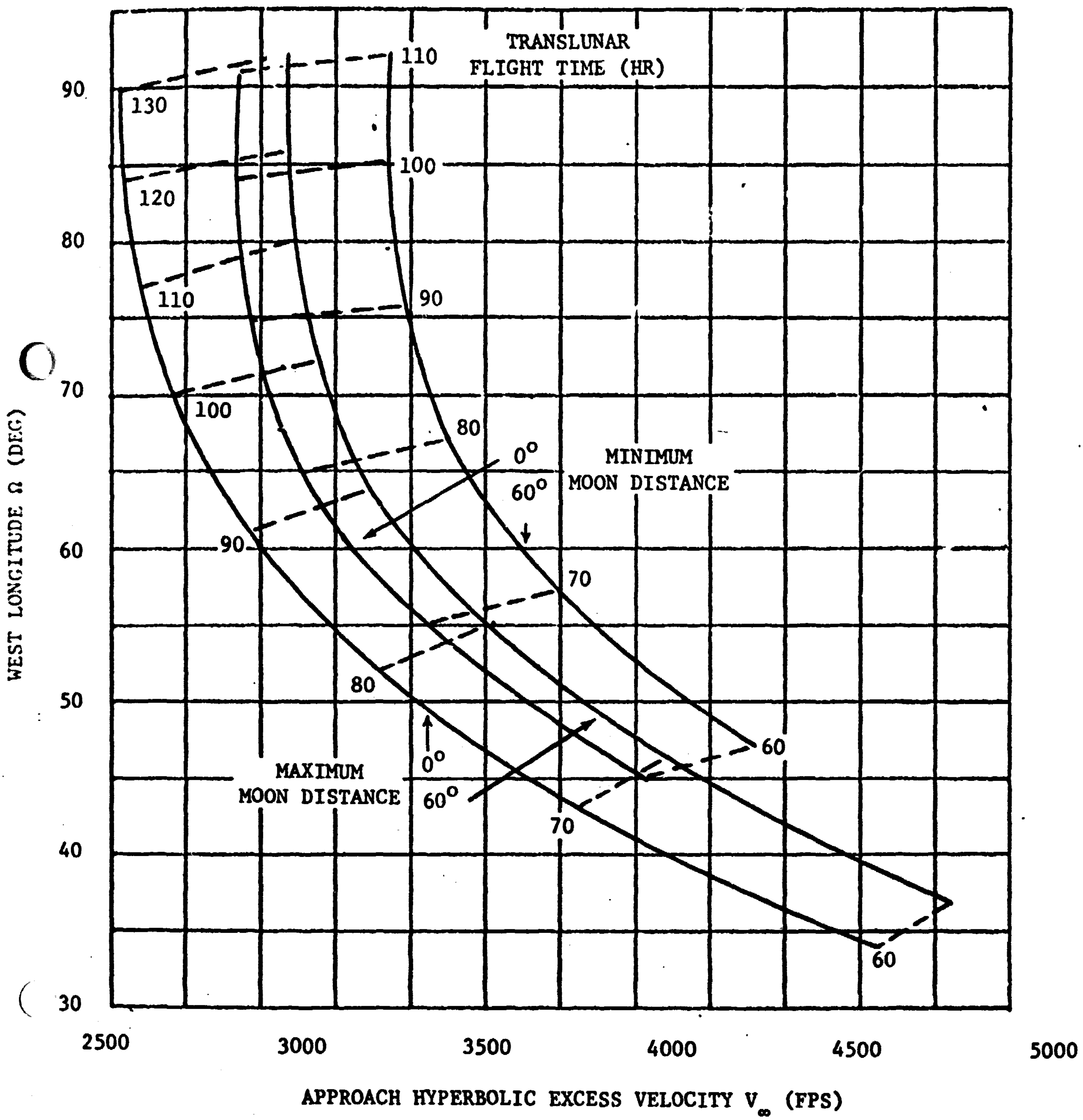

FIGURE 24. WEST EARTH-MOON PLANE LONGITUDE OF THE NODE FOR POLAR ORBITS

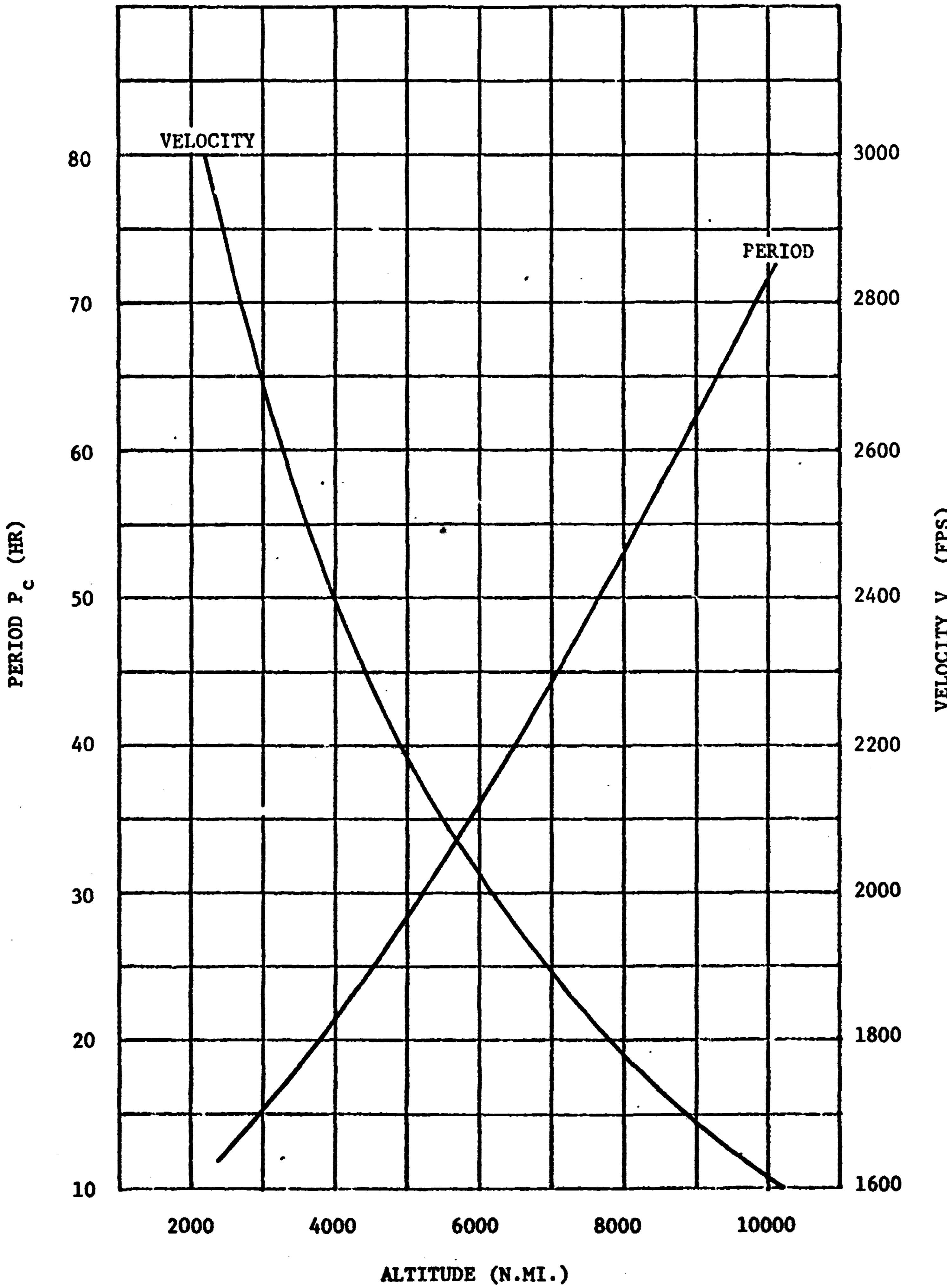

FIGURE 25. PERIOD AND VELOCITY OF CIRCULAR ORBITS ABOUT THE MOON FOR VARIOUS ALTITUDES

The frequency and amcunt of orbital adjustment, which will affect the propulsion system size, depend primarily on the following factors:

(1) The desired lifetime of the satellite system,

(2) The actual deviations of the orbital elements and satellite phase angles from the nominal values as a function of time.

(3) The acceptable deviations of the orbital elements and satellite phase angles from the nominal values.

The actual deviations of the orbital elements and phase angles from nominal will depend primarily on the altitude and inclination of the (near circular) nominal orbit. These effects, as a function of time are presented in the following subsection. If these deviations are acceptable for the desired lifetime of the satellite system, then no adjustment maneuvers will be required. If the deviations are not acceptable (such as, for example, the phase angle increasing to where desired overlap is not provided), then orbital adjustments will have to be made. A technique for such trim maneuvers is presented in Subsection 3.2.

3.1 Satellite Stability

As indicated above, the perturbations acting on the lunar orbit will be the nonspherical effects of the moon and the third body effects of the earth and sun. However, since the orbits considered are relatively high (above 2000 nautical miles), the triaxiality of the moon will have a negligible effect on the lunar orbit. The moon, incidentally, is more spherical than the earth. This is particularly true for the equatorial and polar circular lunar orbits being considered here. Thus, only the third body effects of the earth and sun on the orbits need be considered.

General perturbation theory provides analytic methods for predicting third body effects on a near circular orbit over long periods of time. Greater precision could be obtained with numerical integration; however, the computer time required becomes prohibitive. For this analysis, use was made of an existing satellite lifetime program based on general perturbation equations (see Reference 4-3) which considered only the first order effects on the orbital elements of the motion. Although this program was orginally written for the computation of lifetimes of earth satellites, modifications had been made so that it could apply to lunar orbits as well.

Briefly, the expressions utilized represent the first order variation of the six orbital elements over a single satellite revolution. This variation is computed separately for the effects of the earth and the sun. Thus, correlation effects per orbit are not considered. The variations are then added to the orbital element values to update the perturbed elements for this revolution. The process is repeated for each succeeding revolution.

The formulations presented assume that the third body (sun or earth) remains in a stationary position during the satellite revolution. For the computation, the average position is chosen, which is an approximation and represents a source of error. For example, referring to Figure 25, the period of a 6000 nautical mile altitude satellite is 36 hours. Within this time, the sun will move about 1.5 degrees and the earth about 20 degrees. Thus, the sun will remain essentially stationary during a revolution of the satellite. The earth's position, however, will vary by 10 degrees from the position chosen for the computation. Since, however, this analysis is concerned with long term effects, it is the sun which will make the primary contribution. The earth will cause oscillations in the orbital elements with approximately a 14 day period and, if these oscillations remain within the acceptable deviations for the planned satellite system, then the trim maneuvers need not be directly dependent on the earth's effect.

For this analysis, eight lunar orbits have been chosen for stability computation. Three are near equatorial orbits (5 degrees) and five are near polar (85 degrees). For the equatorial orbits, altitudes of 4000, 6000, and 10,000 nautical miles have been chosen. The polar orbit altitudes range from 2000 to 10,000 nautical miles in 2000 nautical mile steps. The starting eccentricity for these orbits is .001. One reason for choosing this value is that the first order variations of some of the orbital elements are zero for perfectly circular orbits. Thus, the second order effects, which are being ignored here, would become important in causing the <u>initial</u> variations in the elements. Also, it is expected that an eccentricity of .001 will be quite acceptable for an operating system. It represents a deviation of about .001 x R where R is the radius of the satellite orbit. For the extreme case, where the altitude is 10,000 nautical miles, the deviation will be about 10 nautical miles.

The variation of the elements of the eight orbits mentioned above has been computed for a period of 2 years. The variation of eccentricity as a function of time is plotted in Figure 26, where the oscillations due to the earth's effect is not shown. This figure indicates that the near equatorial orbits are quite stable for the period of time considered. In fact, for the cases chosen, the eccentricity decreases with time, implying that the perturbations have a circularizing effect. It is expected, however, that over longer periods of time, the eccentricity will increase. In any case, it is clear that very stable equatorial and near equatorial orbits exist, up to 10,000 nautical miles, which may be used for lunar satellite systems.

The near polar orbits, however, do not behave as well. As shown in Figure 26, the eccentricity increases exponentially with time, which will be an important relation in developing the trimming technique discussed in the next subsection. For an eccentricity of 0.1, for example, the "lifetimes" of the orbits shown are 2.1, 1.0, 0.6, 0.4, and 0.3 years for altitudes ranging from 2000 to 10,000 nautical miles. Here, only the 2000 nautical mile orbit has a lifetime of 2 years, and only if an eccentricity of 0.1 is acceptable. This figure indicates that equatorial orbits will require very little, if any, trim maneuvers to correct eccentricity, whereas polar orbits will require continual eccentricity correction if a lifetime (based on acceptable eccentricity) of several years is required.

Data for the variation in the orientation elements are not presented here since their variations are small and their consideration in the mission design is secondary. For example, assuming orbit times of Figure 26, for which $e \leq 0.1$, the variation in inclination for polar orbits is always less than 10 degrees. The inertial node, however, (again for polar orbits) can vary up to 20 degrees for the 8000 nautical mile altitude orbit and up to 30 degrees for the 10,000 nautical mile altitude orbit. If, for a particular satellite system being considered, a stationary (inertial) longitude is important, then sizable plane change maneuvers may be required to maintain this longitude. The requirement may be considerable for low orbits as well since, although the plane change may be small, the orbital velocity is higher. It is assumed in this analysis, however, that if a lunar communications satellite system consists of satellites in two polar planes normal to each other, then visibility overlap is sufficiently large that no nodal or inclination adjustments will be required for the lifetime of the system.

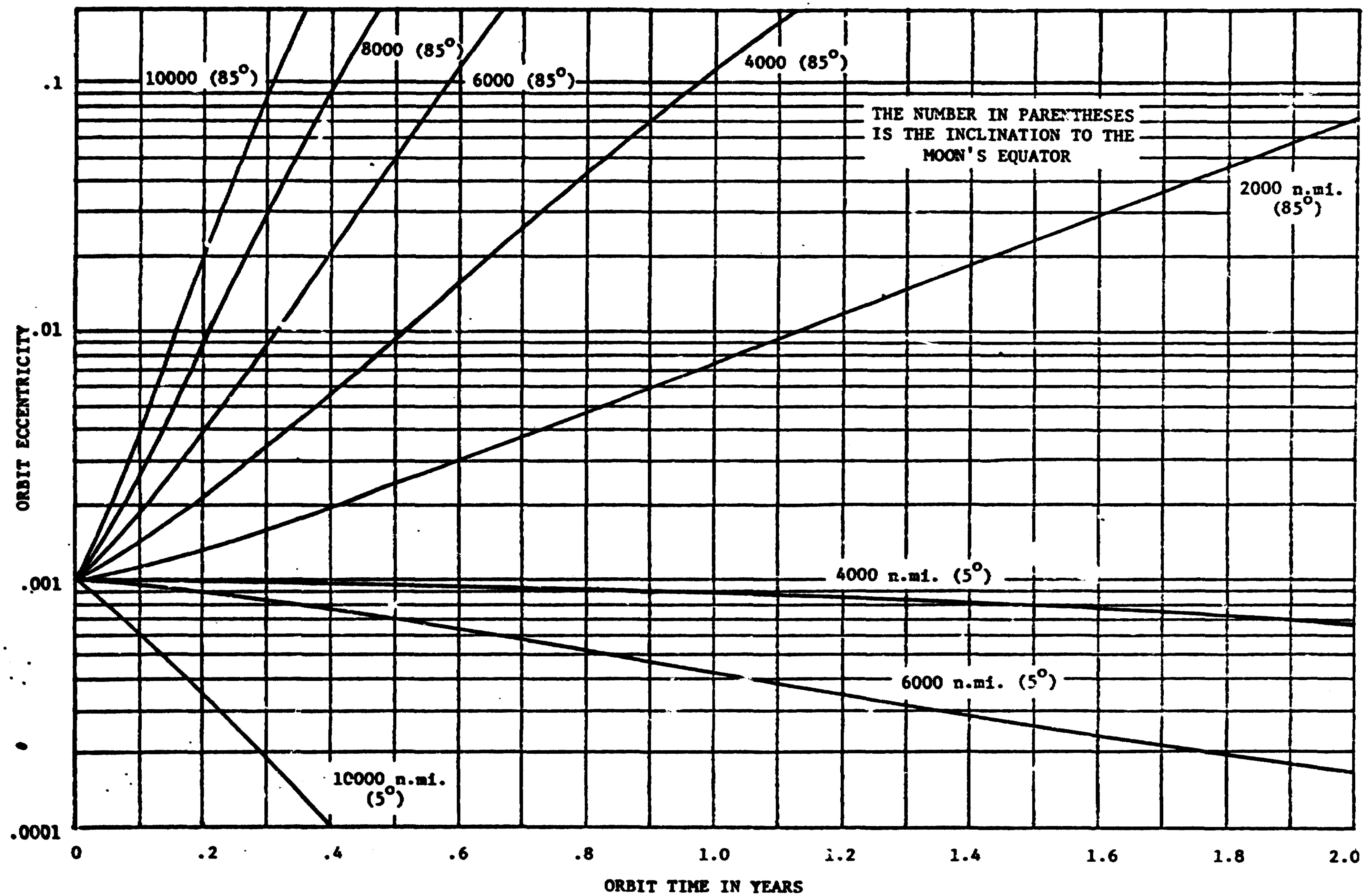

FIGURE 26. ECCENTRICITY VARIATIONS FOR VARIOUS SATELLITE ALTITUDES

3.2 Phase Angle Variation and Control

It is assumed in this analysis that the nominal configuration of a set of communications satellites is such that they are equally spaced and in the same circular orbit. It is also assumed that if there is a similar set in a different orbital plane, then there are no phasing requirements between these two sets. Thus, it is only necessary to analyze the phase relation of the satellites within the same plane.

With respect to the phase angle between satellites which are planned to be equally spaced in the same circular orbit, there are three effects which can cause this angle to be off nominal. These are:

(1) Inaccuracies of the lunar orbit insertion maneuver.

(2) First order effects on phasing due to increasing eccentricity of the orbit which is caused by earth and sun perturbations.

(3) Higher order effects of the earth and sun perturbations on the satellite motion.

Some inaccuracy in lunar orbit insertion cannot be avoided. Thus, a series of trim maneuvers will be required. This trimming falls naturally into two categories. The first is a positioning phase and the second is a circularizing phase. Considerable tracking may be required before and during these trim phases in order to accurately determine the orbit and, hence, the maneuver required. For the positioning phase, where for example, two satellites are too near each other at LOI, it is necessary to change the relative periods. Thus, if one satellite has nearly the correct (nominal) period and an adjacent satellite is too close behind it, then it is necessary to increase the period of the second satellite so that it may lag behind the first. This may be done by increasing the semi-major axis which is most efficiently accomplished with a tangential maneuver. Then, when the phase angle is correct, another tangential retro-maneuver is performed to decrease the period of the second satellite to that of the first. A similar sequence of maneuvers can be performed for all the satellites in the same orbit plane.

The second, or circularizing, trim phase consists of a maneuver, or set of maneuvers, which affect the eccentricity of the orbit but not the period. These maneuvers, if small, are applied normal to the velocity direction at the point of application. Thus, the energy and, hence, the period of the satellite orbit will not be altered. There will be two

positions on the orbit where the circularizing maneuver must be made. These will be at the points where the radial distance will be equal to the semi-major axis of the orbit.

Once the satellites are positioned and the orbit circularized, which may take many days, the phasing and the orbital elements will be affected by the moon, earth, and sun perturbations, as discussed in the previous section. The most important element in the consideration of satellite phasing will be eccentricity. In particular, since the angular rate of the satellites will not be constant for eccentric orbits, the phase angle between adjacent satellites will increase to a maximum and decrease to a minimum during each orbital revolution. The higher the eccentricity, the larger will be this variation. Thus, there may be a particular value of eccentricity above which the operational requirement of continuous coverage is violated. It is obvious that this boundary value of eccentricity will depend on the overlap coverage of two consecutive satellites. For a system of three satellites per orbit plane, the overlap may be minimal and, hence, the tolerable eccentricity will be low. For a system of six satellites, the overlap will be greater so that a higher eccentricity is acceptable. It is assumed here that the system has not been designed at the limit; i.e., where acceptable coverage is obtained only for a system whose satellites must be exactly phased and in a precise circular orbit.

The analysis of the effect of eccentricity on phasing begins with a relation between the time in the orbit and the angle from perifocus. In Figure 27, this angle is shown as η. The time in the orbit can be represented by the mean anomaly, M, which is given by

$$M = \frac{2\pi T}{P}$$

where P is the period of the orbit and T is the time on the orbit. Thus, for a single revolution, the time T = P and M = 2π.

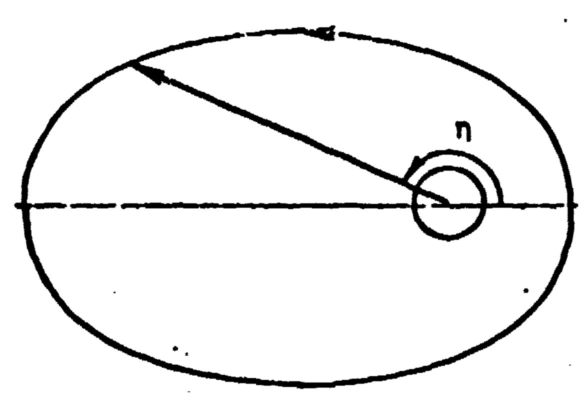

FIGURE 27. IN-PLANE ANGLE DEFINITION

For several satellites on the same orbit, it is assumed that they are equally spaced in time. That is, if there are N satellites, then the time for any one of them to reach the position of the succeeding one will be,

$$t = \frac{P}{N} \tag{1}$$

or,

$$m = \frac{2\pi}{N} \tag{2}$$

In terms of the mean anomaly, the angle from perifocus is given by (see Reference 44),

$$\eta = M + 2e \sin M + \frac{5}{4} e^2 \sin 2 M + \frac{13}{12} e^3 \sin 3M + \ldots \tag{3}$$

Then the phase angle between two consecutive satellites will be

$$\Delta\eta = (M_2 - M_1) + 2e(\sin M_2 - \sin M_1) + \frac{5}{4}e^2 (\sin 2M_2 - \sin 2M_1) + \frac{13}{12}e^3 (\sin 3M_2 - \sin 3M_1) + \ldots \tag{4}$$

where M_1 is the mean anomaly of one satellite and $M_2 = M_1 + m$ is the mean anomaly of the second.

Now, if it is desired to find extremums of $\Delta\eta$, then equation (4) can be differentiated with respect to M_1 and this derivative set equal to zero, or

$$\frac{d\Delta\eta}{dM_1} = 0 = 2e(\cos M_2 - \cos M_1) + \frac{5}{2} e^2(\cos 2M_2 - \cos 2M_1) + \frac{13}{4} e^3(\cos 3M_2 - \cos 3M_1) + \ldots \tag{5}$$

Two extremums exist and these are when

$$\left.\begin{array}{ll} (1) & M_1 = -\frac{m}{2} \text{ and } M_2 = \frac{m}{2} \\ (2) & M_1 = \pi - \frac{m}{2} \text{ and } M_2 = \pi + \frac{m}{2} \end{array}\right\} \tag{6}$$

This is seen by noting that each term in parenthesis of equation (5) is of the form

$$\cos(\frac{km}{2}) - \cos(-\frac{km}{2}) = 0$$

and

$$\cos(k\pi + \frac{km}{2}) - \cos(k\pi - \frac{km}{2}) = 0$$

In addition, sample calculations will show that extremum (1) above is a maximum and extremum (2) is a minimum.

Then, substituting extremum (1) into equation (4) gives

$$\Delta\eta_{max} = m + 4e \sin(\frac{m}{2}) + \frac{5}{2} e^2 \sin m + \frac{13}{6} e^3 \sin \frac{3m}{2} + \quad \ldots \quad (7)$$

Similarly, substituting extremum (2) into equation (4) gives,

$$\Delta\eta_{min} = m - 4e \sin(\frac{m}{2}) + \frac{5}{2} e^2 \sin m - \frac{13}{6} e^3 \sin \frac{3m}{2} + \quad \ldots \quad (8)$$

where

$$\sin[k(\pi + \frac{m}{2})] - \sin[k(\pi - \frac{m}{2})] = (-1)^k \sin \frac{km}{2}$$

and k is an integer.

In this analysis, the range of eccentricities of interest are assumed to be $0 \leq e \leq 0.1$, so that the above four terms in equations (7) and (8) should yield sufficient accuracy. These expressions for the

phase angle extremums have been evaluated for a set of 2 to 6 satellites and are given below. In addition, the extreme deviations of the phase angle relative to the nominal value of phase angle is shown in Figure 28. This figure may be used with the coverage analysis of Part III and the lifetime analysis of the previous section to determine the times that trim maneuvers to correct for eccentricity must be made. Evaluating equations (7) and (8) for a specific number of satellites gives, in radians,

$$\left.\begin{aligned}\Delta\eta_{max} &= \pi + 4e - 2.167e^3 \\ \Delta\eta_{min} &= \pi - 4e + 2.167e^3\end{aligned}\right\} \text{ for } N = 2$$

$$\left.\begin{aligned}\Delta\eta_{max} &= \frac{2\pi}{3} + 3.464e + 2.165e^2 \\ \Delta\eta_{min} &= \frac{2\pi}{3} - 3.464e + 2.165e^2\end{aligned}\right\} \text{ for } N = 3$$

$$\left.\begin{aligned}\Delta\eta_{max} &= \frac{\pi}{2} + 2.828e + 2.5e^2 + 1.532e^3 \\ \Delta\eta_{min} &= \frac{\pi}{2} - 2.828e + 2.5e^2 - 1.532e^3\end{aligned}\right\} \text{ for } N = 4$$

$$\left.\begin{aligned}\Delta\eta_{max} &= \frac{2\pi}{5} + 2.351e + 2.378e^2 + 2.061e^3 \\ \Delta\eta_{min} &= \frac{2\pi}{5} - 2.351e + 2.378e^2 - 2.061e^3\end{aligned}\right\} \text{ for } N = 5$$

$$\left.\begin{aligned}\Delta\eta_{max} &= \frac{\pi}{3} + 2e + 2.165e^2 + 2.167e^3 \\ \Delta\eta_{min} &= \frac{\pi}{3} - 2e + 2.165e^2 - 2.167e^3\end{aligned}\right\} \text{ for } N = 6$$

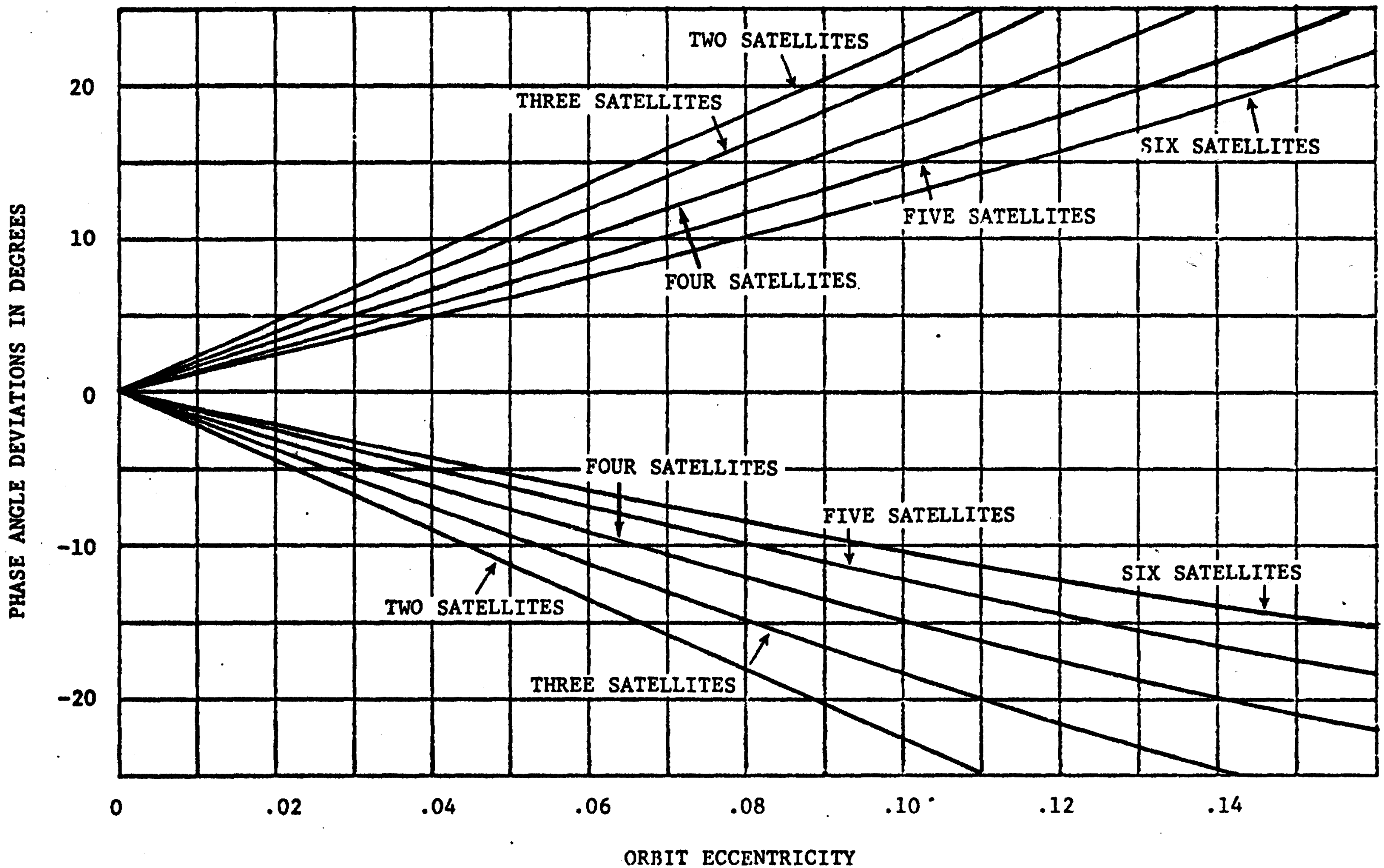

FIGURE 28. PHASE ANGLE DEVIATIONS FOR SELECTED SATELLITE SYSTEMS

It is interesting to notice in Figure 28 that the system with a greater number of satellites can accept a greater variation in eccentricity than a system with a lower number, for a given phase angle deviation. Thus, if the deviation limit is 10 degrees, then the upper limit of eccentricity for a six satellite system is .08, whereas the upper limit for a two satellite system is only .044. To obtain these values, the maximum deviation (upper) curves of Figure 28 were used here, since these represent greater deviations from the nominal value at a given eccentricity. Also, the upper curves represent an increase in phase angle which will result in a decrease in the coverage overlap.

Using this same example and referring to the eccentricity variation curve of Figure 26, it is seen that for a polar satellite system of 6000 nautical mile altitude, an eccentricity of .08 is reached after about 0.56 years, or 200 days. This is for the six satellite system whose phase angle deviation limit is 10 degrees. Thus, after 200 days, the circularizing trim maneuvers discussed above would have to be applied to each of the six satellites.

With the data generated thus far, it is also possible to estimate the velocity requirement for the circularizing trim maneuver. Figure 25 gives the circular velocity of a lunar satellite as a function of altitude. This also happens to be the velocity on the ellipse (perturbed orbit) where the trim maneuver must be made. This circularizing maneuver must be made such that the velocity magnitude does not change and its direction is perpendicular to the position vector. The true anomaly of the trim maneuver can be found by solving the conic equation,

$$r = \frac{a(1 - e^2)}{1 + e \cos \eta} \tag{9}$$

for η when $r = a$. This gives

$$\cos \eta = - e, \sin \eta = \sqrt{1 - e^2} \tag{10}$$

This value of true anomaly may be substituted into the general expression for the flight-path angle, γ, which is

$$\tan \gamma = \frac{e \sin \eta}{1 + e \cos \eta} \tag{11}$$

Substituting equation (10) into this gives,

$$\tan \gamma = \frac{e\sqrt{1 - e^2}}{1 - e^2} = \frac{e}{\sqrt{1 - e^2}}$$

This implies, however, that

$$\sin \gamma = e$$

or, for low values of e,

$$\gamma \cong e \text{ (radians)} \tag{12}$$

Thus, if $e \leq 0.1$ then $\gamma \leq 5.73$ degrees. The velocity requirement is then obtained from the equation

$$\Delta V = 2V_c \sin \frac{\gamma}{2}$$

where V_c is the circular velocity shown in Figure 25. For small angles, this can be approximated by,

$$\Delta V = \gamma V_c$$

or, using equation (12),

$$\Delta V = e V_c \tag{13}$$

Considering the example above, where the satellite altitude is 6000 nautical miles and eccentricity is .08, Figure 25 gives a circular velocity of V_c = 2300 feet per second. Then, using equation (13), ΔV = 184 feet per second. This maneuver could be applied after 200 days of operation, when e reaches .08, to circularize the orbit, allowing it to operate within the deviation limit of 10 degrees for another 200 days. This maneuver would have to be applied to each of the six coplanar satellites in the system.

Thus far, only the most direct method has been considered for performing the circularizing trim maneuver. That is, the maneuver is made only when the satellite system is about to violate an operational constraint. The question arises: Is it possible to perform this maneuver more often (prior to any violation) and obtain a savings in propellant over the lifetime of the system? The answer is definitely yes. The reason is that the perturbing forces have a greater effect on an orbit of greater eccentricity over the same period of time, whereas the ΔV requirement, as shown by equation (13) increases linearly with eccentricity.

For example, in Figure 26, for the 6000 nautical mile polar orbit, the eccentricity increases from .001 to .007 in about 100 days. Then, using equation (13), the ΔV required for circularizing would be 16 feet per second, or 32 feet per second (two maneuvers) for 200 days, which is considerably less than the 184 feet per second computed above for the single maneuver. Introducing a greater number of maneuvers within this 200 day interval may reduce the total ΔV required further; however, two factors should be kept in mind. First, Figure 26, as mentioned previously, is based on a first order theory and, therefore the behavior of eccentricity near zero, shown on this figure, may not be representative of actual behavior. The rates of increase of eccentricity for larger values of eccentricity should be representative, however. Second, the short period effect of the earth can cause eccentricity to vary significantly in a 14 day period (about .005), so that it is the average and not the instantaneous value of eccentricity that is significant. Additional analysis is required to determine the frequency of the trim maneuvers which will result in minimum total ΔV for the lifetime of a given satellite system.

Thus far, only first order effects on the satellite phasing have been discussed. These effects are on the eccentricity of the orbit which, in turn, affects the phase angle as described above. There are also higher order effects on the phase angle which will increase the ΔV requirement for phase angle control. For example, if two satellites are in the same 6000 nautical mile orbit about the moon, but phased 180 degrees apart, the perturbations on each will be almost identical except for a slight shift in the position of the perturbing bodies. That is, the second satellite will arrive at the position of the first satellite about 18 hours later (the period is 36 hours). In this time, the earth will have moved about 10 degrees relative to the orbit plane and the sun 0.75 degree. Thus, the perturbation on the second satellite will be slightly different than on the first. This is a higher order effect whose magnitude has not been calculated for this preliminary analysis. This effect will show up as a variation in all of the orbital elements, including the semi-major axis; however, it is expected that the variation will be slow compared with the first order variation of eccentricity of Figure 26. It is anticipated that the only corrective maneuver required

to maintain acceptable phasing will be on the semi-major axis, which affects the period. Thus, if one satellite acquires a reduced period and has a tendency to catch up with the other, then it is necessary to increase its period. This maneuver can be small since only a small catch-up rate per orbit is required. That is, it may be quite acceptable, operationally, to allow several months, after many revolutions, for one satellite to catch up with the other. It is expected that a detailed analysis will show this maneuver to require a small portion of the total spacecraft ΔV budget.

4. LAUNCH AND MISSION MODE CONSIDERATIONS

There are some trajectory and vehicle considerations, not discussed in Subsection 2, which are concerned with the mission phase from launch to LOI. The launch hardware and the operational constraints associated with it can definitely impact on the satellite system finally chosen. For example, the Centaur stage of the Atlas/Centaur vehicle has a restart capability; however, the time of coast to second ignition is limited to 30 minutes, about a third of an orbit. This constraint, sometimes referred to as a direct injection, will limit the lunar launch windows to one opportunity per day and eight days per month. This compares with two opportunities per day every day of the month for a full orbit coast capability. In addition, this 30 minute coast constraint complicates the launch guidance and decreases the optimum payload for certain launch days. These problems are not insurmountable; however, they must be considered and they may impact on the spacecraft design and the system configuration finally chosen.

The Titan IIIC, on the other hand, has been successfully used several times to launch multiple payloads into high earth orbit. This capability may be also used to launch several satellites into lunar orbit. There are two mission modes possible for this situation. The first is that a single stage may be used to deboost all the satellites into the same coplanar orbit about the moon. For this mode, the individual satellites would then have to perform maneuvers in orbit to get positioned relative to each other. The second mode gives each spacecraft the ability to deboost into lunar orbit. Greater flexibility is possible with this mode. For example, if six satellites were launched with the same vehicle,

then three could be placed in an equatorial orbit and three in a polar orbit. Thus, a complete satellite system may be implemented with a single launch vehicle. Only a moderate midcourse maneuver a few hours from TLI would be required to place three of the satellites on a translunar trajectory having a polar approach to the moon, assuming that an equatorial approach was targeted to at TLI. These midcourses, assuming that they are performed by the individual satellites, could include a translunar flight time variation which would satisfy the required phase angle requirement. The disadvantage of this mission mode is that each satellite must carry its own LOI propulsion system resulting in a lower total useful payload, compared with using a single stage for LOI.

5. SUMMARY AND CONCLUSIONS

The trajectory and vehicle considerations discussed in this report are important to the feasibility and design of a lunar communications satellite system. In particular, the TLI and LOI velocity requirements presented in Subsection 2 are required in establishing the payload in lunar orbit. Figure 23 indicates that this payload will increase for longer translunar flight times (up to 130 hours) and is fairly independent of the lunar orbit altitude and inclination. Figure 24 indicates the location of the node at the time of LOI. This can be important if a certain relation with the sun is desired in order to influence its perturbative effects.

The results of Subsection 3 indicate that satellite stability and phase control can be handled with reasonable midcourse maneuvers. It is pointed out that the most important perturbative effect of the sun and the earth is on eccentricity and that this effect is exponential with time. Thus, it is concluded that frequent circularizing adjustments to the satellite orbit will result in a lower total velocity requirement than adjustments made only when a coverage constraint is violated.

Since eccentricity affects the phase angle between consecutive satellites in the same orbit, an analysis is presented in Subsection 3 to quantize this effect and to determine the trim ΔV maneuver required to correct it. The result has been applied to satellite systems of up to six satellites and is presented in Figure 28. Combining this data with the coverage analysis of Part III will indicate that, for some systems,

the phase angle deviations are within the coverage overlap requirements and, therefore, the continuous communication requirement is always met.

Once the optimum configuration has been chosen, it will be necessary to perform more detailed analysis of the following:

(1) Study of frequency and length of lunar occultations.

(2) Perform detailed analysis of orbit stability and phasing decay.

(3) Investigation of optimum (minimum ΔV) technique to maintain or correct phasing between satellites

(4) Development of daily launch windows and yearly launch opportunities to maximize payload in lunar orbit.

(5) Investigation of midcourse velocity requirements for accurate lunar orbit insertion.

REFERENCES

4-1. "Titan III Standard Space Launch System (SSLS) Definition for Payload Contractors," SSD-CR-65-18 (Rev. 1), Martin Denver, September 1965.

4-2. "Atlas Launch Vehicle Family for Spacecraft Contractor Planning," GDC BGJ 67-002, General Dynamics, Convair Division, April 1967.

4-3. Moe, M. M., "Solar-Lunar Perturbations of the Orbit of an Earth Satellite," ARS Journal, May 1960.

4-4. Moulton, F. R., Celestial Mechanics, MacMillan Co., 1914, p. 171.

V. ERP AND ANTENNA GAIN SPECIFICATIONS FOR LUNAR COMMUNICATIONS SATELLITES

1. INTRODUCTION

Part V presents the analysis and conclusions of lunar communications trade-off studies pertaining to communications link margins in determining the satellite parameters of effective radiated power (ERP) and the receive antenna specifications. (See Figure 29.)

The analysis adheres to the ground rules and parameters specified by NASA/MSC/TCD and are stated in Appendix A. The method of analysis utilizes the Apollo communications math model of Reference 5-1 and certain trigonometric relationships of earth, moon, and satellite to establish maximum expected communication ranges. This entire model, ranges and communications, is explained in detail in Section 3.

The parametric analyses contained in Section 4 were performed using an SRU 1108 program which is described in Reference 5-2.

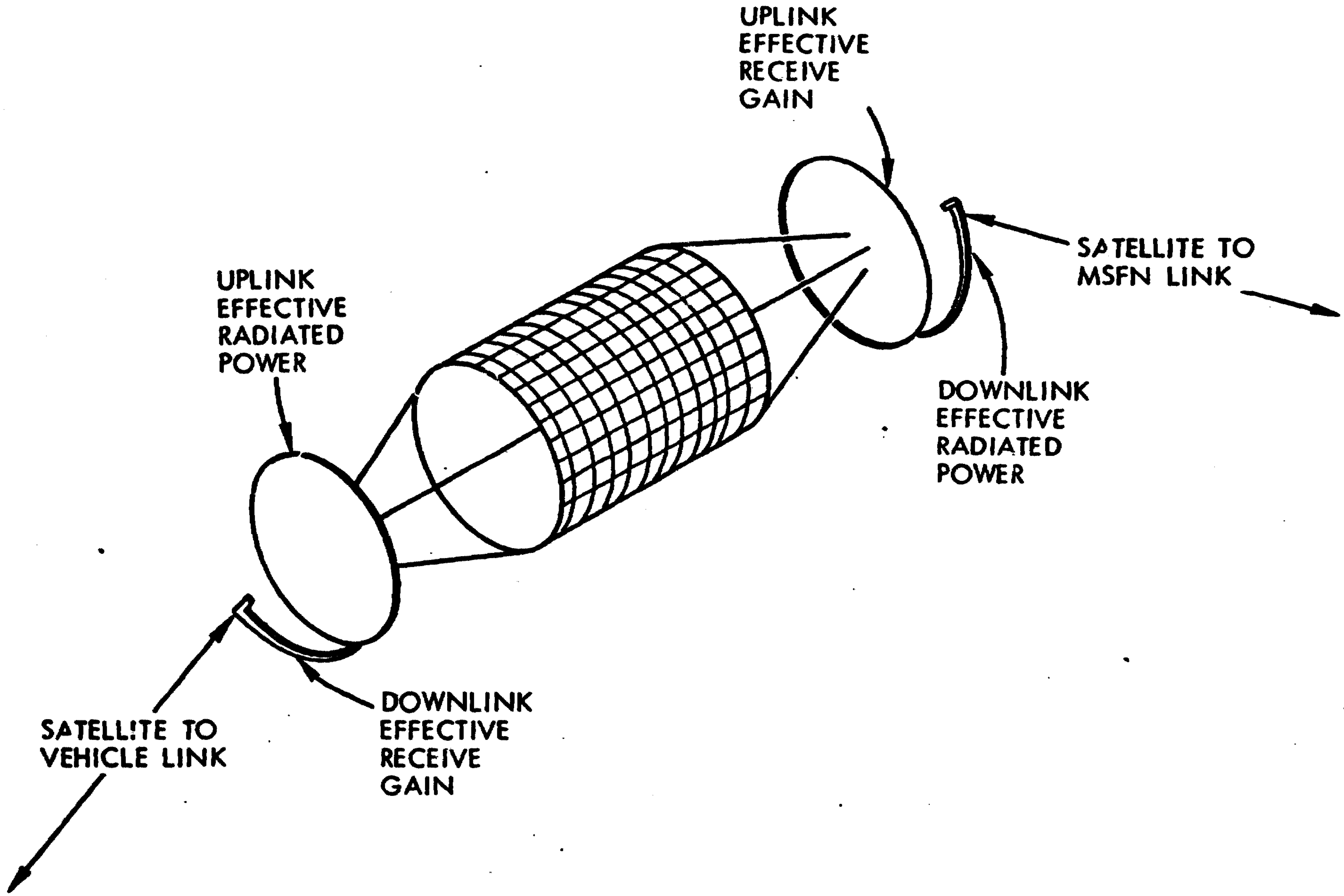

FIGURE 29. Parameters to be determined by Analysis

2. CONCLUSIONS

The analysis discussed in Section 4 using the math model of Section 3 and parameters of Appendix A concerns the determination of required lunar orbiting satellite antenna receive gain and transmit radiated power. The results to date consider only the effect of IF bandwidth and the required SNR in this bandwidth.

Two distinct systems were analyzed--current Apollo and modified Apollo. The basic differences between these systems include: (See Appendix A.)

a) MSFN - satellite link transmit frequency.

b) Required SNR improvements at vehicle and MSFN.

c) Increased vehicle transmit power.

d) Improved noise figures at vehicle, satellite, and MSFN.

For each of the systems, three separate modes of operations were analyzed.

These are:

1) Wideband with High Gain Antenna.

2) Narrowband with Omni Antenna.

3) Narrowband with High Gain Antenna.

Based on the assumptions listed below for lunar orbiting satellites,

Number of Satellites	3
Satellite Altitude	4500 n.m.
Vehicle Altitude	60 n.m.
Lunar Surface Overlap Angle	30 degrees
Vehicle Elevation Angle to Lunar Surface Grazing Plane	5 degrees

application of the trigonometric relationships derived in Section 3.1

result in the following maximum ranges:

Range (MSFN-satellite)	215320 n.m.
Range (satellite-vehicle)	5621 n.m.

Use of these maximum ranges, the parameters listed in Appendix A (Ground Rules) and the math model of Section 3 allows the predictions shown in Figures 30 and 31. These figures show the useable range of combinations of satellite effective receive gain and effective radiated power necessary to achieve the required effective signal to noise ratios at the vehicle or MSFN.

Assuming parabolic antennas, Table 3, Page 5-13, illustrates the antenna specifications and power outputs of a satellite system necessary to achieve the required SNR at the vehicle for selected combinations of ERP and receive gain using the modified system. (See the example in Paragraph 2.1.2.)

2.1 Required Antenna Gains

The relationship of lunar relay satellite receive gain and effective radiated power were analyzed by means of the "Lunar Communications Satellite Analysis Program (SATCOM) HV025A", (Ref. 5-2) and the results are reported in Section 4. Use of the program resulted in generation of a series of plots of terminal receiver IF Bandwidth signal-to-noise ratios versus satellite effective radiated power for families of receive gain curves. The receive gain curves are in 5dB increments increasing in gain from bottom to top of the graph. The bottom curve is labeled in db of gain and the horizontal line across the graph is the required IF SNR for that system (see Appendix A). Thus, any combination of effective receive gain and radiated power on or above this horizontal line will produce positive IF margins in the terminal receiver (vehicle or MSFN). Figures 36 through 47 provide satellite ERP vs received SNR curves for different systems and antenna combinations listed as "cases" in Table 4, Page 5-32.

A pair of plots describe an uplink and downlink for each case. Figure 36 and 37 are the uplink and downlink plots respectively for case No. 1 of Table 4. Each curve in the receive gain family has a flattening shape with increasing radiated power. This shows a constant upper limit in received SNR and is due to the satellite transmitted SNR being the upper limit obtainable in the vehicle (or MSFN) receiver.

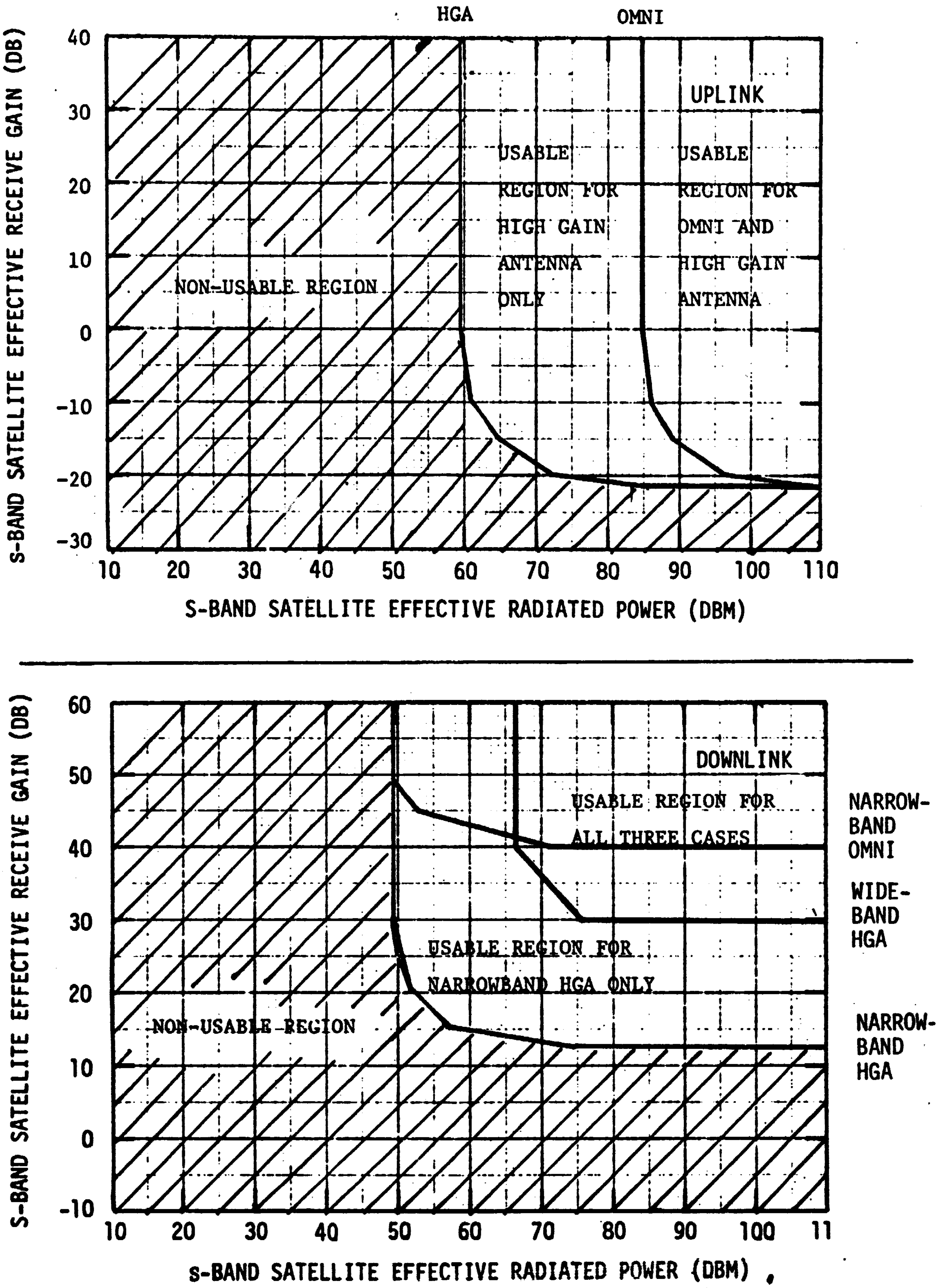

FIGURE 30. SATELLITE ANTENNA REQUIREMENTS FOR APOLLO SYSTEM PARAMETERS FOR THE CASE OF ORBITING SATELLITE AND ORBITING VEHICLE

NOTE: See Figure 29, Page 5-2, for definition of uplink and downlink.

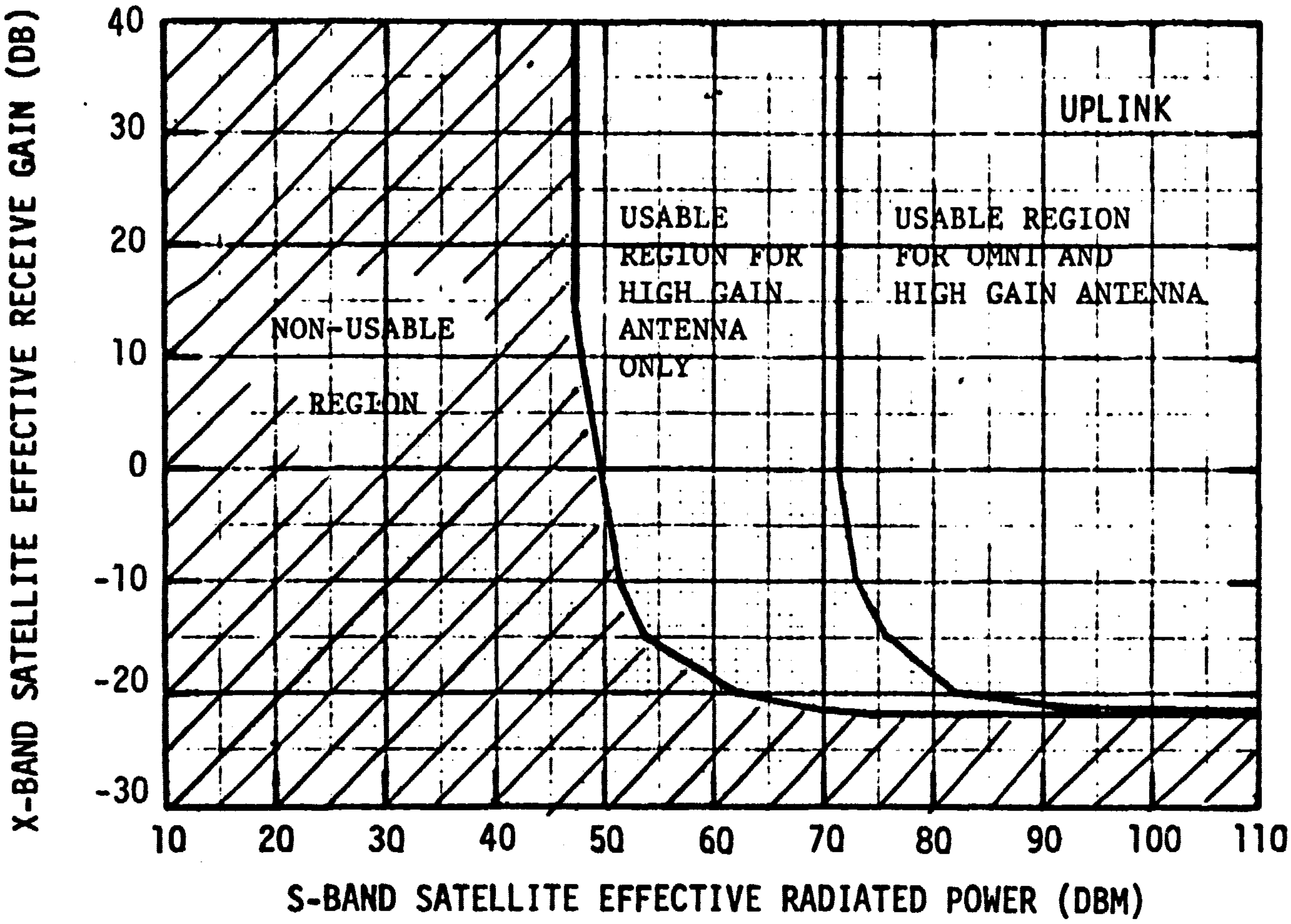

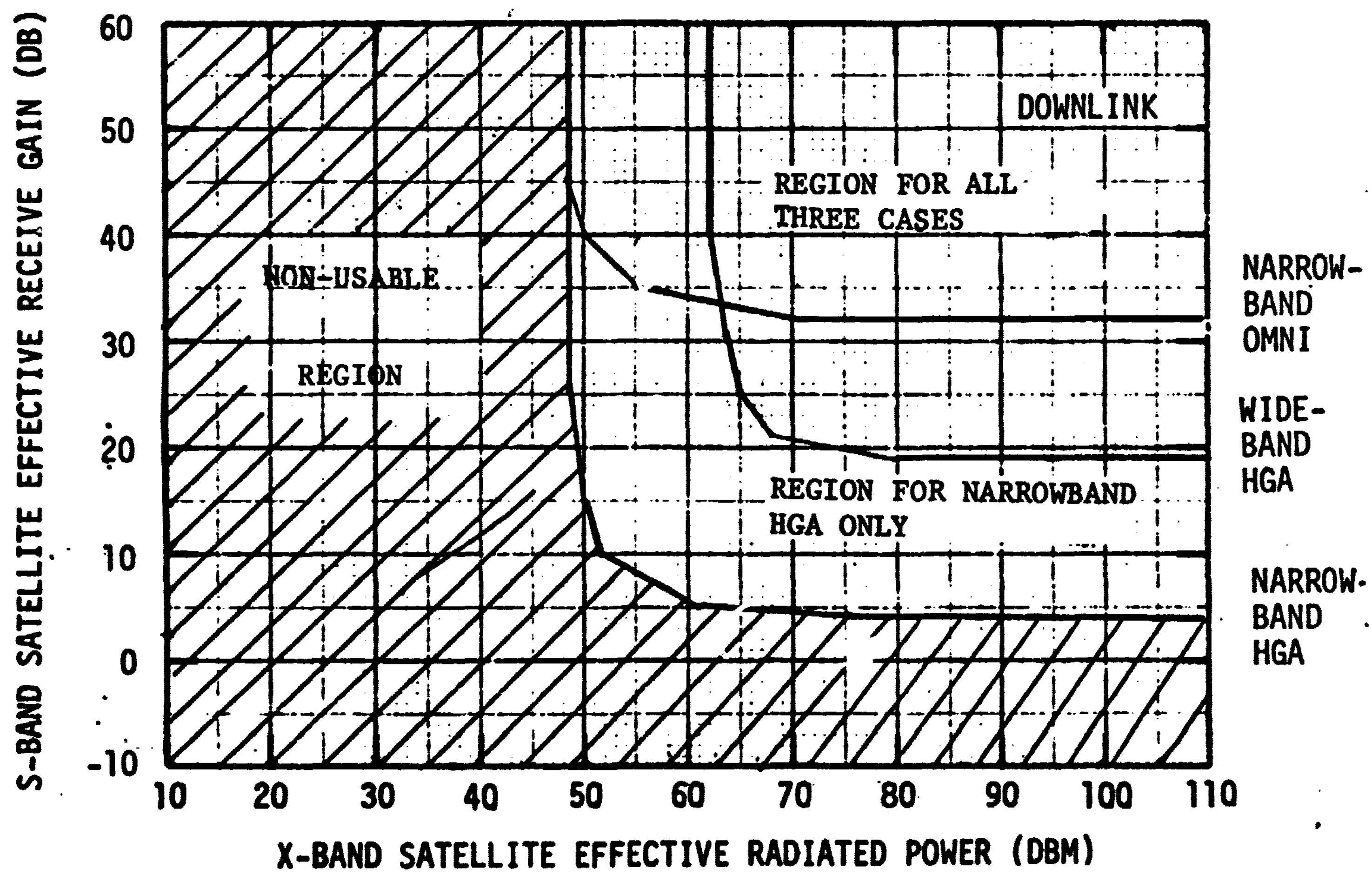

FIGURE 31. SATELLITE ANTENNA REQUIREMENTS FOR MODIFIED SYSTEM PARAMETERS FOR THE CASE OF ORBITING SATELLITE AND ORBITING VEHICLE

NOTE: See Figure 29, Page 5-2, for definition of uplink and downlink.

Also, increasing the satellite receive gain for a constant satellite effective radiated power will reach an upper limit of receive gain, above which no increase in terminal received SNR is obtainable. This is caused by the limiting of the terminal receiver noise.

In order to make the information more useable, the series of plots presented in Section 4 have been consolidated into four plots (Figures 30, and 31) showing satellite effective receive gain and effective radiated power combinations necessary to produce the required SNR at the terminal receiver (lunar vicinity vehicle or MSFN).

In each figure, two graphs are presented for the uplink case and the downlink case. The uplink graph presents two vehicle antennas--high gain and omni. The areas above and to the right of each data line represents the possible combination of satellite receive gain and effective radiated power which will provide positive circuit margins in the vehicle IF bandwidth. A crosshatched area represents combinations of receive gain and radiated power which are not useable for either vehicle antenna.

The downlink graph presents three cases of vehicle antenna and bandwidth. Again, a crosshatched area represents combinations which are not useable in any case.

As noted above, there are limits above which increases in satellite ERP produce no increase in terminal receiver SNR, for a given satellite receive gain. The satellite receive gain curve (-22db curve in Figure 36) which produces the minimum terminal SNR required becomes a line of minimum useable satellite gain in the consolidated plots for that system (Figure 30, upper figure). At the other extreme, the limit is approached where further increase of satellite receive gain results in no increase in terminal receiver SNR for a given satellite ERP. This point is noted at the intersection of the line where the lower values of the increasing satellite receive gain curves "stack up"

on each other and the minimum required terminal receiver SNR line (approximately 59 dbm ERP in Figure 36.). This results in the line of minimum useable ERP shown as the vertical line in the upper figure of Figure 30. Since this point (refer to Figure 36) does not coincide the required SNR line (-6.8 db), it appears that the line of minimun satellite ERP and minimum satellite receive gain (Figure 30) do not intersect but are joined by a continuous curve. Points on this curve are obtained by noting (Figure 36 again) where the satellite receive gain curves greater than the required minimum (-22 db) intersect the required terminal receiver required SNR. (Three of these points in Figure 36 are: receive gain = -20 db, ERP = 72 dbm; receive gain = -15 db, ERP = 65 dbm, and receive gain = -10 db, ERP = 61). These points are then plotted in Figure 30 and joined by straight lines. It, thus, appears that the radius of the curve joining the minimum ERP line and the minimum receive gain line depends upon the required terminal receiver SNR (for a given system). For instance, if the required SNR in Figure 36 were +4db, the minimum satellite receive gain curve of -10db would intersect the required SNR line, at approximately 84 dbm and the minimum ERP point would be approximately 72 dbm,resulting in a radius for the curve joining the minimum satellite receive gain line and the minimum ERP line of approximately 12 db (instead of the approximate 17 db in the actual case when the minimum SNR required is -6.8 db).

Table 2 lists the minimum requirements for the Apollo and modified systems for the uplink and downlink cases, including an emergency VHF voice link between the lunar vicinity vehicle and the lunar orbiting satellite, and an emergency downlink baseband voice system. The parameters used in calculating these emergency links are those used in the present Apollo CSM-MSFN system, where applicable. The arrangement of the tables allows comparison of the two systems requirements for different satellite antennas. Another factor to consider in comparing these tables is the frequency differences on the MSFN-satellite link. The Apollo system uses S-Band and the modified system uses X-Band (both use S-band on the satellite-lunar terminal link). This difference will account for an antenna gain difference of 11 to 12 db assuming the antenna diameter remains constant.

Table 2. Comparative Analysis of Apollo and Modified Systems Relay Satellite Antenna Requirements

Link	Vehicle Antenna	Bandwidth	Satellite Min. Req'd Rec. Gain		Satellite Min. Required ERP	
			Apollo	Modified	Apollo	Modified
MSFN to Vehicle	S-Band Omni	Backup Voice (3 KHz BW)	-33.6 dB (S-Band)	-33.8 dB (X-Band)	+72.5 dBm	+62.0 dBm
	S-Band HGA				+48.5 dBm	+38.0 dBm
Vehicle to MSFN	S-Band Omni	Baseband Voice (3 KHz BW)	+14.8 dB	+7.4 dB	+24.5 dBm (S-Band)	+24.4 dBm (X-Band)
	S-Band HGA		-12.2 dB	-20.6 dB		
MSFN to Vehicle	VHF omni	3 KHz	-20.0 dB (S-Band)	-20.0 dB (X-Band)	+71.1 dBm	+68.1 dBm
Vehicle to MSFN	VHF omni	3 KHz	+8.6 dB	+8.4 dB	+22.0 dBm (S-Band)	+22.0 dBm (X-Band)
MSFN to Vehicle	S-Band Omni	4.8 MHz	-22.0 dB (S-Band)	-22.0 dB (X-Band)	+84.0 dBm	+72.0 dBm
	S-Band HGA				+59.0 dBm	+47.0 dBm
Vehicle to MSFN	S-Band Omni	4.8 MHz	+40.0 dB	+32.0 dB	+49.0 dBm (S-Band)	+49.0 dBm (X-Band)
	S-Band HGA		+13.0 dB	+ 4.0 dB		
	S-Band HGA	5.3 MHz	+30.0 dB	+19.0 dB	+66.0 dBm (S-Band)	+62.0 dBm (X-Band)

NOTE: Values are based on the parameters given in the ground rules (Appendix A), and presently accepted Apollo parameters, where applicable.

2.1.1 Example 1

To determine if a satellite antenna system will produce positive margins on both the uplink and downlink, the following procedure is needed:

1) Assume a vehicle antenna-omni.
2) Assume a system-Apollo.
3) A point is then chosen in the useable portion of Figure 30 (Apollo) uplink above the omni curve.

$$\left.\begin{array}{l}\text{Eff. Receive Gain} = 20\text{ dB} \\ \text{Eff. Radiated Power} = 84\text{ dBm}\end{array}\right\}\text{ Uplink}$$

4) The effective radiated power is composed of an antenna gain and a transmit power. The antenna gain may be assumed to be effective receive gain for the downlink. Referring to the downlink graph of the same figure, the useable region for the Narrowband Omni would dictate an effective receive gain of greater than 40 dB. If we choose a point in this region, say:

$$\left.\begin{array}{l}\text{Eff. Receive Gain} = 45\text{ dB} \\ \text{Eff. Radiated Power} = 55\text{ dBm}\end{array}\right\}\text{ Downlink}$$

The satellite transmit power on the uplink will be:

Eff. Radiated Power - Antenna Gain or,

+ 84 dBm - 45 dB = +39 dBm = 7.9 watts.

5) The downlink effective radiated power is also composed of transmit power and antenna gain. Assuming this antenna gain to be the same as the uplink effective receive gain, the required satellite transmit power on the downlink will be:

+55 dBm - 20 dB = +35 dBm = 3.2 watt.

2.1.2 Example 2

Another example, using the modified system, is calculated for the omni antenna.

1) From Figure 31, a point is chosen on the uplink graph above the omni curve;

   Eff. Receive Gain = +40 dB (X-Band)

   Eff. Radiated Power = +75 dBm (S-Band)

2) From the downlink graph of Figure 31, a point is chosen above the omni curve;

   Eff. Receive Gain = +35 dB (S-Band)

   Eff. Radiated Power = +70 dBm (X-Band)

3) The required satellite S-Band transmit power is then;

   +75 dBm - 35 dB = +40 dBm = 10 watts.

4) The required satellite X-Band transmit power is then;

   +70 dBm - 40 dB = +30 dBm = 1 watt.

2.1.3. Comparison of Example 1 and Example 2

At first glance, it would appear that Example 2 indicates that the S-band transmit power requirement for the modified system is greater than that for the Apollo (S-Band) system. However, this results from the particular satellite receive gain - ERP point chosen for Example 1, which, though allowable, was not very realistic in terms of required antenna size. The antenna gains for the modified system are more realistic; i.e.,

S-Band gain = 35 dB (req. parabolic ant. size - approximately 10.5 ft.)

X-Band gain = 40 dB (req. parabolic ant. size - approximately 5 ft.)

whereas, the Apollo system vehicle-satellite gain is less realistic; i.e.:

Vehicle-Satellite Link = 45 dB (req. parabolic ant. size approximately 33 ft.)

2.2 Satellite Antenna Specifications

Having determined allowable satellite antenna gain for a communication system, the choice of hardware available to provide the required gain is quite broad. Appendix B is a compilation of state-of-the-art information on antennas and RF power amplifiers for use in satellite systems.

Since parabolic reflectors are current, proven antenna design for space applications, Table 3 shows antenna beamwidths and diameters for parabolic antennas to satisfy the conditions of the example in paragraph 2.1.2, with assumed circuit losses of 2 dB (S-Band) and 5 dB (X-Band) added to the derived antenna gains. (Inasmuch as each antenna is used for both transmission and reception, the antenna gains were increased to account for the assumed losses, rather than increasing the RF power outputs). Table 3 also shows antenna specifications for use with lunar vicinity vehicles using high gain antennas as well as omnis. It is obvious that an antenna system which satisfies the omni case will be sufficient for use with high gain antennas.

Table 3. Satellite Parabolic Antenna System Specifications-Modified System

Vehicle Antenna	PA Output Power	Antenna Gain	Frequency	Antenna Efficiency	Antenna 3dB Beamwidth	Diameter
Omni/ Narrowband	10 watts 1 watt	37 dB 45 dB	2300 MHz 8500 MHz	.55 .55	2.27 deg. 0.91 deg.	13.2 feet 8.9 feet
High Gain/ Narrowband	1 watt 0.1 watt	22 dB 35 dB	2300 MHz 8500 MHz	.55 .55	12.8 deg. 2.9 deg.	2.35 feet 2.8 feet
High Gain/ Wideband	0.25 watt 0.32 watt	28 dB 35 dB	2300 MHz 8500 MHz	.55 .55	6.4 deg. 2.9 deg.	4.7 feet 2.8 feet

3. MATHEMATICAL MODEL

The lunar satellite communications parametric analysis is accomplished by a computer program operating on the SRU 1108. This program has two phases of operation; 1) uplink communications from earth MSFN station, via the lunar satellite, to the lunar vehicle, and 2) downlink communications from the lunar vehicle, via the lunar satellite, to the earth MSFN station.

The program is capable of analyzing; 1) lunar surface or lunar orbiting vehicles, 2) any system of lunar satellites described by quantity and lunar surface overlap angle or libration satellites, and 3) any parameters of the vehicle, satellite, and MSFN station which concern communications.

The method of operation initially computes the communications ranges, satellite to vehicle and satellite to MSFN station. Using these ranges, uplink and downlink communication computations are made. For each phase, the satellite signal-to-noise ratio is computed; then, the receive terminal, vehicle or MSFN, signal-to-noise ratios are computed. These calculations are then plotted as effective signal channel SNR versus satellite effective radiated power for a family of satellite receive gains.

3.1 Communication Ranges

The communication ranges are for use in calculating the total received power on a particular link and are derived from the simple trigonometric relationships among the earth, satellites, moon, and vehicles.

3.1.1 Satellite Altitude Above the Lunar Surface

The satellite altitude depends on the number of satellites, the coverage overlap angle on the lunar surface (in the orbital plane), and the elevation look-angle from vehicle horizon to the satellite.

Referring to Figures 32, and 33, the derivation proceeds: The angle θ is derived from the coverage overlap angle, α, and the number of satellites, N, as:

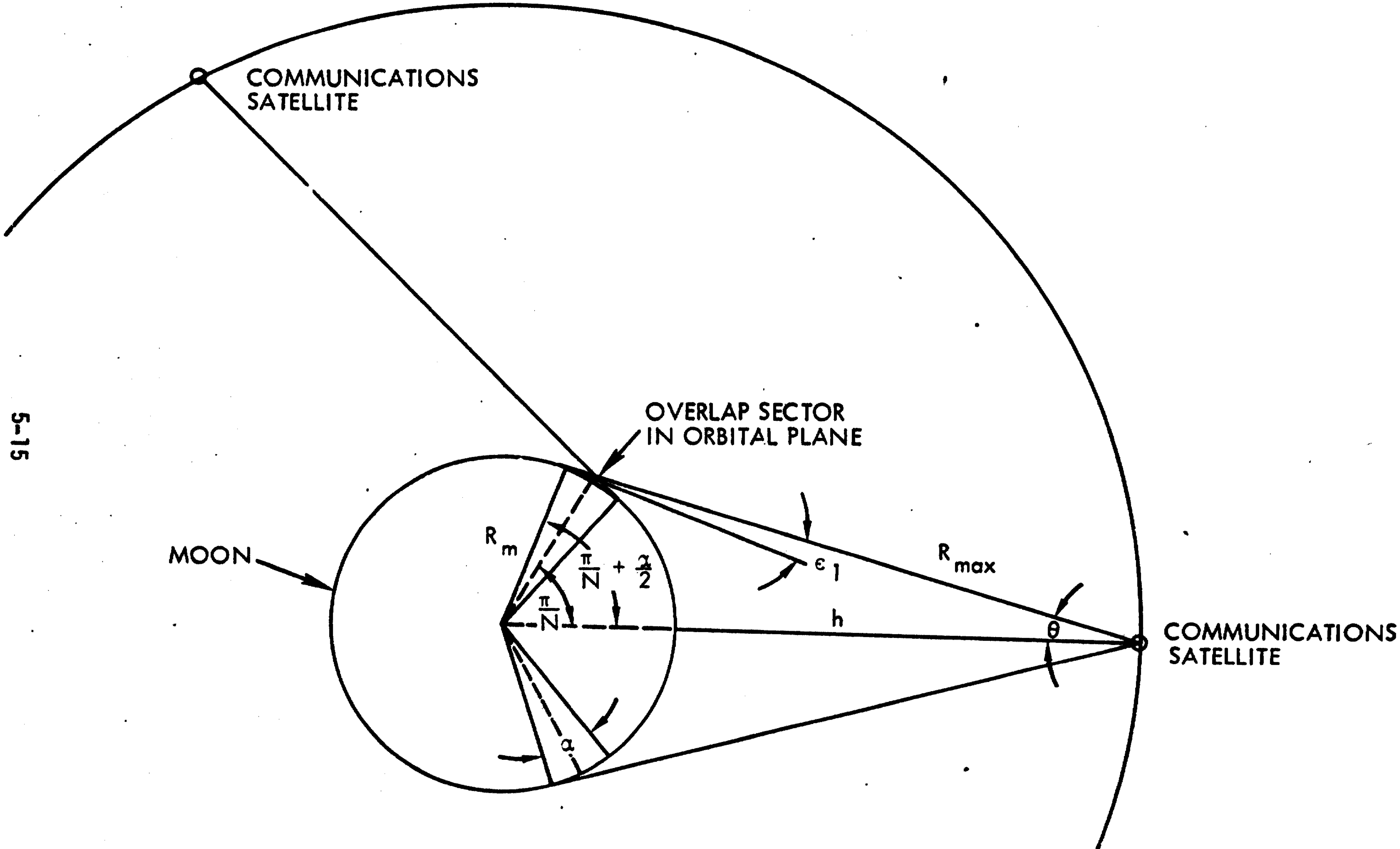

FIGURE 32. BASIC COVERAGE GEOMETRY

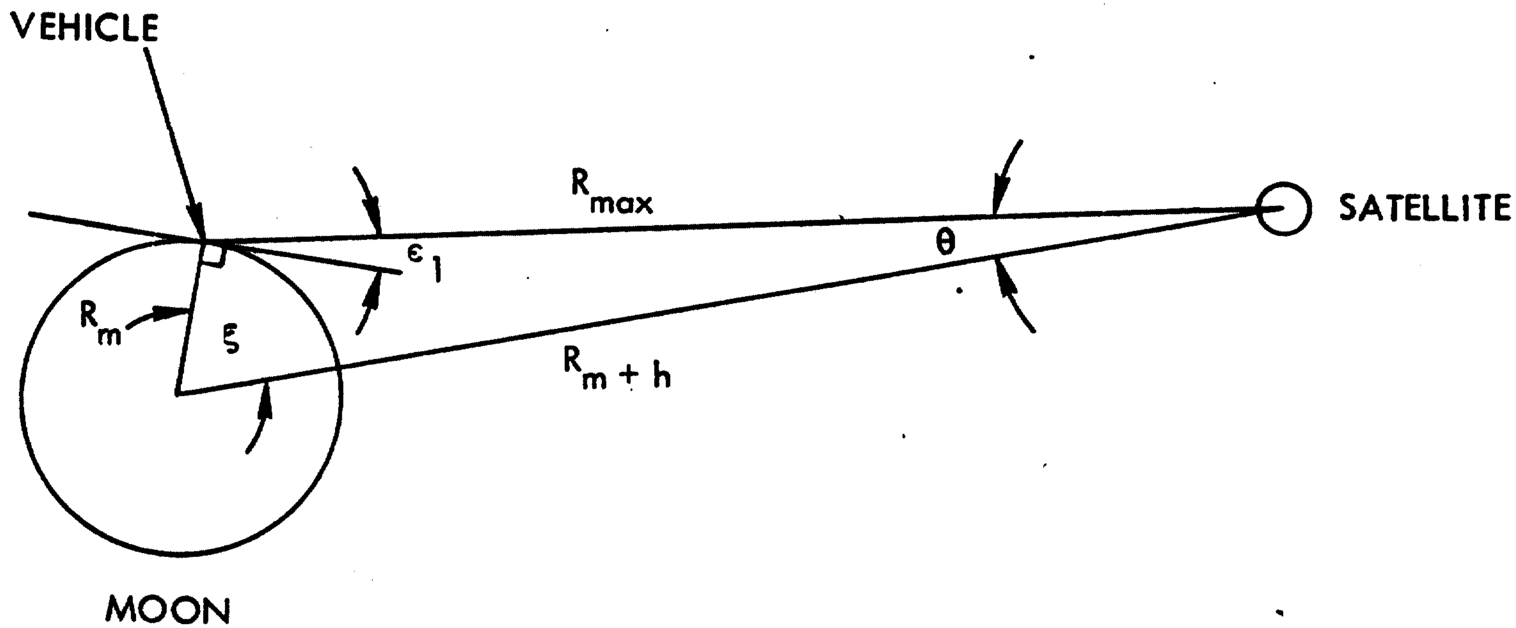

FIGURE 33. Relationship of Moon, Surface Vehicle, and Satellite

$$\pi = \xi + \frac{\pi}{2} + \varepsilon_1 + \theta \tag{1}$$

but, for maximum satellite to vehicle range;

$$\xi = \frac{\pi}{N} + \frac{\alpha}{2}. \tag{2}$$

then,

$$\pi = \theta + \left(\frac{\pi}{2} + \varepsilon_1\right) + \left(\frac{\pi}{N} + \frac{\alpha}{2}\right)$$

$$\theta = \pi/2 - \frac{\pi}{N} - \varepsilon_1 - \frac{\alpha}{2} \tag{3}$$

$$\theta = \pi\left(\frac{1}{2} - \frac{1}{N}\right) - \left(\varepsilon_1 + \frac{\alpha}{2}\right) \tag{4}$$

By the Law of Sines,

$$\frac{\sin \xi}{R_{max}} = \frac{\sin\left(\pi/2 + \varepsilon_1\right)}{R_m + h} = \frac{\sin \theta}{R_m} \tag{5}$$

where R_m = radius of moon
h = satellite altitude
ε_1 = vehicle elevation look angle

and,

$$(R_m + h) \sin \theta = R_m \sin \left(\frac{\pi}{2} + \varepsilon_1\right) \tag{6}$$

thus,

$$h = \frac{R_m \left[\sin \left(\frac{\pi}{2} + \varepsilon_1\right) - \sin \theta\right]}{\sin \theta} \tag{7}$$

3.2.2 Range to Lunar Surface Vehicle

Referring again to Figures 32, and 33, the maximum range from to satellite to lunar surface vehicle is,

$$R_{max} \sin \theta = R_m \sin \left(\frac{\pi}{N} + \frac{\alpha}{2}\right) \tag{8}$$

$$R_{max} = \frac{R_m \sin\left(\frac{\pi}{N} + \frac{\alpha}{2}\right)}{\sin \theta} \quad (9)$$

3.1.3 Range to Lunar Orbiting Vehicle

The case of a lunar orbiting vehicle is similar to that of a surface vehicle; however, the vehicle is placed at a fixed altitude above the mean lunar surface. Referring to Figure 34; the derivation of communication range proceeds using the vehicle altitude, h_v, and the vehicle elevation angle from the lunar surface grazing plane, ε_1.

From Figure 34,

$$\sin \theta_2 = \frac{R_m}{R_m + h_v} \quad (10)$$

By the law of sines,

$$\frac{\sin(\theta_2 + \varepsilon_1)}{R_m + h} = \frac{\sin \theta_1}{R_m + h_v} \quad (11)$$

where h = satellite altitude

then,

$$\theta_1 = \sin^{-1}\left\{\frac{R_m + h_v}{R_m + h} \cdot \sin(\theta_2 + \varepsilon_1)\right\} \quad (12)$$

and, for the larger triangle,

$$\theta_3 = \pi - (\theta_1 + \theta_2 + \varepsilon_1) \quad (13)$$

Again, by the Law of Sines,

$$\frac{\sin \theta_3}{R_{max}} = \frac{\sin(\theta_2 + \varepsilon_1)}{R_m + h} \quad (14)$$

hence,

$$R_{max} = (R_m + h) \frac{\sin \theta_3}{\sin(\theta_2 + \varepsilon_1)} \quad (15)$$

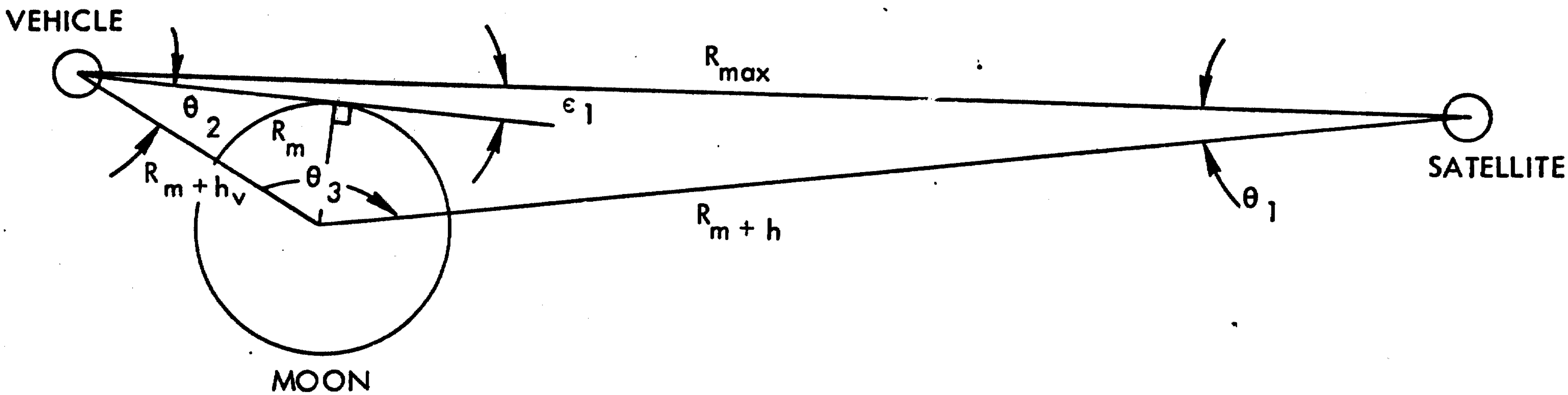

FIGURE 34. Relationship of Moon, Orbiting Vehicle, and Satellite

3.1.4 Range from Satellite to MSFN Station

The maximum range from satellite to earth is shown in Figure 35, as $R_1 + R_2 + R_3$.

The angle, θ_1, is given by Equation 4 when ε_1 is zero, so as to make R_3 the grazing distance from satellite to lunar surface, as,

$$\theta_1 = \pi\left(\frac{1}{2} - \frac{1}{N}\right) - \frac{\alpha}{2} \tag{16}$$

where; α = satellite coverage overlap angle.

$$R_3 = (R_m + h) \sin (90 - \theta_1)$$

$$R_3 = (R_m + h) \cos \theta_1 \tag{17}$$

By the Law of Sines,

$$\beta = \sin^{-1} \frac{R_m}{D_2} = \sin^{-1} \frac{R_e}{D_1} = \sin^{-1} \frac{R_e}{D_m - D_2} \tag{18}$$

where; D_m = mean distance earth to moon = $D_1 + D_2$

$$\theta_2 = \theta_1 + \beta \tag{19}$$

NOTE: Minimum orbital plane separation, such that one of the two orbits is completely visible from earth at all times, is 2 θ_2.

By similiar triangles,

$$\beta = \sin^{-1} \left\{\frac{R_e + R_m}{D_m}\right\} \tag{20}$$

then, $$R_1 + R_2 = (R_e + R_m) \cot \beta \tag{21}$$

$$= (R_e + R_m) \cot \left\{\sin^{-1} \left(\frac{R_e + R_m}{D_m}\right)\right\} \tag{22}$$

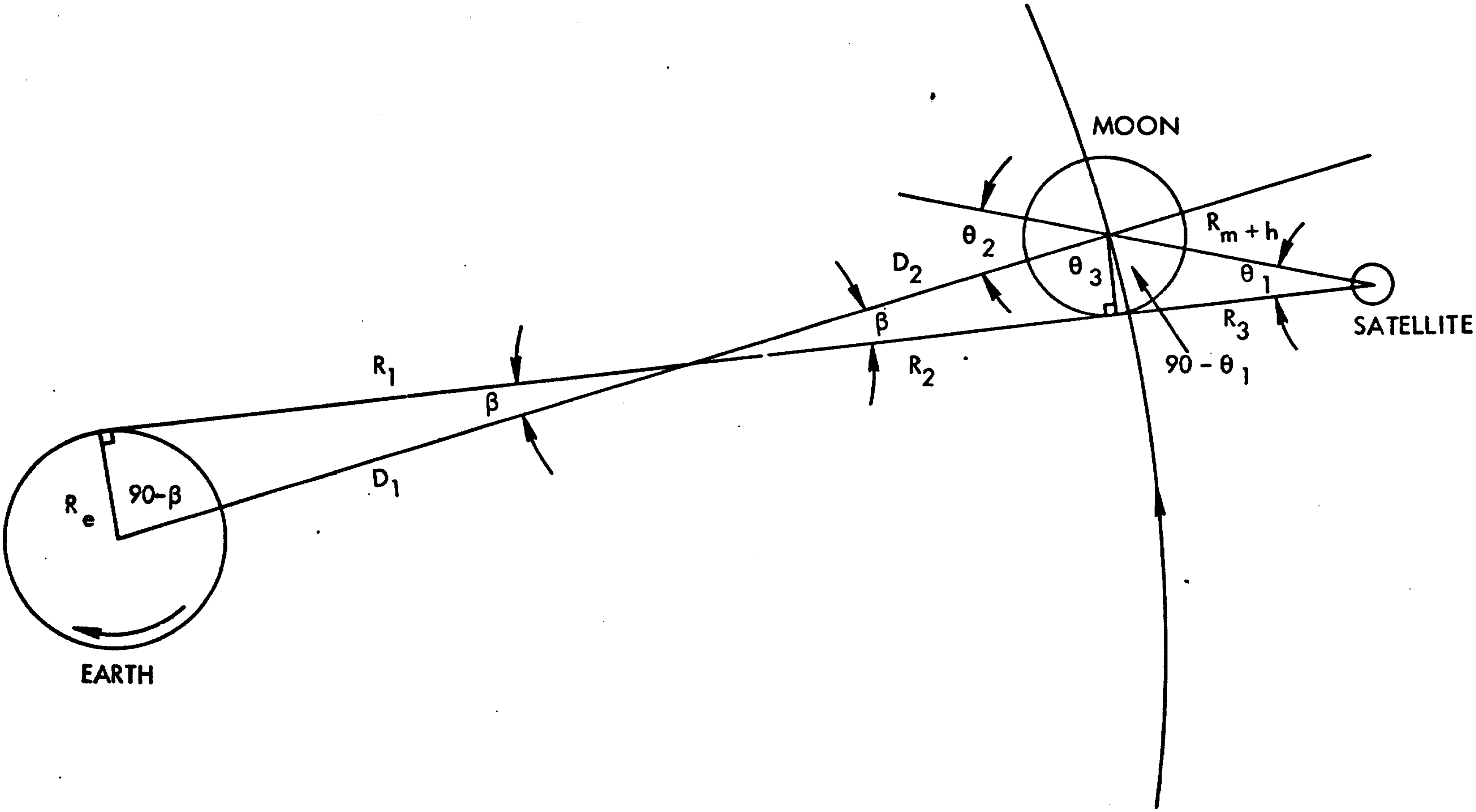

FIGURE 35. Relationship of Earth, Moon, and Satellite

Hence, the maximum distance from earth to satellite is

$$R_{(e-s)max} = R_1 + R_2 + R_3$$

$$= (R_e + R_m) \cot \left\{ \sin^{-1} \left(\frac{R_e + R_m}{D_m} \right) \right\} + (R_m + h) \cos \theta_1 \qquad (23)$$

3.2 Uplink Modulation Loss

The uplink, MSFN-to-vehicle via satellite, modulation losses are calculated for each information service; including carrier, voice, updata, and ranging. The calculations use the uplink PM modulation indices for ranging (ϕ), updata (MTM), and voice (MV).

3.2.1 Uplink Carrier Modulation Loss

$$L_{m/cu} = \cos^2 \phi \bullet J_o^2 (MV) \bullet J_o^2 (MTM) \qquad (24)$$

3.2.2 Uplink Voice Modulation Loss

$$L_{m/vu} = 2 \bullet \cos^2 \phi \bullet J_1^2 (MV) \bullet J_o^2 (MTM) \qquad (25)$$

3.2.3 Updata Modulation Loss

$$L_{m/tu} = 2 \bullet \cos^2 \phi \bullet J_o^2 (MV) \bullet J_1^2 (MTM) \qquad (26)$$

3.2.4 Uplink Ranging Modulation Loss

$$L_{m/ru} = \sin^2 \phi \bullet J_o^2 (MV) \bullet J_o^2 (MTM) \qquad (27)$$

3.3 Satellite Uplink Received Signal-to-Noise Ratio

The satellite received signal-to-noise ratio is calculated in a series of steps beginning with the calculation of total received power at the satellite from the MSFN station. The calculation of satellite receiver noise is then made and divided into the received power.

3.3.1 Total received Power

$$P_{rs} = \frac{P_t G_t G_r}{4\pi R^2} \quad \frac{\lambda^2}{4\pi} \qquad (28)$$

where; P_t is MSFN transmit power

G_t is the MSFN transmit antenna gain (including losses)

G_r is satellite effective receive gain

R is communications range from MSFN to satellite

λ is wavelength of received carrier frequency

3.3.2 Received Carrier Power

$$P_{cs} = P_{rs} \cdot L_{m/cu} \tag{29}$$

3.3.3 Satellite Receiver Noise Power

$$P_{ns} = k \cdot (A + B \cdot P_{cs}) \cdot BW_{IF} \tag{30}$$

where; k is Boltman's constant (1.38×10^{-23})

A is satellite system noise temperature

B is satellite receiver AGC noise factor

BW_{IF} is satellite transponder IF bandwidth

3.3.4 Satellite Received Signal-to-Noise Ratio

$$SNR_{sat} = \frac{P_{cs}}{P_{ns}} \tag{31}$$

NOTE: The satellite transmitted SNR is assumed equal to the satellite received SNR

3.4 Vehicle Effective Uplink Received Signal-to-Noise Ratio (IF Bandwidth)

The effective received SNR considers the transmitted SNR to obtain the true IF signal-to-noise ratio. The total received power is calculated at the vehicle receiver; then, the transmitted signal-to-noise ratio is applied to obtain the total effective signal power received. The vehicle receiver noise power is increased by the amount of noise power transmitted to obtain the total noise power. The ratio of these is the effective IF signal-to-noise ratio.

3.4.1 Vehicle Total Received Power

$$P_{rv} = \frac{P_t G_t G_r}{4\pi R^2} \bullet \frac{\lambda^2}{4\pi} \bullet L_r \tag{32}$$

where; $P_t G_t$ is the satellite effective radiated power

G_r is the vehicle receive antenna gain

R is the satellite-to-vehicle communication range

λ is the wavelength of the received carrier

L_r is the combined receive antenna system losses

3.4.2 Vehicle Total Effective Received Signal Power

$$P_{rv(eff)} = P_{rv} \bullet \frac{P_{cs}}{P_{ns} + P_{cs}} \tag{33}$$

where; P_{cs} is the satellite transmitted signal power

P_{ns} is the satellite transmitted noise power

3.4.3 Vehicle Received Carrier Power

$$P_{cv} = P_{rv} \bullet L_{m/cu} \tag{34}$$

3.4.4 Vehicle Receiver Noise Power

$$P_{nv} = k \bullet (A + B \bullet P_{cv}) \bullet BW_{IF} \tag{35}$$

where; k is Boltzman's constant

A is vehicle receiver system temperature

B is receiver AGC noise factor

BW_{IF} is the IF bandwidth

3.4.5 Vehicle Total Effective Noise Power

$$P_{nv(eff)} = P_{nv} + \frac{P_{ns}}{P_{cs} + P_{ns}} \bullet P_{rv} \tag{36}$$

3.4.6 Vehicle Effective Received Signal-to-Noise Ratio

$$SNR_{veh} = \frac{P_{rv(eff)}}{P_{nv(eff)}} \tag{37}$$

3.5 Uplink Carrier Channel Effective Signal-to-Noise Ratio

The carrier channel effective SNR is obtained from the effective received carrier power and the effective noise power in the carrier loop bandwidth.

3.5.1 Effective Received Carrier Power

$$P_{c(eff)} = P_{rv(eff)} \cdot L_{m/cu} \tag{38}$$

3.5.2 Effective Carrier Loop Noise Power

$$P_{nc} = \frac{BW_c}{BW_{IF}} \cdot P_{nv(eff)} \tag{39}$$

where; BW_c is the carrier loop bandwidth

3.5.3 Effective Received SNR-Carrier Channel

$$SNR_{c(eff)} = \frac{P_{c(eff)}}{P_{nc}} \tag{40}$$

3.6 Upvoice Channel Effective Signal-to-Noise Ratio

The voice channel effective SNR is obtained in a similar manner to the carrier channel effective SNR (above) but using the voice channel predetection bandwidth, BW_v, as

$$SNR_{v(eff)} = \frac{BW_{IF}}{BW_v} \cdot \frac{P_{rv(eff)} \cdot L_{m/vu}}{P_{nv(eff)}} \tag{41}$$

3.7 Updata Channel Effective Signal-to-Noise Ratio

$$SNR_{u(eff)} = \frac{BW_{IF}}{BW_u} \cdot \frac{P_{rv(eff)} \cdot L_{m/tm}}{P_{nv(eff)}} \tag{42}$$

3.8 Transponder Turnaround Modulation Indices

The transponder turnaround modulation indices, α, β, λ, ξ, are computed for every uplink SNR as satellite receive gain and effective radiated power are varied.

3.8.1 Transponder Turnaround Ranging Modulation Index

$$\alpha = TRC \bullet \left(\frac{SNR_{IF}}{1 + SNR_{IF}}\right)^{1/2} \bullet \sin \phi \bullet J_o\,(mv) \bullet J_o(mtm) \tag{43}$$

where; TRC is the transponder ranging gain constant

SNR_{IF} is the transponder IF bandwidth

ϕ is the uplink ranging modulation index

mv is the upvoice modulation index

mtm is the updata modulation index

3.8.2 Transponder Turnaround Updata Modulation Index

$$\beta = 2 \bullet TRC \bullet \left(\frac{SNR_{IF}}{1 + SNR_{IF}}\right)^{1/2} \bullet \cos\phi \bullet J_o(mv) \bullet J_1\,(mtm) \tag{44}$$

3.8.3 Transponder Turnaround Upvoice Modulation Index

$$\lambda = 2 \bullet TRC \bullet \left(\frac{SNR_{IF}}{1 + SNR_{IF}}\right)^{1/2} \bullet \cos\phi \bullet J_1(mv) \bullet J_o\,(mtm) \tag{45}$$

3.8.4 Transponder Turnaround Thermal Modulation Index

$$\xi = TRC \bullet \left(\frac{1}{1 + SNR_{IF}}\right)^{1/2} \bullet \left(\frac{2 \bullet BW_r}{BW_{IF}}\right)^{1/2} \tag{46}$$

where; BW_r is the transponder video bandwidth

BW_{IF} is the transponder IF bandwidth

3.9 Downlink Modulation Losses

The downlink, vehicle-to-MSFN via satellite, modulation losses are calculated for each information service; including carrier, voice, telemetry,

and ranging. The calculations use the PM downlink modulation indices and the turnaround modulation indices. Two cases are allowed; 1) with voice on subcarrier, and 2) with voice at baseband (no ranging).

3.9.1 Downlink Ranging Modulation Loss

$$L_{m/pd} = \sin^2\alpha \bullet J_0^2\,(mv) \bullet J_0^2\,(mtm) \bullet J_0^2(\beta) \bullet J_0^2(\lambda) \bullet J_0^2(\xi) \qquad (47)$$

3.9.2 Downlink Modulation Losses with Voice on Subcarrier

3.9.2.1 Downlink Carrier Modulation Loss

$$L_{m/cd} = \cos^2\alpha \bullet J_0^2(mv) \bullet J_0^2\,(mtm) \bullet J_0^2\,(\beta) \bullet J_0^2(\lambda) \bullet J_0^2(\xi) \qquad (48)$$

3.9.2.2 Downlink Voice Modulation Loss

$$L_{m/vd} = 2 \bullet \cos^2\alpha \bullet J_1^2\,(mv) \bullet J_0^2\,(mtm) \bullet J_0^2(\beta) \bullet J_0^2(\lambda) \bullet J_0^2(\xi) \qquad (49)$$

3.9.2.3 Downlink Telemetry Modulation Loss

$$L_{m/td} = 2 \bullet \cos^2\alpha \bullet J_0^2(mv) \bullet J_1^2(mtm) \bullet J_0^2(\beta) \bullet J_0^2(\lambda) \bullet J_0^2(\xi) \qquad (50)$$

3.9.3 Downlink Modulation Losses with Voice at Baseband

3.9.3.1 Downlink Carrier Modulation Loss

$$L_{m/cd} = \cos^2\,(\rho \bullet mv) \bullet J_0^2(mtm) \qquad (51)$$

where; ρ is the rms-to-peak factor for voice

3.9.3.2 Downlink Voice Modulation Loss

$$L_{m/vd} = \sin^2\,(\rho \bullet mv) \bullet J_0^2(mtm) \qquad (52)$$

3.9.3.3 Downlink Telemetry Modulation Loss

$$L_{m/td} = 2 \bullet \cos^2\,(\rho \bullet mv) \bullet J_1^2(mtm) \qquad (53)$$

3.10 Downlink Satellite Received Signal-to-Noise Ratio

The downlink satellite received SNR is calculated in the same

manner as was the uplink satellite SNR (refer to Paragraph 3.3.4).

3.10.1 Total Received Power

$$P_{rs} = \frac{P_t G_t G_r}{4\pi R^2} \bullet \frac{\lambda^2}{4\pi} \qquad (54)$$

where; P_t is vehicle transmit power

G_t is vehicle transmit antenna gain including losses

G_r is satellite effective receive gain (includes satellite receive system losses)

R is vehicle-to-satellite range

λ is wavelength of received carrier

3.10.2 Received Carrier Power

$$P_{cs} = P_{rs} \bullet L_{m/cd} \qquad (55)$$

3.10.3 Satellite Receiver Noise Power

$$P_{ns} = k \bullet (A + B \bullet P_{cs}) \bullet BW_{IF} \qquad (56)$$

where; k is Boltzman's constant

A is satellite system noise temperature

B is satellite receiver AGC noise factor

BW_{IF} is satellite transponder IF bandwidth

3.10.4 Satellite Received Signal-to-Noise Ratio

$$SNR_{sat} = \frac{P_{cs}}{P_{ns}} \qquad (57)$$

NOTE: The satellite transmitted SNR is assumed equal to the satellite received SNR.

3.11 MSFN Effective Downlink Received Signal-to-Noise Ratio

3.11.1 MSFN Total Received Power

$$P_{rm} = \frac{P_t G_t G_r}{4\pi R^2} \bullet \frac{\lambda^2}{4\pi} \qquad (58)$$

where; P_tG_t is the satellite effective radiated power

G_r is the MSFN receive gain including losses

R is the satellite-to-MSFN range

λ is the received carrier wavelength

3.11.2 MSFN Total Effective Received Signal Power

$$P_{rm(eff)} = P_{rm} \bullet \frac{P_{cs}}{P_{cs} + P_{ns}} \quad (59)$$

3.11.3 MSFN Received Carrier Power

$$P_{cm} = P_{rm} \bullet L_{m/cd} \quad (60)$$

3.11.4 MSFN Receiver Noise Power

$$P_{nm} = k \bullet (A + B \bullet P_{cm}) \bullet BW_{IF} \quad (61)$$

where; k is Boltzman's constant

A is MSFN system noise temperature

B is MSFN receiver AGC noise factor

BW_{IF} is MSFN receiver IF bandwidth

3.11.5 MSFN Total Effective Noise Power

$$P_{nm(eff)} = P_{nm} + \frac{P_{ns}}{P_{cs} + P_{ns}} \bullet P_{rm} \quad (62)$$

3.11.6 MSFN Effective Received Signal-to-Noise Ratio

$$SNR_m = \frac{P_{rm(eff)}}{P_{nm(eff)}} \quad (63)$$

3.12 Downlink Carrier Channel Effective Signal-to-Noise Ratio

$$SNR_{c(eff)} = \frac{BW_{IF}}{BW_c} \bullet \frac{P_{rm(eff)} \bullet L_{m/cd}}{P_{nm(eff)}} \quad (64)$$

3.13 Downlink Voice Channel Effective Signal-to-Noise Ratio

$$SNR_{v(eff)} = \frac{BW_{IF}}{BW_v} \bullet \frac{P_{rm(eff)} \bullet L_{m/vd}}{P_{nm(eff)}} \tag{65}$$

3.14 Downlink Telemetry Channel Effective Signal-to-Noise Ratio

$$SNR_{t(eff)} = \frac{BW_{IF}}{BW_t} \bullet \frac{P_{rm(eff)} \bullet L_{m/bd}}{P_{nm(eff)}} \tag{66}$$

3.15 Downlink Ranging Channel Effective Signal-to-Noise Ratio

$$SNR_{p(eff)} = \frac{BW_{IF}}{BW_p} \bullet \frac{P_{rm(eff)} \bullet L_{m/pd}}{P_{nm(eff)}} \tag{67}$$

4. ANALYSIS OF SATELLITE ERP AND ANTENNA GAIN USING SATCOM COMPUTER PROGRAM

This section discusses the analyses performed to determine the required satellite effective radiated power and effective receiver gain. Uplink and downlink computations were made for the six cases of Table 4 using the parameters as described in Appendix A. The common parameters for all cases include:

No. of Satellites	3
Vehicle Altitude (orbiting)	60 n.m.
Range (MSFN - Satellite)	215320 n.m.
Range (Satellite - Vehicle)	5621 n.m.
Lunar Surface Overlap Angle	30 degrees
Satellite Altitude	4500 n.m.
Vehicle Elevation Angle to Lunar Surface Grazing Plane	5 degrees

In each case a representative Apollo mode was used to determine the satellite antenna requirements. This paper reports the analysis of the effect of bandwidth and required SNR in this bandwidth on the satellite antenna requirements.

Figure 36 through 47 present the results of the analysis as obtained using the computer program described by Reference 5-2. These plots are of required satellite effective radiated power versus IF bandwidth signal-to-noise ratio for a family of satellite effective received gain curves. The receive gain curves are in 5 dB increments increasing in gain from bottom to top of the graph. The bottom curve is labeled in db of gain and the horizontal line across the graph is the required IF SNR for that system (see Appendix A). Thus, any combination of effective receive gain and radiated power on or above this horizontal line will produce positive IF margins in the terminal receiver (vehicle or MSFN).

A pair of plots describe an uplink and downlink for each case. Figure 36 and 37 are the uplink and downlink plots respectively for the wideband Apollo using the high gain antennas, case No. 1 of Table 4 listed below. Each curve in the receive gain family has a flattening shape with increasing radiated power. This shows a constant upper limit in received SNR and is due to the satellite transmitted SNR being the upper limit obtainable in the vehicle (or MSFN) receiver. Also, increasing the satellite receive gain for a constant satellite effective radiated power will reach an upper limit of receive gain, above which no increase in received SNR is obtainable. This is caused by the limiting of the terminal receiver noise.

The results of this analysis have been summarized in Section 2, Conclusions. Figures 30 and 31 are curves of the intersections of required SNR and the family of curves shown in Figures 36 through 47.

Table 4. Summary of Link Usage

Case	System	Bandwidth	Vehicle Antenna	Apollo Mode
1	Apollo	Wideband	High Gain	6.2
2	Apollo	Narrowband	Omni	7.10
3	Apollo	Narrowband	High Gain	7.4
4	Modified	Wideband	High Gain	6.2
5	Modified	Narrowband	Omni	7.10
6	Modified	Narrowband	High Gain	7.4

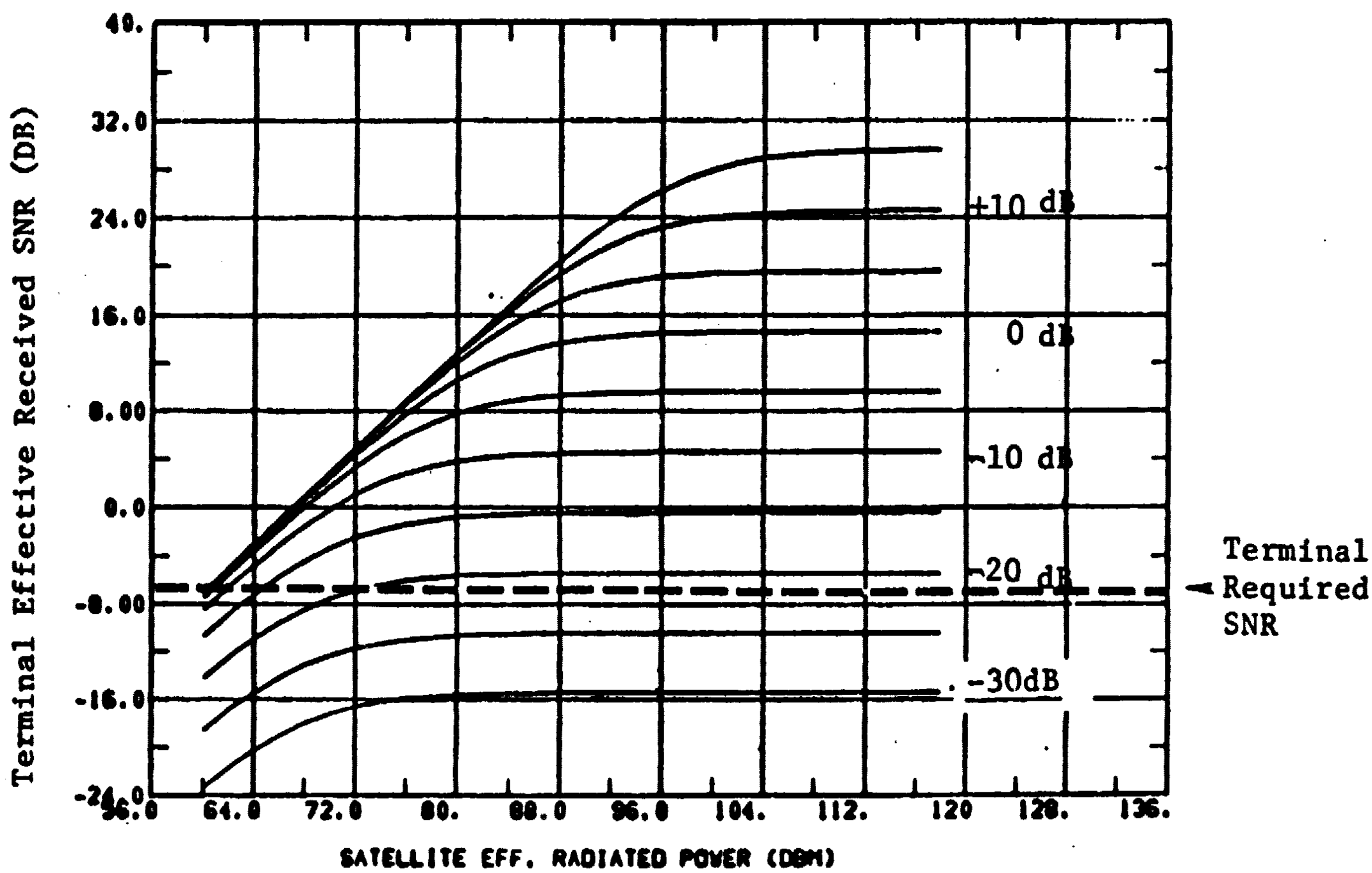

NO. OF SATELLITES	= 3.0000	SATELLITE ALTITUDE	= 4500.0
COMMUNICATION MODE	= 6.2000	SAT.-VEH. RANGE	= 5620.6
MSFN ELV. ANGLE	= 5.0000	TRANS. POWER	= 10000.
VEHICLE ELV. ANGLE	= 5.0000	TRANS. ANT. GAIN	= 52.500
OVERLAP ANGLE	= 30.000	RECIEVED ANT. GAIN	= 23.000

FIGURE 36. SATELLITE ERP VS TERMINAL RECEIVED SNR FOR DIFFERENT SATELLITE RECEIVER GAINS

WIDEBAND APOLLO SYSTEM - CSM-UPLINK (HGA)

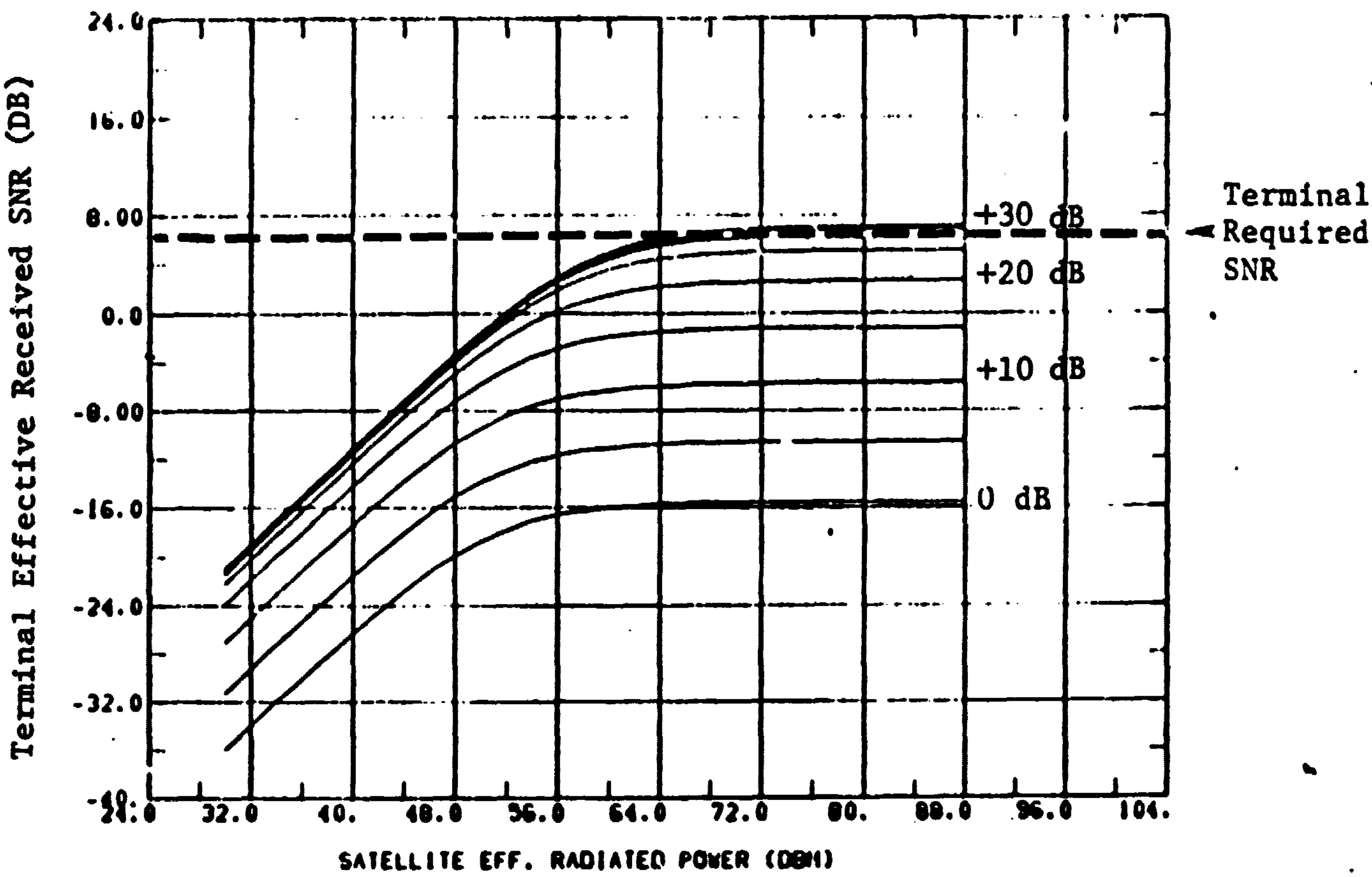

NO. OF SATELLITES	= 3.0000	SATELLITE ALTITUDE	= 4500.0
COMMUNICATION MODE	= 6.2000	SAT.-VEH. RANGE	= 5620.6
MIN ELV. ANGLE	= 5.0000	TRANS. POWER	= 12.000
VEHICLE ELV. ANGLE	= 5.0000	TRANS. ANT. GAIN	= 26.000
OVERLAP ANGLE	= 30.000	RECIEVED ANT. GAIN	= 53.000

FIGURE 37. SATELLITE ERP VS TERMINAL RECEIVED SNR FOR DIFFERENT SATELLITE RECEIVER GAINS

WIDEBAND APOLLO SYSTEM - CSM-DOWNLINK (HGA)

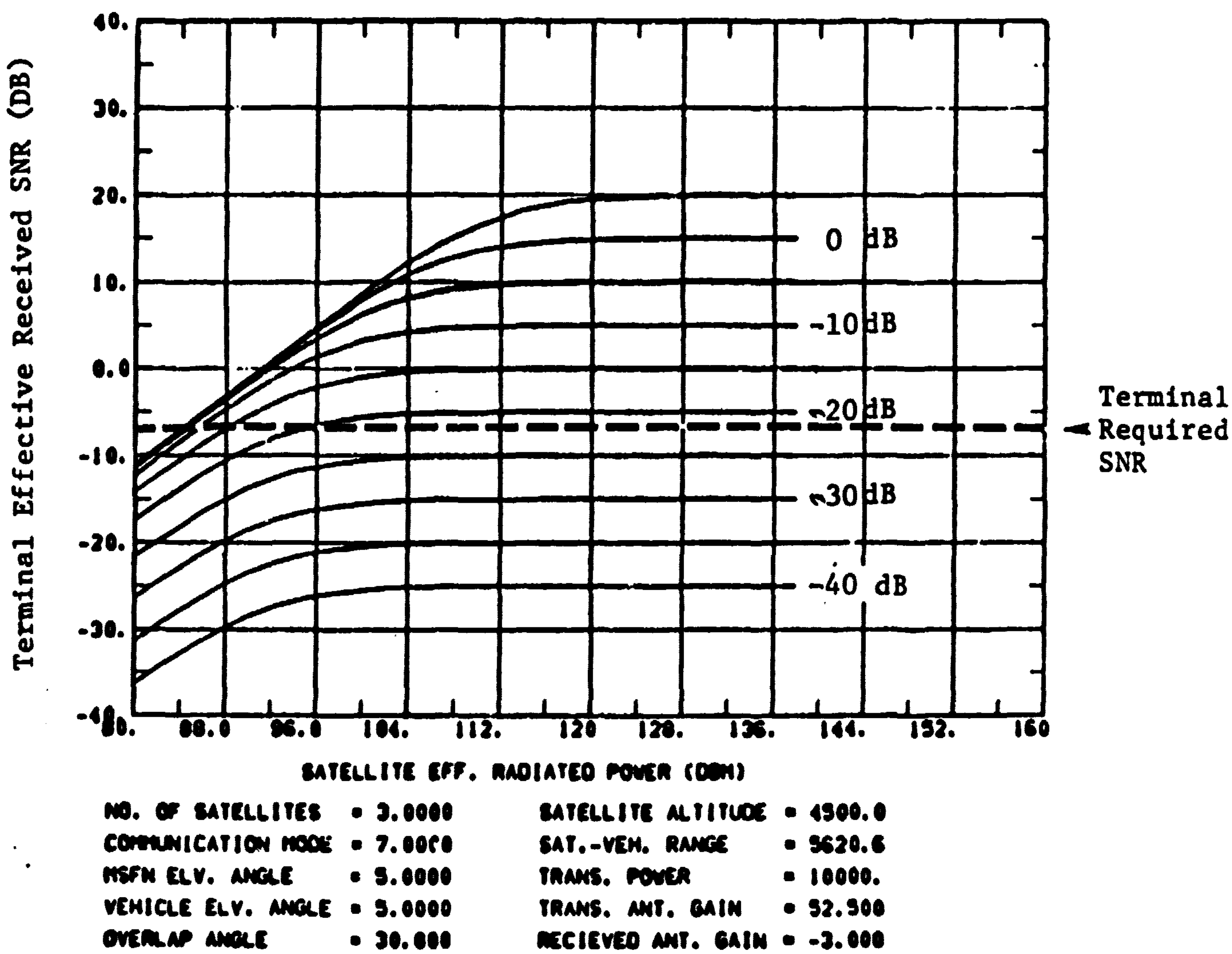

FIGURE 38. SATELLITE ERP VS TERMINAL RECEIVED SNR FOR DIFFERENT SATELLITE RECEIVER GAINS

NARROWBAND APOLLO SYSTEM - CSM-UPLINK (OMNI)

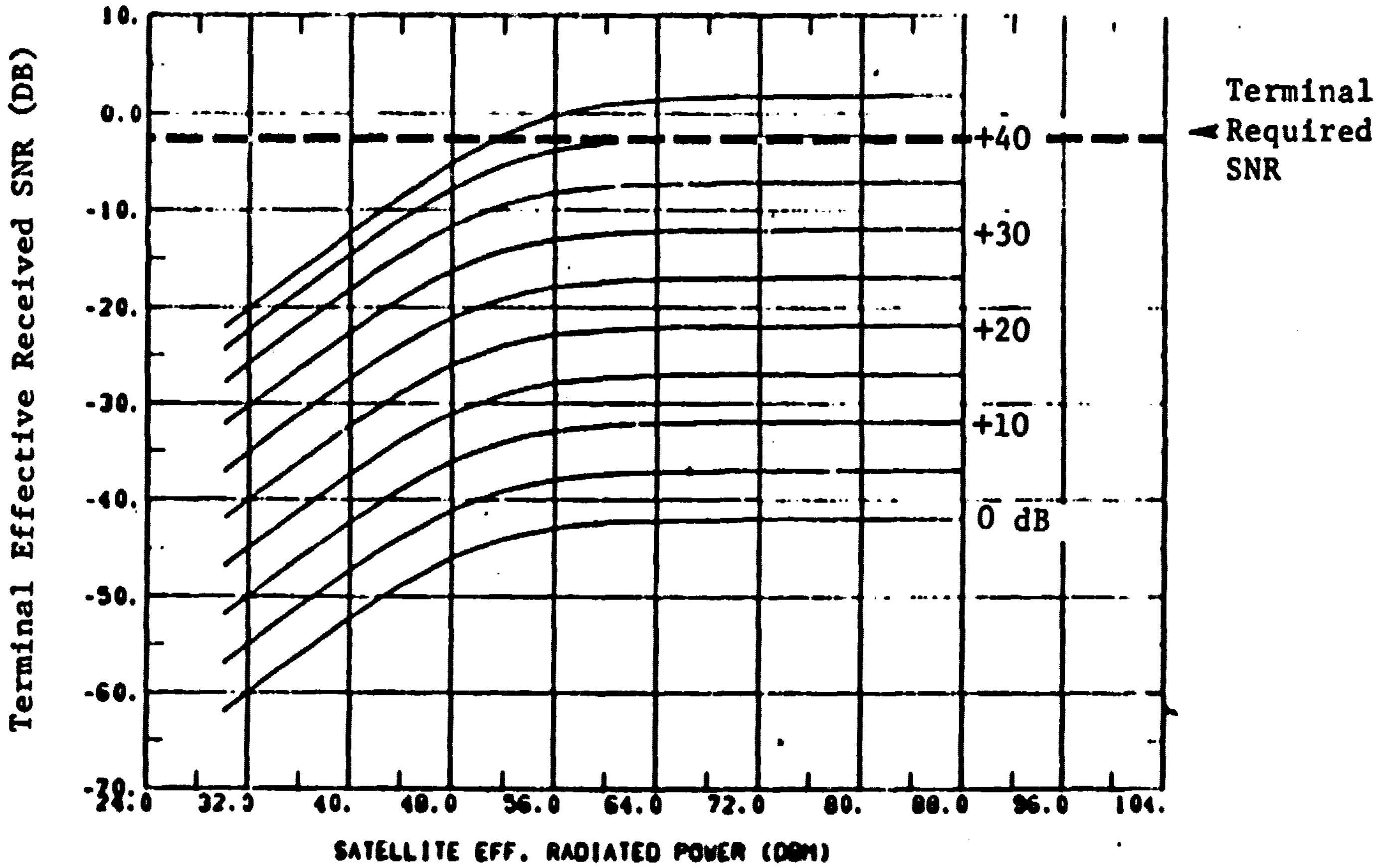

NO. OF SATELLITES	= 3.0000	SATELLITE ALTITUDE	= 4500.0
COMMUNICATION MODE	= 7.0000	SAT.-VEH. RANGE	= 5620.6
MSFN ELV. ANGLE	= 5.0000	TRANS. POWER	= 12.000
VEHICLE ELV. ANGLE	= 5.0000	TRANS. ANT. GAIN	= -3.000
OVERLAP ANGLE	= 30.000	RECIEVED ANT. GAIN	= 53.000

FIGURE 39. SATELLITE ERP VS TERMINAL RECEIVED SNR FOR DIFFERENT SATELLITE RECEIVER GAINS

NARROWBAND APOLLO SYSTEM - CSM-DOWNLINK (OMNI)

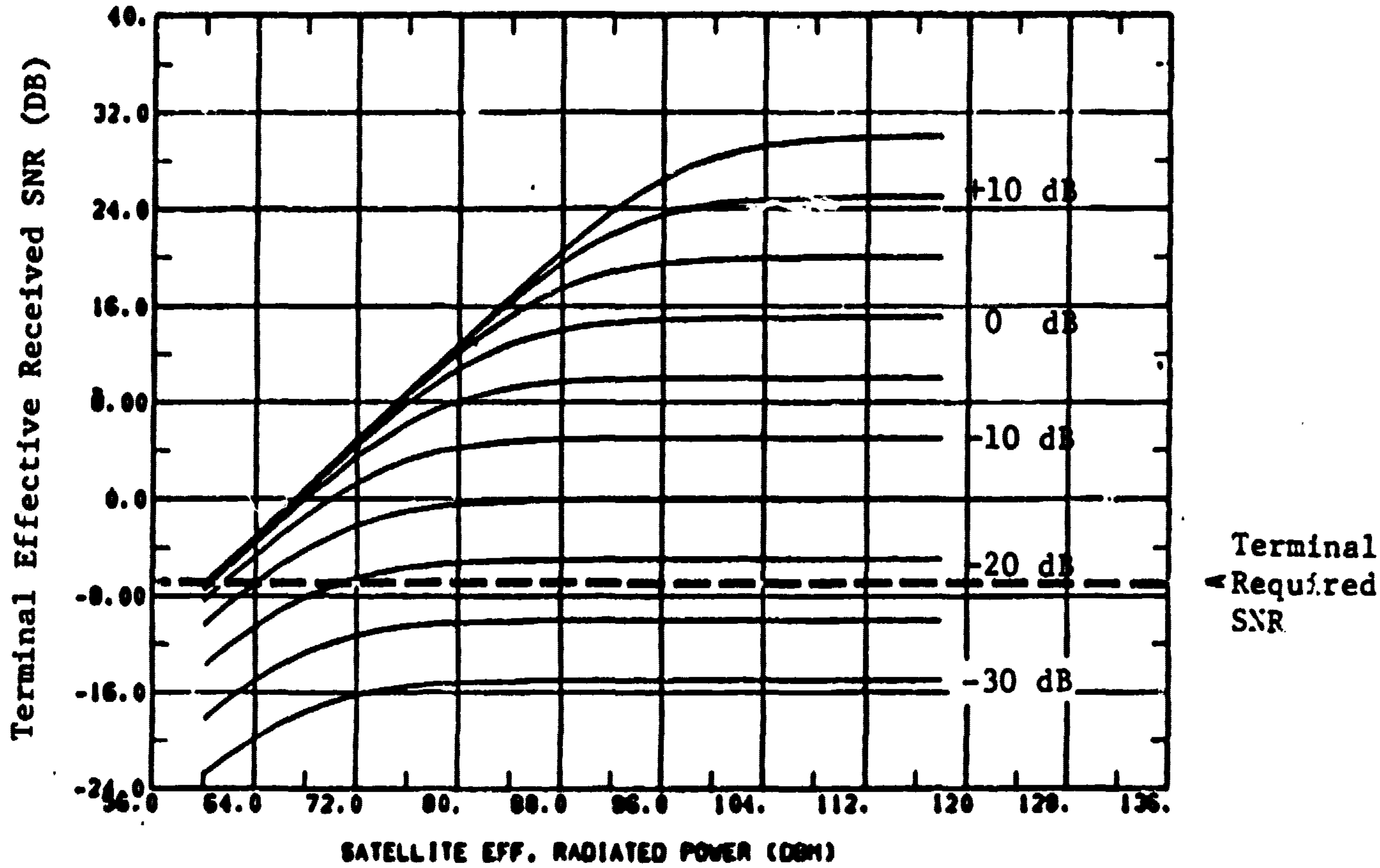

NO. OF SATELLITES	= 3.0000	SATELLITE ALTITUDE	= 4500.0
COMMUNICATION MODE	= 7.4000	SAT.-VEH. RANGE	= 5620.6
MSFN ELV. ANGLE	= 5.0000	TRANS. POWER	= 10000.
VEHICLE ELV. ANGLE	= 5.0000	TRANS. ANT. GAIN	= 52.500
OVERLAP ANGLE	= 30.000	RECIEVED ANT. GAIN	= 23.000

FIGURE 40. SATELLITE ERP VS TERMINAL RECEIVED SNR FOR DIFFERENT SATELLITE RECEIVER GAINS

NARROWBAND APOLLO SYSTEM - CSM UPLINK (HGA)

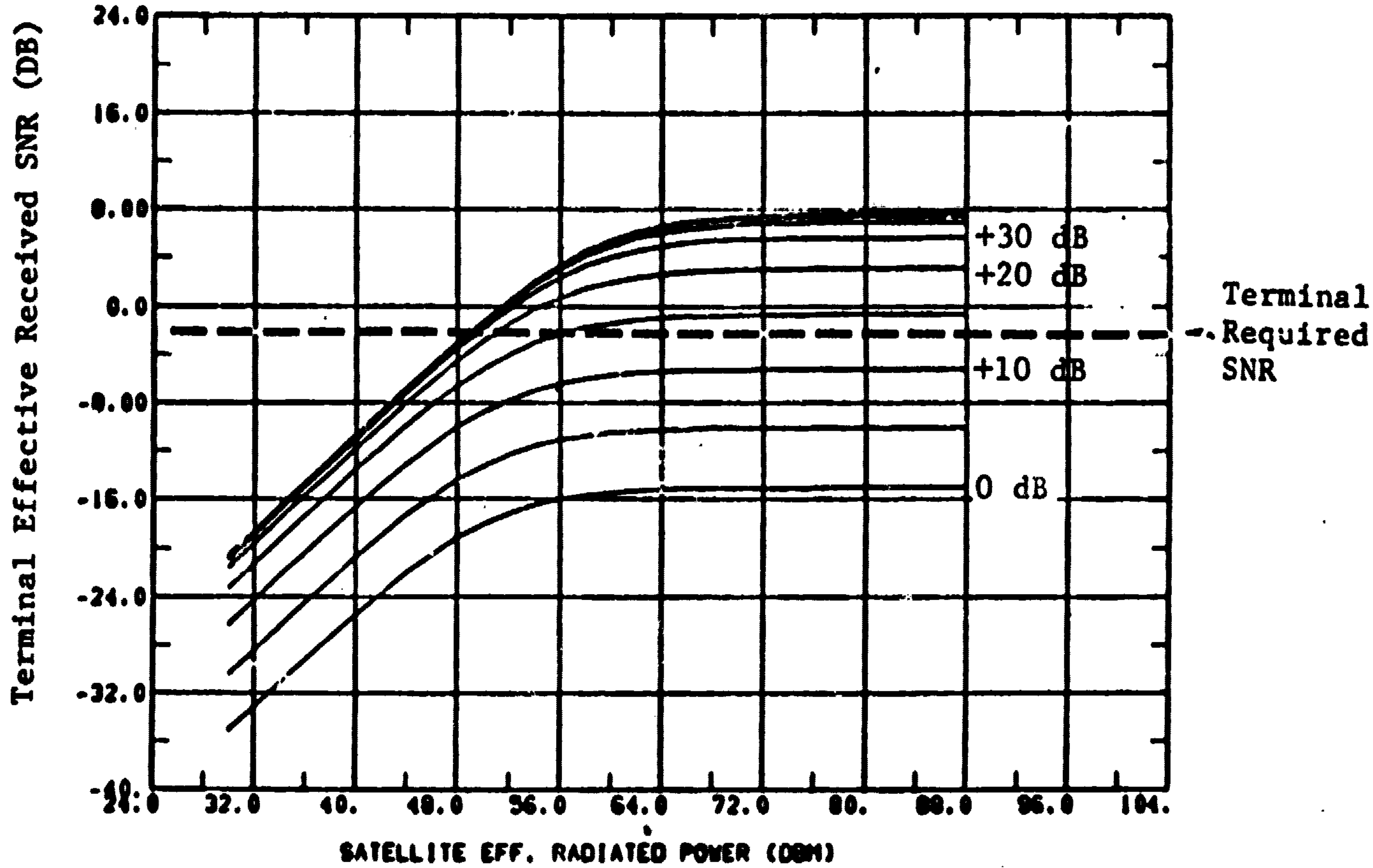

NO. OF SATELLITES	= 3.0000	SATELLITE ALTITUDE	= 4500.0
COMMUNICATION MODE	= 7.4000	SAT.-VEH. RANGE	= 5620.6
MSFN ELV. ANGLE	= 5.0000	TRANS. POWER	= 12.000
VEHICLE ELV. ANGLE	= 5.0000	TRANS. ANT. GAIN	= 26.000
OVERLAP ANGLE	= 30.000	RECIEVED ANT. GAIN	= 53.000

FIGURE 41. SATELLITE ERP VS TERMINAL RECEIVED SNR FOR DIFFERENT SATELLITE RECEIVER GAINS

NARROWBAND APOLLO SYSTEM - CSM-DOWNLINK (HGA)

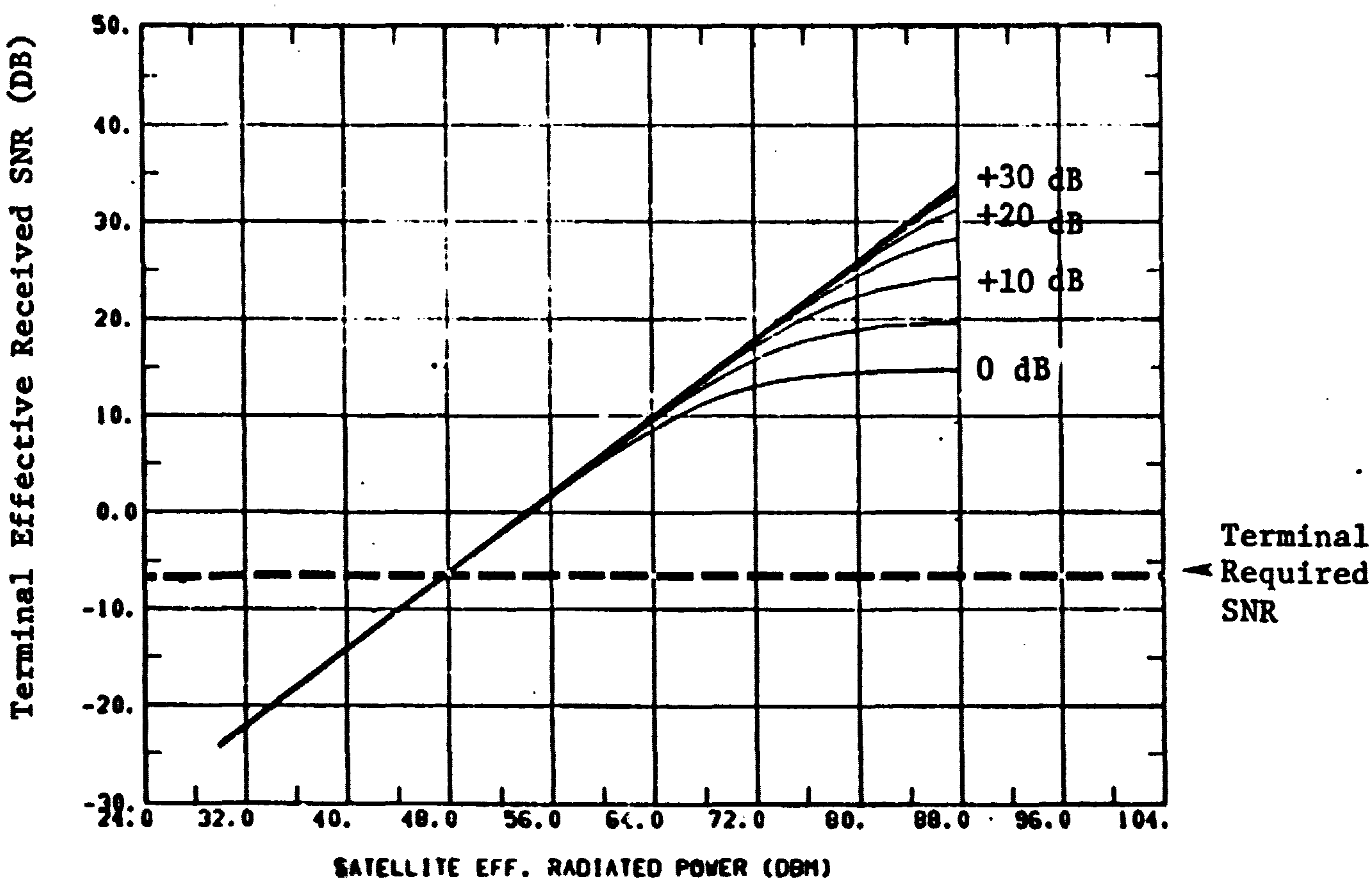

NO. OF SATELLITES	= 3.0000	SATELLITE ALTITUDE	= 4500.0
COMMUNICATION MODE	= 6.2000	SAT.-VEH. RANGE	= 5620.6
MSFN ELV. ANGLE	= 5.0000	TRANS. POWER	= 10000.
VEHICLE ELV. ANGLE	= 5.0000	TRANS. ANT. GAIN	= 64.500
OVERLAP ANGLE	= 30.000	RECIEVED ANT. GAIN	= 23.000

FIGURE 42. SATELLITE ERP VS TERMINAL RECEIVED SNR FOR DIFFERENT SATELLITE RECEIVER GAINS

WIDEBAND MODIFIED SYSTEM - CSM UPLINK (HGA)

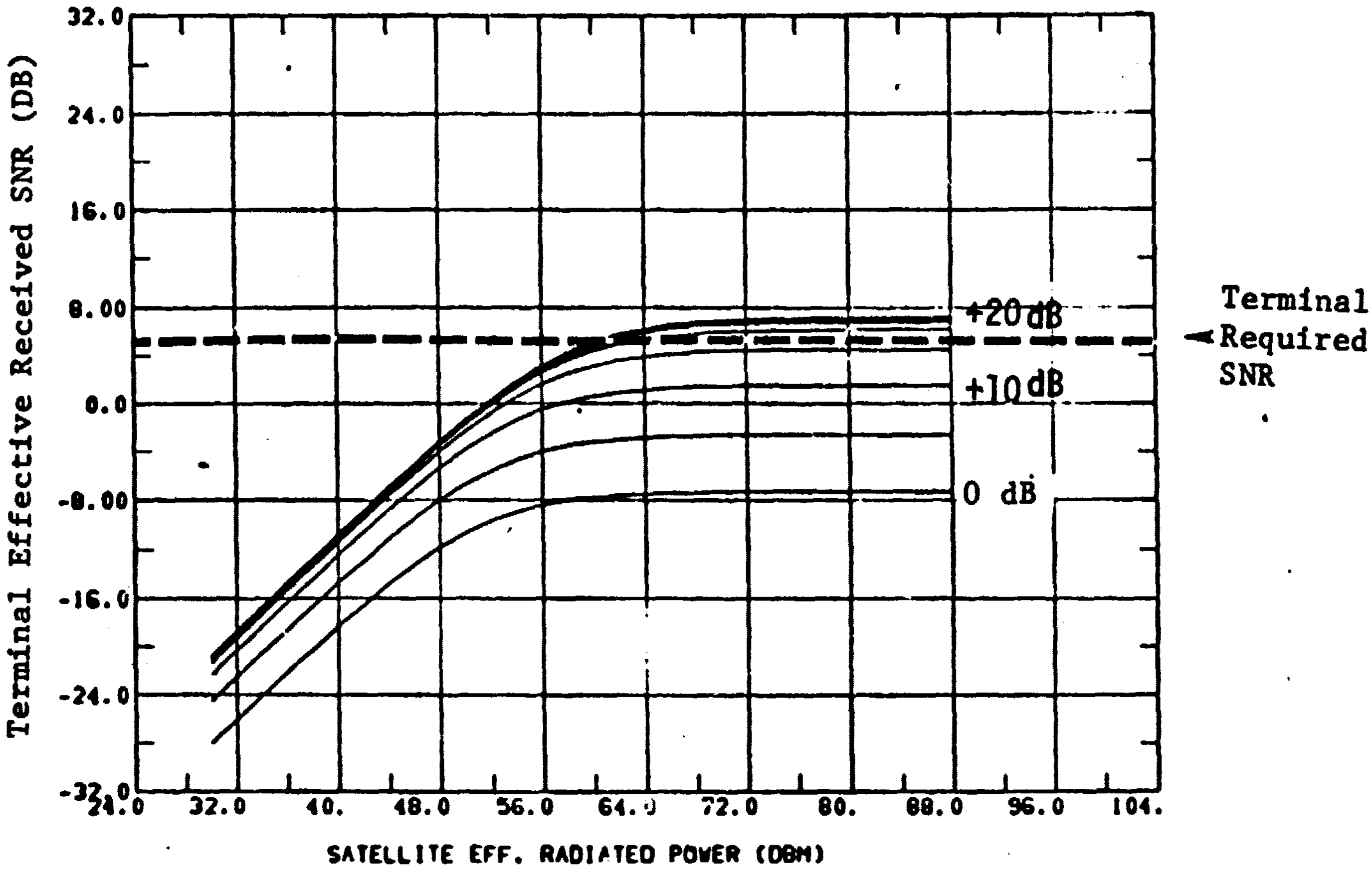

NO. OF SATELLITES	= 3.0000	SATELLITE ALTITUDE	= 4500.0
COMMUNICATION MODE	= 6.2000	SAT.-VEH. RANGE	= 5620.6
MSFN ELV. ANGLE	= 5.0000	TRANS. POWER	= 50.000
VEHICLE ELV. ANGLE	= 5.0000	TRANS. ANT. GAIN	= 26.000
OVERLAP ANGLE	= 30.000	RECIEVED ANT. GAIN	= 64.600

FIGURE 43. SATELLITE ERP VS TERMINAL RECEIVED SNR FOR DIFFERENT SATELLITE RECEIVER GAINS

WIDEBAND MODIFIED SYSTEM - CSM-DOWNLINK (HGA)

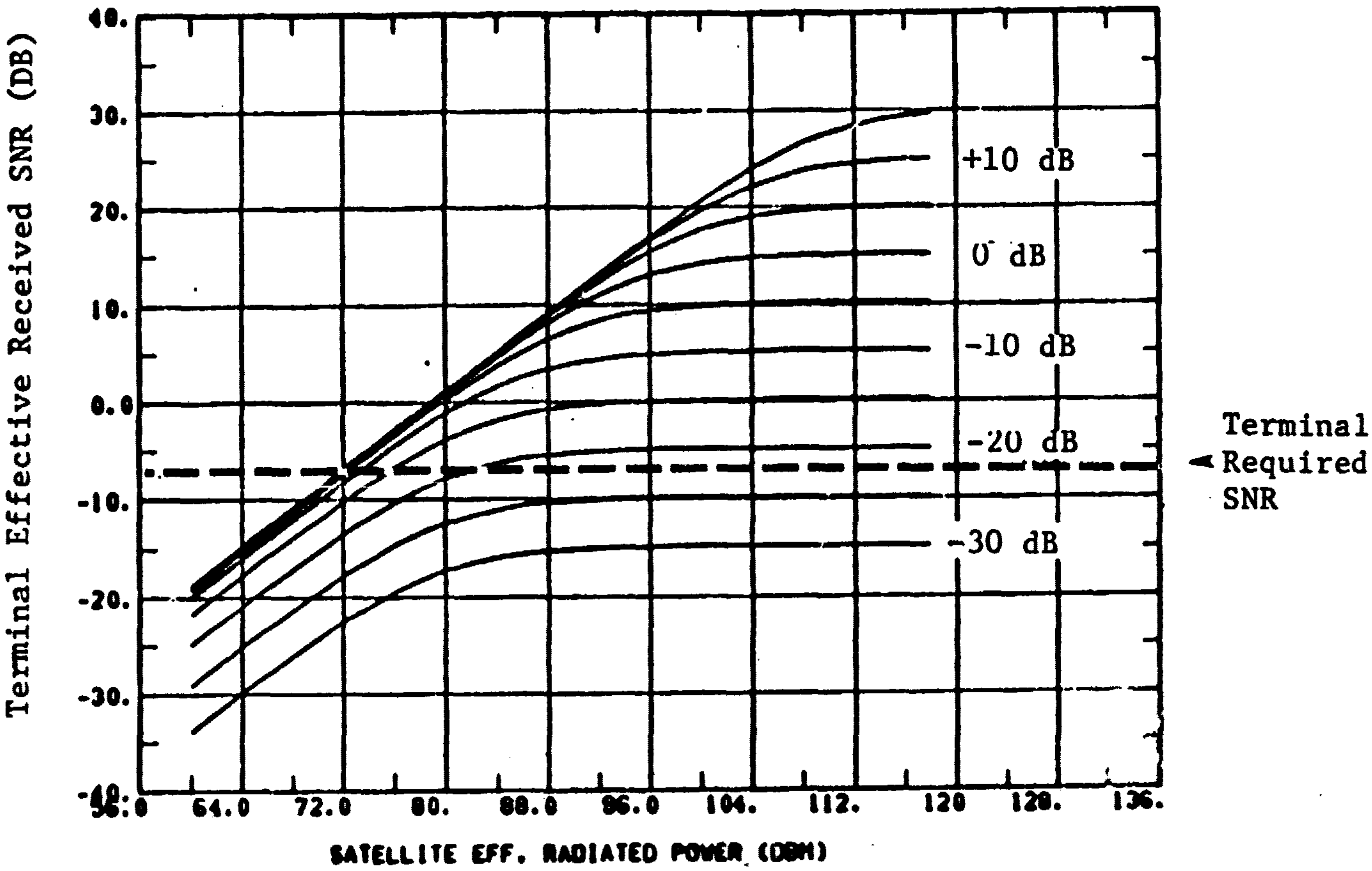

NO. OF SATELLITES	= 3.0000	SATELLITE ALTITUDE	= 4500.0
COMMUNICATION MODE	= 7.0000	SAT.-VEH. RANGE	= 5620.6
MSFN ELV. ANGLE	= 5.0000	TRANS. POWER	= 10000.
VEHICLE ELV. ANGLE	= 5.0000	TRANS. ANT. GAIN	= 64.500
OVERLAP ANGLE	= 30.000	RECIEVED ANT. GAIN	= -3.000

FIGURE 44. SATELLITE ERP VS TERMINAL RECEIVED SNR FOR DIFFERENT SATELLITE RECEIVER GAINS

NARROWBAND MODIFIED SYSTEM - CSM-UPLINK (OMNI)

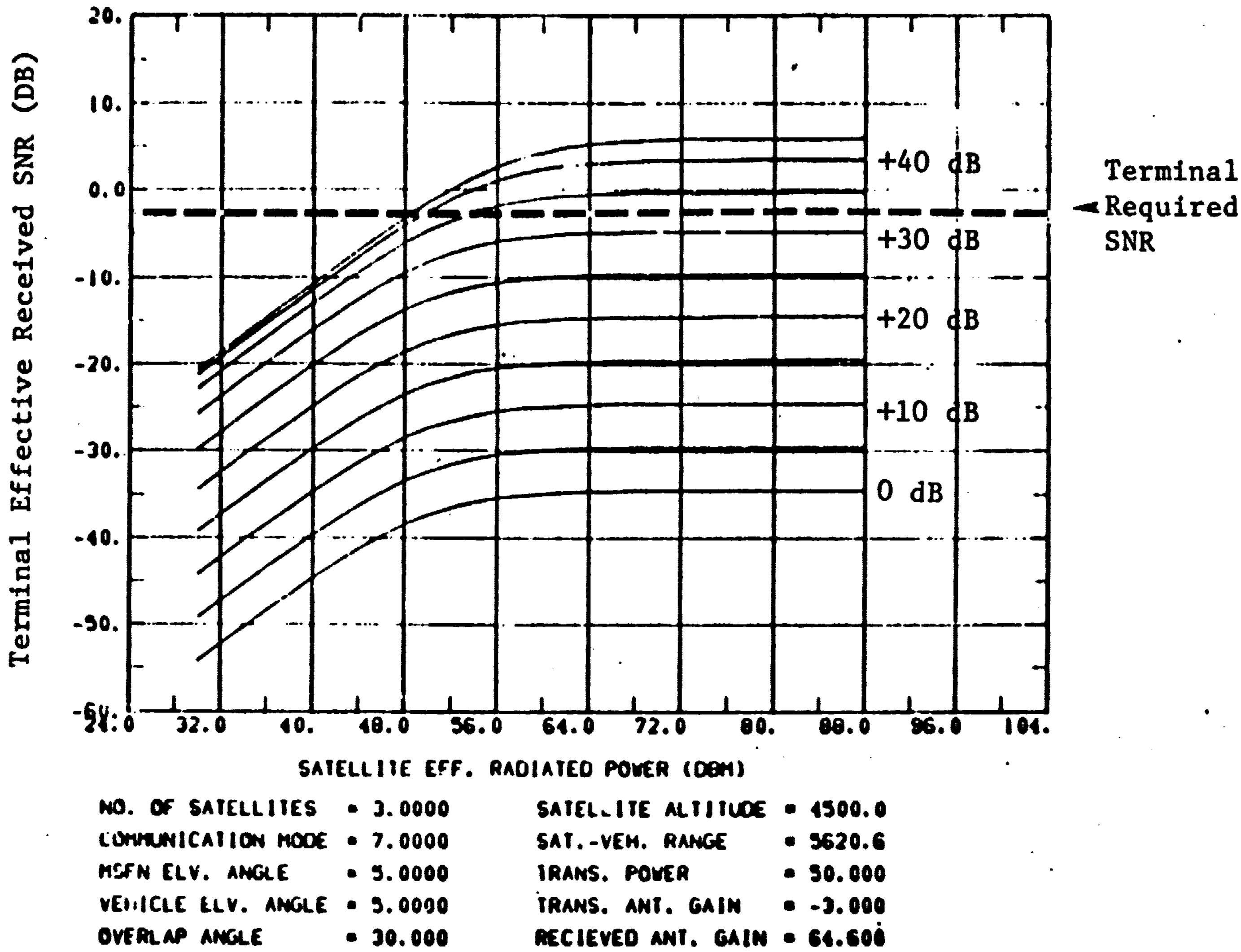

FIGURE 45. SATELLITE ERP VS TERMINAL RECEIVED SNR FOR DIFFERENT SATELLITE RECEIVER GAINS

NARROWBAND MODIFIED SYSTEM - CSM-DOWNLINK (OMNI)

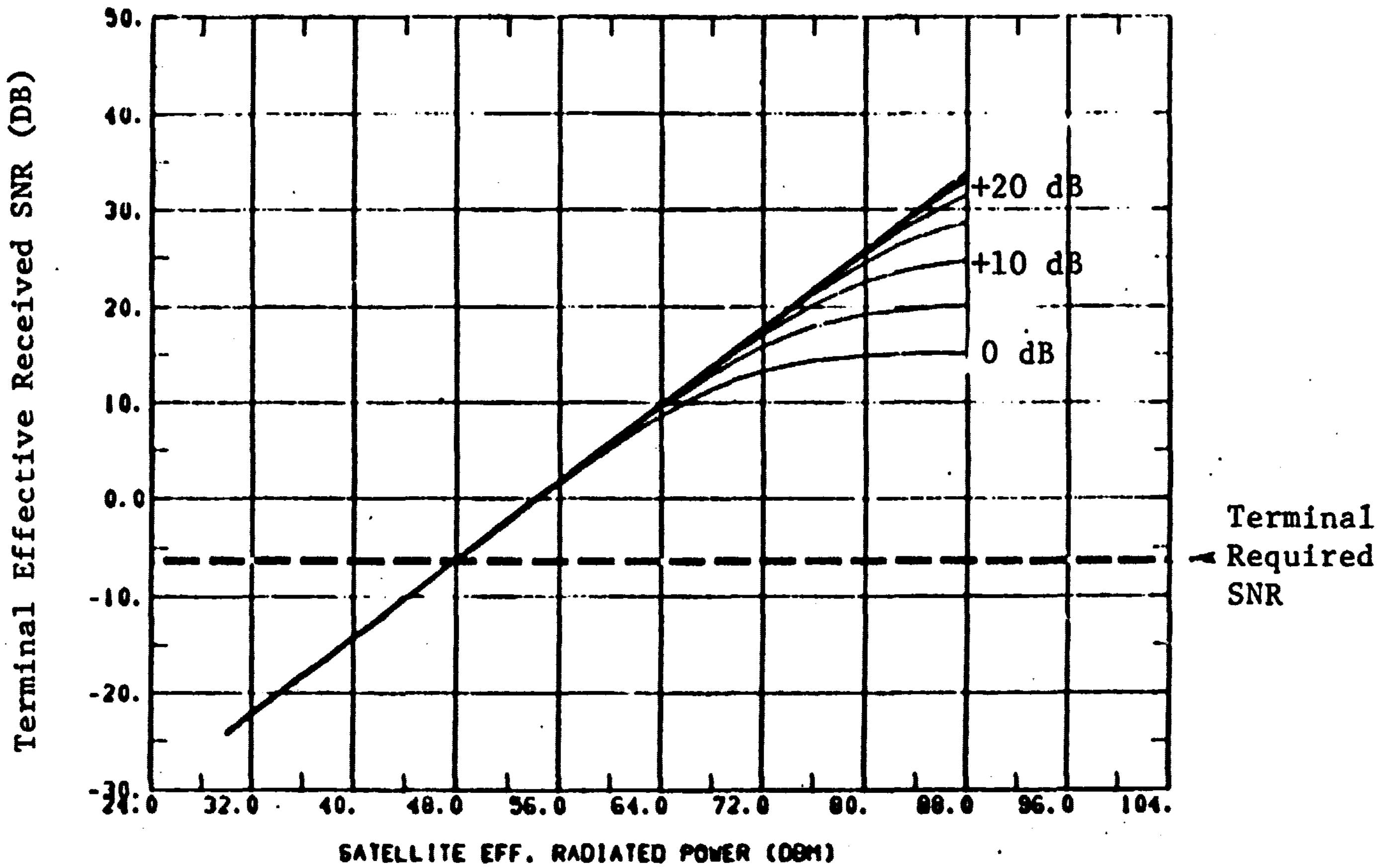

NO. OF SATELLITES	= 3.0000	SATELLITE ALTITUDE	= 4500.0
COMMUNICATION MODE	= 7.4000	SAT.-VEH. RANGE	= 5620.6
MSFN ELV. ANGLE	= 5.0000	TRANS. POWER	= 10000.
VEHICLE ELV. ANGLE	= 5.0000	TRANS. ANT. GAIN	= 64.500
OVERLAP ANGLE	= 30.000	RECIEVED ANT. GAIN	= 23.000

FIGURE 46. SATELLITE ERP VS TERMINAL RECEIVED SNR FOR DIFFERENT SATELLITE RECEIVER GAINS

NARROWBAND MODIFIED SYSTEM - CSM-UPLINK (HGA)

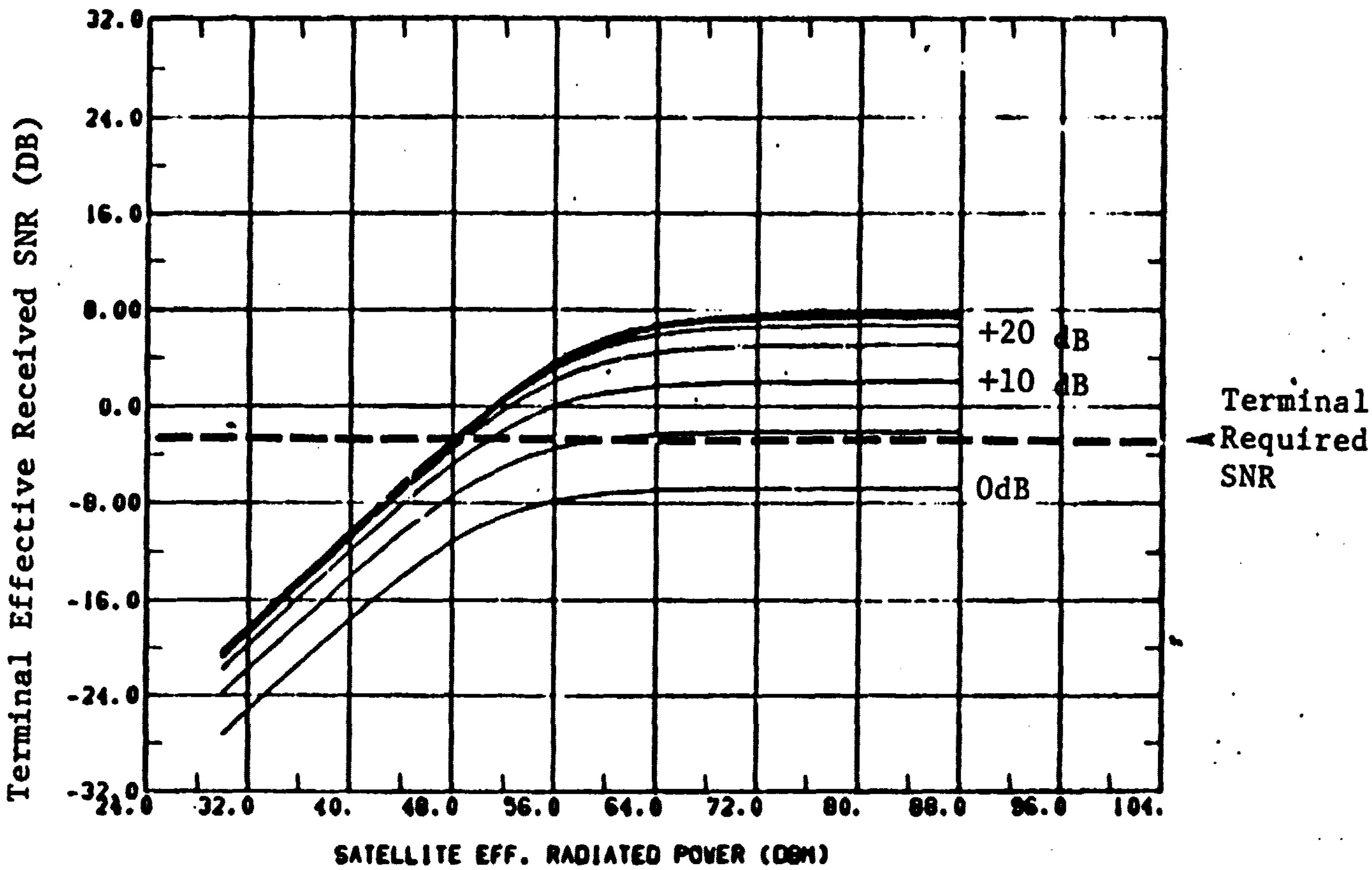

NO. OF SATELLITES	= 3.0000	SATELLITE ALTITUDE	= 4500.0
COMMUNICATION MODE	= 7.4000	SAT.-VEH. RANGE	= 5620.6
MSFN ELV. ANGLE	= 5.0000	TRANS. POWER	= 50.000
VEHICLE ELV. ANGLE	= 5.0000	TRANS. ANT. GAIN	= 26.000
OVERLAP ANGLE	= 30.000	RECIEVED ANT. GAIN	= 64.600

FIGURE 47. SATELLITE ERP VS TERMINAL RECEIVED SNR FOR DIFFERENT SATELLITE RECEIVER GAINS

NARROWBAND MODIFIED SYSTEM - CSM-DOWNLINK (HGA)

REFERENCES

5-1. G. D. Arndt and G. A. Jaegers, "A Computer Program and Math Model for the Unified S-Band System", MSC/ISD Report EB-66-200-U.

5-2. G. L. Houser, "Lunar Communications Satellite Analysis Program (SATCOM), HVO2SA", TRW Report #11176-H398-RO-OO.

APPENDIX A

GROUND RULES FOR LUNAR COMMUNICATION SATELLITE TRADE-OFF STUDIES

Emphasis on the tradeoff studies will be on lunar far side communications for a 1975 launch date. PHO will undertake a study of libration point satellite systems. TRW will undertake a study of low-medium orbit satellite systems. Both PHO and TRW will apply the ground rules listed in this report to the following areas of concentration:

1) Communication Coverage
2) Communication Link Margins (satellite ERP and antenna specifications)
3) Station-Keeping
4) Lifetime
5) Deployment
6) Listing of Advantages and Disadvantages

GROUND RULES

1. <u>Communication Coverage</u>

The relay satellite shall communicate between an 85 foot MSFN ground station and multiple lunar vicinity communication systems located beyond line-of-sight of the earth on either the lunar surface or in a 100 nautical mile lunar orbit.

2. <u>Communication Link Margins (Satellite ERP and Antenna Specifications)</u>

The relay satellite ERP, antenna diameter, beamwidth, gain, and losses, for downlink (lunar vicinity-to-satellite-to-earth) communications shall be calculated for both a narrowband system (via a lunar vicinity omni antenna or high gain antenna) and a wideband system (via a lunar vicinity high gain antenna). The same information for uplink (earth-to-satellite-to-lunar-vicinity) communications shall be calculated only for a narrowband system. <u>A frequency translation repeater is assumed to be the basic relay device</u> Communication parameters to be used for both studies are the following:

TABLE A-1. UPLINK PARAMETERS

Parameter	APOLLO COMMUNICATION SYSTEM		MODIFIED COMMUNICATION SYSTEM		
	Omni	Hi-Gain	Omni	Hi-Gain	Units
Ground Station transmitting frequency TFRMS	2.1	2.1	8.4	8.4	GHz
Ground Station transmitting power PTMSFN	10	10	10	10	Kw
Ground Station transmitting circuit loss TLMSFN	0.5	0.5	0.5	0.5	dB
Ground Station transmitting antenna gain GTMSFN	52.5	52.5	64.5	64.5	dB
Satellite receiver circuit loss	3	3	2	2	dB
Satellite receiver system temp. (NF=3dB) ASAT	610	610	580	580	^{o}K
Satellite transmitter frequency TFUSAT	2.1	2.1	2.1	2.1	GHz
Lunar Vicinity receiver antenna gain GRVEH*	-3	23	-3	23	dB
Lunar vicinity receiver circuit loss RLVEH	3	5	2	3	dB
Lunar vicinity receiver system temp. AVEH**	5685	5727	435	564	^{o}K
Lunar vicinity receiver SNR	-6.8	-6.8	-6.8	-6.8	dB
Lunar vicinity receiver margin	0	0	0	0	dB
Uplink IF noise BW (Satellite and Lunar receiver) BWIFSA & SWIFVE	4.8	4.8	4.8	4.8	MHz

* (Omni antenna gain includes 3 dB multipath loss.

** Receiver noise figure is 13 dB for the Apollo system; 4 dB for the modified system.

TABLE A-2. DOWNLINK PARAMETERS

	Narrowband				Wideband		
	Apollo Comm. System		Modified Comm. System		Apollo Comm. System	Modified Comm. System	
Parameter	Omni	Hi-Gain	Omni	Hi-Gain	Hi-Gain	Hi-Gain	Units
Lunar Vicinity trans. freq. TFRVEH	2.3	2.3	2.3	2.3	2.3	2.3	GHz
Lunar Vicinity trans. power PTVEH	12	12	50	50	12	50	watts
Lunar Vicinity trans. cir. loss TLVEH	3	5	2	3	5	3	dB
Lunar Vicinity trans. ant. gain GTVEH*	-3	26	-3	26	26	26	dB
Satellite receiver circuit loss	3	3	2	2	3	2	dB
Sat. Rec. System temp. (NR=4dB) ASAT	638	638	615	615	638	615	^oK
Satellite trans. frequency TFDSAT	2.3	2.3	8.5	8.5	2.3	8.5	GHz
Ground station rec. antenna gain GRMSFN	53	53	64.5	64.5	53	64.5	dB
Ground station rec. cir. loss RLMSFN	0.5	0.5	0.5	0.5	0.5	0.5	dB
Ground station rec. system temp AMSFN**	209	209	207	207	209	207	^oK
Ground station receiver required SNR	-2.4	-2.4	-2.4	-2.4	6.5	6.5	dB
Ground station receiver margin	0	0	0	0	0	0	dB
Downlink IF noise BW (Sat. and ground) BWIFMS & BWIFSA	4.8	4.8	4.8	4.8	5.3	5.3	MHz

* Omni antenna gain includes 3 dB multipath loss

** Receiver noise figure is 0.8 dB for the Apollo system; 0.7 dB for the modified system

APPENDIX B

SURVEY OF APPLICABLE TECHNOLOGY

1. ANTENNA TECHNOLOGY

1.1 Antenna Technology Summary

The results of a survey of the current state-of-the-art in antenna technology for satellites are shown in Tables B-1 through B-5.

Tables B-1, B-2, and B-4 list high gain antennas; while Table B-3 lists primarily antennas with gains less than 20 dB. Table B-5 contains information on antennas for some past, present, and future NASA communications satellites. These tables do not contain any information on the current Apollo antennas.

Along the top of each chart are listed brief descriptions of the information contained in the respective vertical columns. The information contained in each horizontal row of the charts pertains to the antenna listed in the "Type of Antenna" column. The source of this information for Tables B-1 through B-4 is identified by consecutively numbered references appearing in the "Authors" column. The information source for Table B-5 is given at the bottom of the chart. A complete list of references is given starting on Page B-19.

In cases where blocks of a chart are subdivided by thin horizontal lines, the entries across a horizontal row within the same respective sets of horizontal lines are associated. For example, for the retrodirective Van Atta array antenna in Reference 10, a 6 ft. by 6 ft. array of 1000 elements has a gain of 34 dB at S-band.

Spacecraft antennas with gains up to 44 dB at S-band and up to 55 dB at X-band are shown. Reference 14 discusses a cassegrainian telescope antenna for a 10.6 micron carbon-dioxide laser which is expected to have a gain of 98.5 dB. It should be noted that some of these entries are based on theoretical calculations for envisioned antennas which haven't actually been constructed. This is particularly true for the higher gain antennas. The maximum gain in the tables for an antenna which has been successfully flown is 27 dB for the one on the Surveyor spacecraft (References 8 and 29). The Apollo CSM high-

gain antenna has a transmitting gain of 25.8 dB in the narrow-beam mode at S-band.

By way of comparison, Reference 14 gives an empirical expression for maximum attainable gain for future spaceborne antennas:

$$G = 1.95 \times 10^{-9} f^{1.52} \qquad \text{(B-1)}$$

where f is the transmitted carrier frequency in Hz. This gain limitation is imposed by difficulties in mechanical fabrication and alignment tolerances. Equation (B-1) gives gains of 49.7 dB at 1 GHz and 64.9 dB at 10 GHz.

1.2 Parabolic Reflectors

Three parabolic-reflector antennas (References 5, 6, and 24) which can be unfurled after the spacecraft has attained orbit are shown. Gains of 27 to 30 dB at 2 GHz are achieved with diameters of 6 to 9 feet, beamwidths of a few degrees, and weights from 20 to 30 pounds (not including steering mechanisms). Gain increases with reflector size and operating frequency. Narrow-beam reflector antennas require precise spatial orientation and several beams simultaneously in different directions is difficult to achieve.

Korvin and Mills (Reference 27) have invented a feed for a parabolic reflector which is capable of acquiring and tracking a communications station that lies within 15° of the reflector axis. An additional station within an annulus of 5° to 15° of the reflector axis could be simultaneously tracked. This could be accomplished with four different frequencies (two for transmit and two for receive). The feed consists of an arrangement of 600 or more waveguide elements into an annular array which is coplanar and concentric with a linear array of waveguide elements within the annulus. The plane of the feed is perpendicular to the reflector axis and the linear array is mechanically rotatable about the reflector axis. Normally four elements are excited for one beam position.

1.3 Array Antennas

Arrays of a large number of elements provide high antenna gains at the experse of weight and complex phasing networks for beam steering. However, precise spatial orientation of the array is not required. Increasing the frequency of operation allows a smaller physical size for the same gain.

Array type antennas with gains ranging from 20 to 45 dB are discussed in References 7, 9, 10, 12, 13, 21, 22, and 26. The Van Atta retrodirective array of Reference 10 uses 1000 elements arranged in a square to achieve a gain of 34 dB. The linear dimensions are 6 ft. at S-band and 2 ft. at X-band. An increase of 10 dB in antenna gain requires 10 times the number of elements. Typical weights of array antennas: 170 lb. for 26.5 dB gain at 2.3 GHz (Reference 12); 175 lb. for 34 dB gain at 4 GHz (Reference 13); and 100 lbs. for 30 dB gain at 7.4 GHz (Reference 26).

1.4 Despun Antennas

Mechanically and electronically despun antennas for spin stabilized spacecraft are discussed in References 1, 2, 3, 4, 22, and 23. Gains of 16 to 21 dB with 20° beamwidths (generally earth coverage from orbit) and beam pointing accuracies of $\pm 0.7^{\circ}$ are typical.

1.5 Antenna Pointing Systems

Ball Brothers Research Corporation has developed a biaxial control and drive system (Reference 28) which is capable of positioning a spacecraft antenna with respect to the spacecraft to within $\pm 0.3^{\circ}$ in less than 10 seconds. Command from an external input is required. An autotrack mode provides for tracking a moving target to within $\pm 0.2^{\circ}$. The unit weighs 22 lbs. and consumes 5 watts of power. The gimbal angular range is $\pm 100^{\circ}$ for the primary axis and $\pm 85^{\circ}$ for the secondary axis.

The ATS-F satellite, expected to be launched early in 1972, will test techniques for pointing a 30 ft. space-erectable antenna with an accuracy of $\pm 0.1^{\circ}$. A study by Lockheed (Reference 26) concludes this is feasible.

DATE OF ARTICLE	AUTHORS	COMPANY AFFILIATION	TYPE OF ANTENNA	GAIN OF ANT.	FREQUENCY	SIZE	WEIGHT	BEAM DIMENSIONS	NUMBER OF BEAMS
July 1969	Donnelly, Graunas, Killian References 1, 2	Sylvania	Mechanically Despun; Conical horn with 45° Reflecting Plate	17 dB 21 dB (Meas.)	3.7-4.2 GHz Trans. 5.9-6.4 GHz Receive	 24.5" α = 45° cone = 28° 8" dia.	<32 lb.	19.3°	1-Receive 1-Transmit
July 1969	Blaisdell, Rubin, Mahr References 2, 3	Sylvania	Mechanically Despun; Line source illuminating parabolic cylindrical reflector.	17.1 dB Meas.	4.107-4.191 GHz trans. 6.200-6.313 Receive	Picture 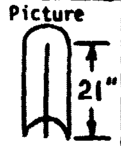 21"	13.5 lb	20° x 20°	1-Receive 1-Transmit
July 1966	Backus Reference 4	Grumman A/C	Mechanically Despun Phased Array	21 dB Eval.	S-Band	3.4' x 4.3' (Oblate Spheroid)	Not Given	6.5° x 22°	1 can quick scan 20° acquisit[ion] volume
July 1968	Holst Reference 5	Martin Marietta	Erectable Parabolic reflector	30.5 dB 32.5 dB (Meas.) 37 dB (Calculated)	1.7 GHz 2.5 GHz 4.0 GHz	8' dia. 3.84" focal Distance 8' Dia.	<30 lb	5.0° 3.2° 2.5°	1
July 1969	Fager, Garriott Reference 6	Convair	Erectable Parabolic Reflector (Expandable Truss) (Meas) → (Cal.) →	44 dB Meas. 35 dB 27.5 dB	15 GHz 4 GHz 2 GHz	6' Dia. 6' Dia. 6' Dia.	20 lb. 20 lb. 20 lb.	0.75° 3° 6°	1
July 1969	Das, Delaney Reference 7	TRW	Phased Array	44 dB Estimated	2.28 GHz	28.5' x 28.5' Aperture	2800-4300 lb (Ant. & Spacecraft)		2- Indep[en]dently Steerabl[e] by integrated C[...]
April 1964	Report Reference 8	Hughes A/C	Planar Array (Crossed and Complex Slots)	27 dB	?	?	?	?	
Apr 1964	Report Reference 8	Hughes A/C	Conical Reflector with Cylindrical feed (dipoles outside cyl, reflecting surface or slots on cylindrical waveguide)	28.1 dB (Meas.) 33.5 dB (Calculated)	9.375 GHz	19.1" Dia. x 8.8" feed length		40°, 20°, 10°, 5°, or 2.5° theoretical	5 (Beamwi[dth] on exp. model = [...]) beam
Mar 1964	Belfi, Rothenberg Reference 9	Sperry Gyroscope	Retrodirective planar array. (Switched-beam hybrid matrix).	24.3 dB expected	2 GHz	26" x 26" printed ckt.board	Printed Ckts.		32 beam positio[ns]
Mar 1964	Gruenberg, Johnson Reference 10	IBM	Retrodirective Van Atta Array "Comarray"=quasi-passive	44 dB 39 dB 34 dB 29 dB theoretical	S, C, or X-band	21 14 7 10.5 7 3.5 6 4 2 3.6 2.4 1.2 S C X Linear Dim. of Sq.Array (ft)		Field of view=±60°	Several ground station[s] can use simulta[n]eously
Apr 1969	Das Reference 11	TRW	Helix Antenna - 24 turns	16.5 dB (Meas.) 18.5 dB (Cal.)	2.3 GHz	1.9" Dia. 30" length	0.35 lb. rigid 0.13 lb. Deployable	21.7° meas.	1
July 1969	Williams & Schroeder Reference 12	TRW	Planar Hybrid Matrix Array	26.5 dB (Estim.) 28.2 dB	2.3 GHz 3.15 GHz	7' Dia. (hexagonal) 7' Dia.	220#-2 beams 170# -1 beam	3.45° 2.6°	Any num[ber]

FOLDOUT FRAME

Table B-1. High Gain Spacecraft Antennas

ONS	NUMBER OF BEAMS	BAND-WIDTH	ARRAYS		ANT. BUILT	ANTENNA FLOWN	DEPLOYABLE	PACKAGING	COMMENTS
			NO. ELEMENTS	TYPF ELEME					
	1-Receive 1-Transmit	0.5 GHz	—	—	Yes	Intelstat-III (2) Successful	No	—	Circular polarization; VSWR ·1.20:1; Satellite spin 65-117 rpm; Infrared earth sensors to track to 0.7^0
20^0	1-Receive 1-Transmit	8% (100MHz)	—	—	Yes	ATS-III Successful	No	—	Linearly polarized; VSWR = 1.35:1 max.; Satellite spin = 50-150 rpm; sun sensor to despin and ground command points antenna to $\pm 0.7^0$; Sidelobes 10-12 dB down
22^0	1 quickly 20^0 quisition volume	7%	10	Yagis	Yes	Motor flown on 3rd ATS. Antenna not	Partially (antenna raised above motor after orbit obtained)	—	Horizontal polarization; earth sensor to despin; 100 watts R.F power; side lobes -25 dB Azimuth; - 9dB Elev.
—	1		—	—	Yes — No	No	Yes	Cylinder 30" Dia. X 7" depth	12 ribs; (24 rib version being fabricated with weight less than 30 lb.); Sidelobes: measured (horizontal and vertical) -18 dB at 1.7 GHz; measured -14 dB at 2.5 GHz (-24 dB calculated at 2.5 GHz)
—	1				Yes	No	Yes Expandable Truss type	Cylinder 9" Dia. X 9" high	Gain increases with diameter and frequency; Sidelobes 16-23 dB down (Measured); Polarization used; Circular - S, X bands, Linear - Above X band
	2- Independently Steerable by integrated Cir		1024	Helix (Deployable)	No	No	Yes	Can be stowed in Tital III C Rocket	Simultaneously communicates with 2 vehicles; 1800 watts (includes all antenna and spacecraft power) for use on 3 axis stabilized satellite
				Slots	Yes	? says for surveyor S/C	No		Circularly polarized; Sidelobes -14 dB
0^0, ^{0}, or tical	5 (Beamwidth on exp. model $\approx 5^0$; 1 beam)				Yes	No	Possible	Small	Circularly polarized; Beamwidth switched by exciting different parts of cylindrical feed; cross polarization components = -13 dB; rudimentary form built
	32 beam positions		64	printed ckt.	Partially	No	No		Gain loss = 1.8 dB max. at crossover of 4 beams; 1-2 watts RF power on satellite; Antenna transmits data, which it has collected, to ground station upon interrogation; Hybrid phasing matrix & interrogation signal determine direction of beam
of 60^0	eral und stations can use simultaneously		10,000 3,000 1,000 300	conjugate elements of Van Atta array	No	No			Power < $\frac{1}{2}$ mw. (could be supplied from ground); Incoming continuous wave (A) is modulated with information from other incoming wave (B) & modulated wave returned to origin of A: No power splitting when simultaneously used by several ground stations
meas.	1				Yes	No	Under Development		Such elements can be used for phased arrays; VSWR = 2.0 (can be improved)
—	Any number		108 192	Helix (Deployable)	No	No	No	Can be stowed in Titan III C Rocket	At present practical for 24-30 dB net gain & 10 or more beams; Sidelobes -15 dB; Beam crossover (3 beams) within-2.2 dB possible; Power required low

FOLDOUT FRAME

PRECEDING PAGE BLANK NOT FILMED.

DATE OF ARTICLE	AUTHORS	COMPANY AFFILIATION	TYPE OF ANTENNA	GAIN OF ANTENNA	FREQUENCY (T-TRANSMIT R-RECEIVE)	SIZE	[illegible]
Mar. 1966	Kummer, Birgenheier Reference 13	Hughes A/C	8 turn helix with cup at base (for beam shaping)	6.7 dB Theor.	6.301 GHz	0.56" dia X 4.55" long	Not given
Mar 1966	Kummer, Birgenheier Reference 13	Hughes A/C	"Transdirective" array, a switched multiple-beam, self-steerable antenna	Receive: 20.8 dB peak, 15.0 dB min measured) Transmit: 21 dB peak, 17.4 dB min Measured)	6.301 GHzR 4.081 GHzT	Receive: 14" X 14" Transmit: 22" X 22" (excludes circuitry req'd)	Not given
Mar 1966	Kummer, Birgenheier Reference 13	Hughes A/C	Self-phasing retrodirective array (self-steering)	Transmit: 21 dB peak, 18 dB min measured) Receive: 6.7 dB (Theor.)	4.081 GHzT 6.301 GHzR	Transmit: 22" X 22" (excludes circuitry req'd)	Not given
Mar 1966	Kummer, Birgenheier Reference 13	Hughes A/C	Multiple - beam "Transdirective" array	34 dB, 24 dB min (Theor.)			175 lb
Mar 1966	Kummer, Birgenheier Reference 13	Hughes A/C	Self-phasing array	34 dB, 30 dB min (Theor)			175 lb
Nov. 1968	McElroy, McAvoy, Richard, Richards, Flagiello Reference 14	Goddard SFC	10.6 μ carbon dioxide laser transmiter with a cassegrainian telescope antenna	98.5 dB (with 0.12w into trans. antenna) 98.5 dB R 92.4 dB T (with 0.11w into trans. antenna)	10.6 micron wavelength	25 cm dia. ant. 25 cm dia receive 12.5 cm dia transmit	mass: 34 kg mass: 20 kg

FOLDOUT FRAME

Table B-2. High Gain Spacecraft Antennas

IGHT	BEAM DIMENSIONS	NUMBER OF BEAMS	BANDWIDTH	ARRAYS No. OF ELEMENTS	ARRAYS TYPE ELEMENTS	ANT. BUILT	ANT. FLOWN	DEPLOYABLE	COMMENTS
given	40°	1				yes	no	no	Helix wound on plexiglass rod with bored out center; Sidelobes 13 dB down; VSWR ≤ 1.1:1 for 6301 ± 150 MHz.
given	Receive: 12.5° each (measured) [illegible]nsmit [illegible] each beam (measured) Coverage for receive or transmit fills cone whose subtended total angle is 50°	Receive: 16 discrete Transmit: Continuously scanned beam by using 4 adjacent, weighted beams to form 1 composite beam.	10 MHz	Receive: 16 Transmit: 16 (2-4X4 arrays)	Helix (above)	yes (Breadboard)	no	no	Array receives incident signals from arbitrary directions and after processing, the signals are transmitted to other arbitrarily desired directions. Pilot tones on uplink signals identify them. For proper redirecting need either pilot tones from receiving stations or command signals from uplink stations. Pilots used: 6.310 GHz from uplink station; 6.313 GHz from downlink (receiving) station. Logic circuits used more than 1000 transistors. Designed for gravity gradient satellite but probably could be modified for spin stabilized satellites. 2 beam forming matrices (1 - R, 1 - T); TWT amplifier; 23.0 dBw ERP; Power req'd = 67.2 watts, excluding local oscillators and TWT.
given	Transmit: 13° (measured) Receive: ± 25° coverage angle	1 - Transmit (Steerable) 1 - Receive	10 MHz	Transmit 16 (4 X 4 array) Receive used 1 helix element	Helix (above)	yes (Breadboard)	no	no	Same 4 GHz array as above used for transmit; self-phasing by phase reversal through mixing. Information which was previously received is relayed in direction of a received pilot signal. Pilot = 4.159 GHz. Sidelobes 10 dB down on transmit; power req'd = 418.5 watts excluding TWT amplifier and local oscillators. Designed for gravity gradient satellite but probably could be modified for spin stabilized satellites. TWT amplifier. N element array requires N phase-matched modules (N complete transmitters and receivers). ERP = 13.7 dBw measured, + 0.75 dBw predicted.
lb	30° Coverage	4 independent (2 R, 2T)	2 independent 125 MHz channels	2-8X8 arrays		no	no	no	Envisioned extension of above 4 X 4 "transdirective" array to an 8 X 8 system. Components nearly all proven, except for matrix which should be straight forward. ERP = 33 dBw.
b.				8X8 array		no	no	no	Envisioned extension of above 4 X 4 self-phasing array to an 8X8 system. ERP = 25 dBw. Except for final r-f amplifiers, components close to state-of-the-art. Authors expect 2-3 years for r-f amplifiers to reach the state required at 2 GHz.
: 3	40 arc second beam	Wide for acquisition; pencil for auto tracking	100 MHz			no	no	no	Envisioned laser communication systems expected to be breadboarded by 1972 and available for satellite communication use by 1975. The ATS-F (1972) and ATS-G (1973) laser communications experiments are expected to develop the hardware for these systems. First system requires 200 watts, second system requires 75 watts. An earth-oriented satellite with some degree of stabilization and which permits pointing the main antenna to ±0.1° is satisfactory for the experiment. The course beam-pointing mechanism may be required to steer the laser beam ±40 degrees from local nadir. The 25 cm telecope has a 0.1° field of view. System is autotrack and acquisition time is much less than 1 minute.
			5 MHz			no	no	no	

FOLDOUT FRAME 2

FOLDOUT FRAME

PRECEDING PAGE BLANK NOT FILMED.

DATE OF ARTICLE	AUTHORS	COMPANY AFFILIATION	TYPE OF ANTENNA	GAIN OF ANT.	FREQUENCY (T-TRANSMIT) (R-RECEIVE)	SIZE	[illegible]
Mar 1964	Andre, Leonard Reference 15	Sylvania	Active retrodirective array	14 dB (Meas.)	2.15 GHz T 2.00 GHz R	All solid state	All solid state
July 1969	Rankin, Devane, Rosenthal Reference 16	M.I.T.	Cluster of 8 circularly polarized horns pointed radially outward every 45° about spin axis	10.7±0.6 dB (Meas.) (includes switch)	X-band-T	10" [illegible] x 8" high package of 3 antennas	Package [illegible] 4.5 lb
			Circularly polarized biconical horn	4.4 dB (Meas.)	X-band-R		
			Omnidirectional longitudinally polarized-by exiciting gap between biconical horn & rest of structure.	1 dB (Meas.)	VHF Telemetry		
Sept 1966	King, Wong, Zamites Reference 17	Aerospace Corp.	Polyrod antenna	12.4 dB calculated at θ=±20°	7.3 GHz	5.1" dia. max. x 9.7" long	
			Circular horn with special lens	9.9 dB (Meas.) at θ=±24°	6.4 GHz	4.85" dia.	
Mar 1969	Tokumaru Reference 18	Keio Univ, Japan	Double-sheath helices, leaky-wave antenna 1 - Uniform pitch	10-20 dB theoretical	9.6 GHz	5 cm dia. x 45 cm long	
			2 - Tapered pitch	Not given	9.6 GHz	10 cm dia. x 65 cm long	
Jan 1969	Nair, Srivastava, Hariharan Reference 19	Univ of Delhi & Govt. Victoria College (India)	See comments. Gain & beamwidth values are in E-plane. First value is without grill and second value is with double grill. Each value represents average of several horns. All values are measured.	13.6 to 20.5 dB	9.4 GHz		
				15.8 to 22.0 dB	7.5 GHz		
				14.8 to 20.0 dB	6.66 GHz		
				13.2 to 18.9 dB	6.00 GHz		
Sept 1965	Irmer Reference 20	Technische Universitaet Berlin	Two uniform open slots cut into the metallic surface of sphere	18.94 dB theoretical			

FOLDOUT FRAME 1

Table B-3. Low Gain Spacecraft Antennas

	WEIGHT	BEAM DIMENSIONS	NUMBER OF BEAMS	BAND-WIDTH	ARRAYS		ANT. BUILT	ANTENNA FLOWN	DEPLOY-ABLE	COMMENTS
					NO. ELEMENTS	TYPE ELEMENTS				
d	All solid state	Redirects beam from ±40° off axis	Redirects several (Tested 3 simultaneously)	120 MHz	9 pairs	Dipoles (printed circuit)	Yes	No	No	Tunnel diode amplifiers and mixers used; completely solid state; power supplied by 3 small dry cells; receiving and transmitting elements orthogonally polarized and intermeshed on common aperture surface.
re h of ss	Package less [illegible] 4.5	58° x 28° each horn		60 MHz			Yes	No	No	For X-band transmit antenna: Horns energized by slots. An 8 throw switch turns on horn most currently pointing to earth (operates on information from earth swnsors); VSWR < 1.25 for f_0 ±10 MHz.
		35^0 longitudinal								
		135^0 longitudinal								
.		θ=±24°		±3%			Yes	No	No	Purpose was to shape antenna beam (by proper choice of aperture amplitude and phase distributions) to enhance gain at line of sight angles to horizon (this provides uniform earth coverage.) Primarily for attitude-stabilized satellite. (Here maximum gain occurs at horizon angles).
i.		θ=±30°		±1.5%			Yes	No	No	
		3-6° (Meas.)					Yes	No	No	1: sidelobes -10 dB, 2: sidelobes -20 dB meas.
.		6° (Meas.)								
		48° to 18°					Yes	No	No	Experimental study. Placed 2 conducting grills (metallic rectangular strips) at apertures of E-plane sectoral horns to improve gain and beamwidth in E-plane. Grills had negligible effect on H-plane radiation patterns.
		39° to 17°								
		55° to 18°								
		58° to 17°								
							No	No	No	

FOLDOUT FRAME 2

PRECEDING PAGE BLANK NOT FILMED.

DATE OF ARTICLE	AUTHORS	COMPANY AFFILIATION	TYPE OF ANTENNA	GAIN OF ANT.	FREQUENCY (T-TRANSMIT) (R RECEIVE)	SIZE	WEIGHT	BEAM DIMENSIONS	
Autumn, 1965	Backus Reference 21	Grumman	Linear phased array of 16 circularly polarized waveguide elements (part of a broadband digital communications system.)	17 db	[illegible]-55 GHz			3° azimuth 70° elev.	
			Planar retrodirective array	30 dB theor.	4 GHz T	3' X 3'		4°	
			Planar retrodirective array	38 dB	4 GHz	8.5' X 8.5'		2°	
			Planar retrodirective array	44.2 dB	4 GHz	17' X 17'		1°	
			Dish, lens, or planar array	43 dB	55 GHz	15"		1°	
May 1966	Korvin, Chadwick, Reference 22	Goddard SFC & Radiation Sys.	Clyindrical phased array: 64 circular apertures (16 banks of 4) around circumference plus 12 circular apertures on each end (planar array)	13 to 16 dB meas. (T or R)	1.7 GHz, 2.27 GHz	18.7" dia. X 35" high	65 lb entire system	Cyl. array: 18° X 23° planar array: 23°-30°	S s e d d
Oct 1963	Erhardt, Gerson, Mead Reference 23	Hughes	Electronically despun phased array. 16 elements, parallel to spin axis and perpendicular to orbital plan, are arranged around circle whose diameter is one wavelength	19 dB theor; 17 dB meas.	4 GHz T			21° cone theoretical	1
April 1964	Haylett Reference 24	Goodyear	9-ft. diameter, 12 rib, parabolic reflector	32 dB meas.	2.1 GHz R 2.3 GHz T	9' dia.	32 lb		1
December 1966	Fager Reference 25	Convair	Envisioned erectable phased array	38.8 dB	850 MHz	956 ft^2	1720 lb	2.32°	
				43.2 dB		2595 ft^2	4670 lb	1.41°	
November 1966	Reference 26	Lockheed	20 rib unfurlable, flexirib parabolic reflector	43.3 dB	2.1 GHz	30' dia.	208 lb.		1
				55.0 dB Theor.	8.0 GHz				
November 1966	Reference 26	Lockheed	Electronically phased array: metallic lens with electronic switching of feeds.	45 dB theor.	7.4 GHz	12' X 12'	394 lb	0.9°	4 (
				30 dB Theor.		2.5' dia. (lens size)	100 lb estimated; includes electronics		

FOLDOUT FRAME

Table B-4. High Gain Spacecraft Antennas

BEAM DIMENSIONS	NUMBER OF BEAMS	BAND-WIDTH	ARRAYS		ANT. BUILT	ANTENNA FLOWN	DEPLOYABLE	PACKAGING	COMMENTS
			NO. ELEMENTS	TYPE ELEMENTS					
3° azimuth 70° elev.			16		Yes	No			Capable of search, acquisition, and track operations; transmitter power output of 10 W; receiver noise figure of 10 dB; scan angle of $\pm 30^\circ$; beam switching time of 3 μs; antenna electronically scanned.
4°			600		No	No			Theoretical electronically steerable antenna; transmitter power is 33 dBm (2 W).
2°			2500		No	No			40 mW/element; 640 kW ERP. These antennas based on theoretical calculations.
1°			10,000		No	No			0.4 mW/element; 105 kW ERP
1°			-		No	No			Xmtr. power 15 W, 300 kW ERP
Cyl. array: 18° X 23° planar array: 23°-30°	Several, simultaneously in different directions	Signals cover BW up to 100%	88 circular apertures		Yes	No	No		Provides total spherical coverage; 88 discrete beams; beam crossover level - 1 dB; Sidelobes: -18 dB to -12 dB for planar arrays, -13 dB for cyl. array; switches & Butler matrices used; circularly polarized signals; system can handle kilowatts of peak power.
21° cone theoretical	1	2.5% req'd	16	half-wave dipoles 0.25" dia. X 13" long	Yes	Not at time of article	No		Advanced SYNCOM antenna system. All elements in array driven in proper phase. Sun sensor and command signals used to drive ferrite phase shifters to orient beam. Beam pointing accuracy is 0.7°; sidelobes -10 dB. Total circuitry required weighs 3.6 lb, vol = 0.053 cu. ft. System fails gracefully. Spin modulation less than 0.4 dB.
	1	10 MHz			Yes	No	Yes	43" dia	Antenna is circular paraboloid type consisting of a fixed center hub with outer sections (12 curved radial ribs) that unfurl. Radiated power is 100 W. Total losses = 1.66 dB predicted.
2.32° 1.41°			1274 3458	horns 12.75" dia. X 7" high	No	No	Yes	185" dia.	For Saturn-V launch vehicle. All values are theoretical. Critical phase coupling of this large number of elements under study at time of article. Antenna folded by stacking hexagonal modules.
	1	10%			Models built & Tested	No	Yes, by 0.25 hp elec. motor	4.5' dia. X 1.5' deep	Antenna experiment for ATS-4, 3-axis stabilized satellite; Centaur launched; Study concludes it is feasible to point antenna to $\pm 0.1^\circ$ using a unique adaptive digital autopilot concept together with a radio-interferometer which uses reference signals from two ground transmitters. Interferometer has range of 15.5° for nonambiguous readout of attitude angle.
0.9°	4-steerable (2-T, 2-R)	11% total for 4 beams (800 MHz)	256 feeds 16 feeds		No	No	Yes	12' long X 8" sq.	Proposed antenna for ATS-4 satellite experiment; steering of beams to 0.1 degree by electrical means feasible; command or pilot signals for control; beam scanning of ± 10 to ± 15 beamwidths possible; here about 17° scan used for 45 dB gain antenna; each feed illuminates entire lens; 408 watts estimated power required (unknown as to which antenna).

FOLDOUT FRAME

PRECEDING PAGE BLANK NOT FILMED.

DATE OF LAUNCH	SATELLITE	COMPANY	TYPE OF ANTENNA	GAIN OF ANTENNA	FREQUENCY (R-RECEIVE) (T-TRANSMIT)	ANTENNA SIZE	SPACE-CRAFT WEIGHT
April 1965	Intelsat I	Hughes	Co-linear slot array (transmit)	9 dB	4.08,4.16 GHz		85 lb.
			Omni (receive)	4 dB	6.3,6.39 GHz		
Oct 1966 Sept 1967	Intelsat II	Hughes	Electronically despun multiple element biconical horn	8 dB	4.06-4.19 GHz T 6.3-6.4 GHz R	18"	195 lb.
Sept 1968-Feb 1970	Intelsat III	TRW, ITT, Sylvania	Mechanically despun conical beam	17-18 dB	3.7-4.2 GHz T 5.9-6.4 GHz R		258 lb (Satellite proper)
1971-1972	Intelsat IV	Hughes,	All electronically despun		3.7-4.2 GHz T 5.9-6.4 GHz R		1225 lb.
Dec 1966	ATS-1 (B)	Hughes, JPL	Electronically despun; colinear array for receive; phased array for transmit	14 dB	6 GHz R 4 GHz T		775 lb.
April 1967	ATS-2 (A)	Hughes, G.E., TRW, RCA, deHavilland	Horns for communications		6 GHz R 4 GHz T		815 lb.
Nov 1967	ATS-3 (C)	Hughes	Mechanically despun linear parabolic	18 dB	6 GHz R 4 GHz T	21"	850 lb.
Aug 1968	ATS-4 (D)	Hughes	Linearly polarized horn antennas		6 GHz R 4 GHz T		801 lb.
May 1969	ATS-E	Hughes	Two of unknown type for millimeter wave experiment	20 dB specs	31.6 GHz R 15.3 GHz T		895 lb.
Early 1972	ATS-F	Goodyear (antenna)	Multibeam phased array	50 dB Expected	8 GHz (also will have S&L bands)	30 ft.	1500-2000 lb.
Early 1973	ATS-G (basically same as ATS-F)	Goodyear (Antenna)	Multibeam phased array	50 dB 40 dB expected	7.3-8.0 GHz S-band	30 ft.	1200-1400 lb.
1974	GRSS	RCA, Lockheed, Hughes	Multiple beam electronically phased array (originally desired)	40-45 dB required	1.7-2.3 GHz 7.6-8.5 GHz	3.0°	
			Proposed by Lockheed			21' sq(R) 11' sq(T)	
				44 dB	9-10 GHz	8' dish	
Deployed from one or more AAP missions	SCATR	Hughes	Mechanically despun planar array (right circularly polarized)	26.4 dB R 25.3 dB T	2.1-2.3 GHz	10' x 2'	
			Possibly electrostatically deployed 30' parabolic reflector	42.5 dB expected			
1966-1968	IDCSS (Phase I)	Philco-Ford	Circularly polarized, bi-conical array. (in plane normal to spin axis)	4.5-6.5 dB	8 GHz R 7.3 GHz T		100 lb.
1967-1972	TAC SATCOM	Hughes-prime	Quint-helix UHF array	16 dB expected	240-315 MHz	8' long (approx.)	1600 lb. expected
Late 1971	Multipurpose Satellite	Hughes	4 separately steerable S-band dishes	32 dB each	4-6 GHz T 10 GHz + T		1750 lb. estimated
		Lockheed	Two 6' x 9' microwave antennas	25-30 dB each			

Source: "Communications Satellite Handbook", NASA-MSC, February 1969, Revision 2.

FOLDOUT FRAME

Table B-5. Past, Present and Future Communications Satellites

SPACECRAFT WEIGHT	BEAM DIMENSIONS	NUMBER OF BEAMS	BANDWIDTH	S/C POWER FROM SOLAR CELLS	SPACECRAFT SIZE	ANT. BUILT	ANTENNA FLOWN	SPACECRAFT STABILIZATION	COMMENTS
85 lb.	11^0 squinted		25 MHz each repeater	45 W	24" dia.	Yes	Yes Successful	Spin	6 watt TWT; 6 watts ERP; two independent frequency translation repeaters.
195 lb.	12^0 (Transmit)		126 MHz	100 W	56" dia.x 26.5" high	Yes	Yes Successful	Spin	Four 6 watt TWTS (all can operate simultaneously). Antenna linearly polarized for transmit (15 watts ERP), orthogonally polarized for receive.
268 lb (Satellite proper)	19^0		500 MHz (Antenna	132-181 watts	56" dia.x 63" high (incl.ant)	Yes	Yes (but some problems)	Spin 65-117 rpm	ERP=22.0 dbw/transponder; 2 TWTS @ 11 W each; 2 independent channels; omnidirectional command antenna.
12[illegible]	4.5^0 (33.7 dBW) 17^0 (22.0 dBW)	2 spot beams plus earth coverage	432 MHz total com.	435-565 W	93.5 dia x 17.5' high	No	No	Spin	$\pm 0.1^0$ antenna pointing accuracy (4.5^0 beam); command switching to direct outputs into spot or earth coverage beams; 24 TWT's at 7.2 watts.
775 lb.	24^0			185 W initial	56" dia.x 57" high	Yes	Yes Successful	Spin 100 rpm	Sun sensor; TWT; also has VHF capability (10 db ant. gain; 50^0 beam)
815 lb.				185 W initial	56" dia.x 72" high	Yes	Yes -(S/C has orbit problems)	Gravity Gradient, 3 axis	8 whips extend from top for command and telemetry.
850 lb.	19.7^0				6' long x 5' dia.	Yes	Yes Successful	Spin 100 rpm	12 watt TWT's provide ERP of 1 kW; has auxiliary array antennas.
801 lb.						Yes	Yes (S/C orbit problems)	Gravity Gradient 3 axis	4 TWTS
895 lb.	20^0						Unknown	Gravity Gradient 3 axis	Also 6 GHz receive and 4 GHz transmit with linearly polarized horn antennas
1500-2000 lb.	0.3^0	1000-10,000			Folded S/C dia. = 9'	No	No	3 axis (see comments)	Will test techniques for pointing large space-erectable antennas with accuracy of $\pm 0.1^0$-0.2^0 by phase comparison system; data relay experiments; spin stab wrt geocentric coordinate system; RF loss = 10 dB; operational with up to 4 stations by time sharing.
1200-1400 lb.	3^0				Folded S/C dia. = 9'	No	No	See Comments	Spin stabilized with 0.1^0, 3 axis stabilized; phase comparison system for antenna orientation; operation with up to 4 stations by time sharing; to demonstrate precise pointing required for lasers.
	1^0		50 MHz required	700 W (Solar cells & battery)		No	No	See Comments	Data Relay Satellite System; RCA proposed 3' dish antenna, 24dB gain at about 8 GHz; stabilization: Lockheed proposed Gravity Gradient for roll & pitch axis and momentum wheel for yaw axis control.
	$17^0 \times 2^0$		Equivalent to CSM	332 W (operational system)		No	No	Spin	Synchronous Communications & Tracking Relay System; will provide coverage for 2 or more vehicles of CSM capacity; also low gain colinear array with gain of 3 dB receive; 8 dB transmit.
100 lb.	28^0 (Toroidal)		20 MHz			Yes	Yes (Successful)	Spin 150 rpm	Initial Defense Communications Satellite System. Radiates 2.5 W.
1600 lb. expected	50^0 expected		10 MHz		9' dia x 16' high (expected)	No	No	Spin	2 SHF horns; experimental launches successful so far. Also will have 7-8 GHz capability.
1750 lb. estimated	$2.2^0 \times 3.5^0$ each dish 4.5^0 each		12 color TV ch.			No	No	GYROSTAT 3 axis	Antenna pointing of $\pm 0.1^0$ required.

 FOLDOUT FRAME

2. RF TECHNOLOGY

2.1 Introduction

A brief summary of the state of the art in RF power generation and detection for frequencies in the S-band or greater is presented in this section. Extensive use was made of two recent reports by Philco-Ford: "RF Hardware Study, One to Forty GHz", and "Advanced RF and Optical Hardware Study, One to 300 GHz, 0.1 to 100 μ". (References 30, and 31). In addition, use was made of References 31 through 34.

2.2 RF Transmitters

2.2.1 Traveling-Wave Tubes

Up to the present time traveling-wave tubes (TWT) have been the primary elements for RF transmitters on spacecraft operating at S-band. Disadvantages of TWT's include the requirement of stable high voltages and limited life caused by cathode coating depletion.

As noted in Table B-5, Intelsat I and II used 6 watt TWT's; Intelsat III uses 2 TWT's at 11 watts each; and the ATS-3 (C) used 12 watt TWT's to provide an output power of 15.8 watts, operating at a transmitting carrier frequency of 4 GHz. In the current Apollo program, S-band TWT's provide transmitted powers of 12.5 watts for the CSM and 19.2 watts for the LM.

Two typical TWT's from Reference 30 which are currently available for use as RF transmitters for spacecraft are:

1. Watkins-Johnson model 274-1 which operates in the 2 to 4 GHz range produces 22 watts of output power with an input power of 75 watts. It has an RF bandwidth of 300 MHz, a gain of 26 dB, and a weight of 1.10 lb.

2. Varian model VTV-6180A1 which operates in the 8 to 12 GHz range produces 20 watts of output power with an input power of 290 watts. It has an RF bandwidth of 4 GHz, a gain of 35 dB, and a weight of 2.5 lb.

In addition, References 32 and 33 mention 50 watt TWT's at S-band with dc-to-RF efficiencies of 37% and bandwidths of 50%. These are currently available for spacecraft.

2.2.2 Transistor RF Power Sources

Reference 31 gives mid 1969 capabilities and projected 1980 capabilities for power transistors. Power output of 7 watts at 2.3 GHz is given for the mid 1969 capability. Practical power transistor sources that produce any reasonable amount of output power above 3 GHz are not expected to become available until 1975. A 1980 projection of output power for power transistor sources is 17 watts at 2.3 GHz and 2 watts at 8.5 GHz.

At S-band dc-to-RF efficiencies are presently about 35% for power transistors (Reference 32). Wide bandwidth if no problem to achieve and can be as high as 80% of the operating frequency with proper circuit design (Reference 31).

In order to produce higher output power, 5 to 10 watt power sources can be combined together in a series-parallel structure. With present solid-state technology, practical power levels exceeding 100 watts at S-band are achievable with overall dc-to-RF efficiencies exceeding 30% (Reference 32). Furthermore, failure of a single unit in such a structure is not disastrous.

By generating power at a lower frequency and then using varactor diodes to multiply the frequency, output power at a higher frequency is produced. In the present Apollo system, this technique is used in the landing radar to produce X-band RF energy with power outputs less than one watt. A continuous wave source consisting of parallel power transistors feeding varactor diodes has been breadboarded using thin-film microstrip circuitry (Reference 34). This unit had an output power of 9.8 watts at 3.0 GHz, a 1 dB bandwidth of 6.7%, and a dc-to-RF efficiency from 9 to 14.5% over the band. Overall gain was 12.2 dB and total volume was 3 cubic inches.

2.3 RF Receivers

Table B-6 shows mid 1969 state of the art and 1980 projected noise figures for various types of millimeter-wave front ends. In addition, typical parameter values of currently available devices are given. Taken from References 31 and 32, these data show that current state of the art noise figures range upward from about 2 dB for S-band and 2.5 dB for X-band. By 1980, the projected figures are less than 1 dB for both S and X band. These figures are for uncooled parametric amplifiers. If cooling paramps to 77°K is feasible, the lower figures shown in Table B-6 are applicable as noted.

Table B-6. Receiver Front Ends

Type of Device	Noise Figures (dB)				Typical 2-12 GHz Current Devices			
	at 2.3 GHz		at 8.5 GHz					
	Mid 1969	1980 Proj.	Mid 1969	1980 Proj.	Gain (dB)	Bandwidth (MHz)	Weight (lb)	Power Req. (Watts)
Low Noise TWT	3.9	2.5	5.1	3.5	20-25	> 90	2-18	1-25
Cooled Paramp ($77^{o}K$)[(a)]	0.5	0.25	0.7	0.4	10-20	> 50	24-35	10-32
Uncooled Paramp	1.9	0.65	2.6	0.9	10-20	> 50	4-15	10-32
Transistor Amplifier[(b)]	3.2	1.9	N/A	7.1	15-30	> 100	4 oz	0.5
Tunnel Diode Amplifier	3.8	2.5	5.1	3.2	10-17	> 100	< 1 lb	1.0

(a) Assumes a Peltier or thermoelectric cooler, which weighs 20 lb., can cool the diode to $77^{o}K$. Gain, bandwidth, weight, and power required values are for klystron paramps. 20 lb. was assumed for the cooler for the cooled paramp.

(b) Values are for several stages of germanium transistors with an overall gain of 15 to 30 dB.

REFERENCES

1. F. E. Donnelly, Jr., R. P. Garunas, and J. D. Killian, "The Design of the Mechanically Despun Antenna for the Intelsat - III Communications Satellite", IEEE Trans. Antennas and Propagation, vol. AP-17, pp. 407-415, July 1969.

2. L. Blaisdell, F. Donnelly, J. Killian, O. Mahr, "Design Evolution of Mechanically Despun Antennas from ATS to Intelsat", EASCON 1968 Record, Washington, D. C., pp. 485-495, September 9-11, 1968.

3. L. Blaisdell, R. Rubin, and O. Mahr, "ATS Mechanically Despun Communications Satellite Antenna", IEEE Trans. Antennas and Propagation, vol. AP-17, pp. 415-428, July 1969.

4. D. L. Backus, "A Low Sidelobe Mechanically Despun Antenna for Aerospace Application", Conference of Advisory Group for Aerospace Research and Development (AGARD), at Duesseldorf, July 1966, in Radio Antennas for Aircraft and Aerospace Vehicles, pp. 267-293, November 1967.

5. D. W. Holst, "Electrical Measurements of an Erectable Parabola for Space Missions", Conference in Space Projections from the Rocky Mountain Region, Proceedings of the Symposium, Denver, Colorado, Vol. 1, July 15, 16, 1968.

6. J. A. Fager and R. Garriott, "Large Aperture Expandable Truss Microwave Antenna", IEEE Trans. Antennas and Propagation, vol. AP-17, pp. 452-458, July 1969.

7. A. Das and J. A. Delaney, "Spacecraft Phased Array Configurations", IEEE Trans. Antennas and Propagation (Communications), vol. AP-17, pp. 522-524, July 1969.

8. , "Manned Spacecraft Deep Space Antenna Study", Hughes Aircraft Company, Culver City, Calif., NASA contract NAS 9-2099, Report P64-51, Final Report, April 15, 1964.

9. C. A. Belfi, C. Rothenberg, L. Schwartzman, R. E. Tilley, and A. Wills, "A Satellite Data Transmission Antenna", IEEE Trans. Antennas and Propagation, vol. AP-12, pp. 200-206, March 1964.

10. E. L. Gruenberg and C. M. Johnson, "Satellite Communications Relay System Using a Retrodirective Space Antenna", IEEE Trans. Antennas and Propagation, vol. AP-12, pp. 215-223, March 1964.

11. A. Das, "Helix Antenna for Spacecraft", The Radio and Electronic Engineer, vol. 37,pp. 237-240, April 1969.

12. W. F. Williams and K. G. Schroeder, "Performance Analysis of Planar Hybrid Matrix Arrays", IEEE Trans. Antennas and Propagation (Communications), Vol. AP-17, pp. 526-528, July 1969.

13. W. H. Kummer and R. A. Birgenheier, "Spacecraft Antenna Systems", Hughes Aircraft Company, Culver City, Calif., NASA contract NAS 5-3545, Report P66-66, Final Report, March 1966.

14. J. H. McElroy, N. McAvoy, H. L. Richard, W. E. Richards, and S. C. Flagiello, "An Advanced 10.6 - Micron Laser Communication Experiment", Goddard Space Flight Center, Greenbelt, Maryland, Report X-524-68-478, NASA TM X-63441, November 1968.

15. S. N. Andre and D. J.Leonard, "An Active Retrodirective Array for Satellite Communications", IEEE Trans. Antennas and Propagation, vol. AP-12, pp. 181-186, March 1964.

16. J. B. Rankin, M. E. Devane, and M. L. Rosenthal, "Multifunction Single-Package Antenna System for Spin-Stabilized Near-Synchronous Satellite", IEEE Trans. Antennas and Propagation, vol. AP-17, pp. 435-442, July 1969.

17. H. E. King, J. L. Wong, and C. J. Zamites, "Shaped-Beam Antennas for Satellites", IEEE Trans. Antennas and Propagation (Communications), vol. AP-14, pp. 641-643, September 1966.

18. S. Tokumaru, "Double-Sheath Helices: Leaky-Wave Antennas", IEEE Trans. Antennas and Propagation, vol. AP-17, pp. 138-145, March 1969.

19. K. G. Nair, G. P. Srivastava, and S. Hariharan, "Sharpening of E-Plane Radiation Patterns of E-Plane Sectoral Horns by Metallic Grills", IEEE Trans. Antennas and Propagation (Communications), vol. AP-17, pp. 91-93, January 1969.

20. R. J. Irmer, "Spherical Antennas with High Gain", IEEE Trans. Antennas and Propagation (Communications), vol. AP-13, pp. 827-828, September 1965.

21. D. L. Backus, "Electronically Steerable Antennas for Spacecraft-to-Spacecraft Communications", Journal of the Institute of Navigation, vol. 12, pp. 227-251, Autumn 1965.

22. W. Korvin and G. G. Chadwick, "Latest Word in Space Talk: It Can Come from Anywhere", Electronics, pp. 117-126, May 30, 1966.

23. H. R. Erhardt, G. Gerson, and D. C. Mead, "The Advanced SYNCOM Communication Antenna System - A Directive Array for a Spin-Stabilized Satellite", Record 1963 National Space Electronics Symposium, October 1963.

24. J. W. Haylett, "High-Gain Spacecraft Antenna Design and Development", Goodyear Aerospace Corporation, Akron, Ohio, Report GER 11156, Contract No. 950467 (JPL), Final Report, April 1964.

REFERENCES (CONTINUED)

25. J. A. Fager, "Feasibility Study of Large Space Erectable Antennas", General Dynamics/Convair, San Diego, California, Report NASA-CR-80639, Contract No. NASW-1438, Monthly Progress Report, December 1966.

26. ,"Advance Study of an Applications Technology Satellite (ATS-4) Mission", Lockheed Missiles and Space Company, Sunnyvale, California, Report LMSC-A847537, Report NASA-CR-81765, Final Report, November 1966.

27. W. Korvin and M. K. Mills, "Tracking Antenna System", Goddard Space Flight Center, Greenbelt, Maryland, NASA Case No. GSC 10.553-1, Patent Application Serial No. 820,963, May 1, 1969.

28. G. R. Strevey, "A Biaxial Control and Drive System for Spacecraft Antenna Orientation", Ball Brothers Research Corporation, Boulder, Colorado, Report TN67-05, February 4, 1967.

29. C. Kirsten, "Surveyor Spacecraft Telecommunications", Jet Propulsion Lab, Pasadena, Calif., Report NASA CR-83553, Report JPL-TR-32-1105, March 15, 1967.

30. J. C. Baker, "RF Hardware Study, 1 to 40 GHz", Philco-Ford Corp., Houston, Texas, NASA contract NAS 9-1261, Report PHO-TN377, August 20, 1969.

31. J. C. Baker, "Advanced RF and Optical Hardware Study, 1 to 300 GHz, 0.1 to 100μ", Philco-Ford Corp. Houston, Texas NASA contract 9-1261, Report PHO-TN379, October 3, 1969.

32. S. D. McCaskey, "Communications", Space/Aeronautics, vol. 52, pp. 35-46, July 1969.

33. , "Advanced Planetary Probe Study", TRW Systems, Redondo Beach, Calif., Report NASA-CR-79504, Report TRW 4547-5007-R000, Final Technical Report, vol. 4, Appendices, pp. 42-45, July 27, 1966.

34. E. F. Belohoubek, A. Rosen, D. M. Stevenson, and A. Presser, "Hybrid Integrated 10-watt CW Broad-Band Power Source at S Band", IEEE J. Solid-State Circuits, vol. SC-4, pp. 360-366, December 1969.